Spring 1976

Separations of multicomponent mixtures via thermal parametric pumping

John Daniel Stokes
New Jersey Institute of Technology

76-23,734

STOKES, John Daniel, 1925-
    SEPARATIONS OF MULTICOMPONENT MIXTURES
    VIA THERMAL PARAMETRIC PUMPING.

    New Jersey Institute of Technology
    D.Eng.Sc., 1976
    Engineering, chemical

SEPARATIONS OF MULTICOMPONENT MIXTURES

VIA THERMAL PARAMETRIC PUMPING

BY

JOHN DANIEL STOKES

A DISSERTATION

PRESENTED IN PARTIAL FULFILLMENT OF

THE REQUIREMENTS FOR THE DEGREE

OF

DOCTOR OF ENGINEERING SCIENCE IN CHEMICAL ENGINEERING

AT

NEW JERSEY INSTITUTE OF TECHNOLOGY

Newark, New Jersey

1976

ABSTRACT

This dissertation covers the separation of solutes
from multicomponent solutions via direct mode thermal
parametric pumping.

Dilute solution separations were predicted from
existing binary equations by assuming the existence of
pseudo binary systems, each system consisting of one
solute and the common solvent. Two systems, toluene-
aniline-n-heptane and toluene-acetophenone-n-heptane
with a silica gel adsorbent were used to experimentally
demonstrate the separation. Experimental results were
in good agreement with the mathematical predictions.

For concentrated multicomponent solutions, the
separation was demonstrated by the system, toluene-
acetophenone-n-heptane on silica gel. The effects of
mass transfer and nonlinear adsorption isotherms became
significant and a numerical solution of the basic mass
balance, rate, and equilibrium expressions was used to
predict the product concentration profiles. These pre-
dictions were in reasonable agreement with the experimental
results. Separation efficiency was increased by decreasing
the bottom product rate and increasing the cycle time.
Separation efficiency fell off sharply and the system
appeared to be saturated as the total solute concentration

reached 40 volume percent.

The dilute solution (pseudo binary) theory was
used to develop design equations for pilot plant and
commercial systems. The parametric pumping assembly has
the configuration of a multi-tube heat exchanger due to
the necessity of "instantaneous" temperature changes
between the hot and cold half-cycles. In addition to
the main assembly, the requirements for auxiliary tanks,
pumps, and instrumentation are outlined along with a
process description for the operation of the entire
system.

Equations are also given for the required
energies (steam, refrigeration, electrical) and the
total energies compare favorably with conventional
separation processes such as distillation. For the
system studied, energy requirements were estimated at
600-900 BTU/lb. of bottom product for separation
efficiencies of 50-100%. This was compared to distil-
lation stripping and fractionating column separations
where, for similar product purities, 310 and 1,250 BTU/lb.
of bottom product are required.

APPROVAL OF DISSERTATION

SEPARATIONS OF MULTICOMPONENT MIXTURES

VIA THERMAL PARAMETRIC PUMPING

BY

JOHN DANIEL STOKES

FOR

DEPARTMENT OF CHEMICAL ENGINEERING

NEW JERSEY INSTITUTE OF TECHNOLOGY

BY

FACULTY COMMITTEE

APPROVED: _____ Chairman

_____

_____

_____

_____

NEWARK, NEW JERSEY

1976

iii

PREFACE

Parametric pumping is a new separation technique that should rightfully take its place alongside unit operations such as distillation, adsorption, and extraction. It is hoped that this dissertation with emphasis on the separation of solutes in concentrated solutions and on design and scale-up will further this goal.

ACKNOWLEDGEMENTS

This dissertation is dedicated to Professor H. T. Chen, my advisor and friend whose enthusiasm, guidance, and encouragement made this work possible.

I also express my gratitude to Professor W. Snyder and the other members of my advisory committee for their help and encouragement.

To Dr. William J. Knebel and Mr. Sol Bravman I express my thanks for their valuable advice and suggestions regarding the analytical work.

And for their expert help and guidance in the drafting and textual aspects of the dissertation I wish to thank Mr. Cassius F. Brown and Ms. Anne Toto.

And in conclusion I thank my wife, Sabina, for her patience and encouragement, without which this work could not have been completed.

TABLE OF CONTENTS

LIST OF FIGURES

LIST OF TABLES

CHAPTER 1

INTRODUCTION

Thermal parametric pumping is a new unit operation that combines the effect of temperature change on solute adsorption with a reciprocating flow of the solute bearing stream. By alternately adsorbing and releasing the solute into the synchronously reversing stream, a wave front of concentrated solute is "pumped" up the packed adsorbent bed, thereby resulting in a purified solvent or solution leaving the bottom of the column and a concentrated stream leaving the top.

The most convenient basis for analyzing a thermal parametric pumping system is the equilibrium theory originated by Pigford et al (1969), generalized by Aris (1969), and extended to continuous and semicontinuous single solute operation by Chen et al (1972, 1973) and to continuous multicomponent operation by Chen et al (1974).

The equilibrium theory postulates that local interphase equilibrium exists with a linear distribution law having a temperature-dependent distribution coefficient and that there is negligible axial diffusion. This model generally applies to dilute solutions and has led to relatively simple analytical equations. These basic equations and their extension from binary systems to

multicomponent systems is covered in Chapter 3.

Many systems of commercial interest, however, are not only multicomponent systems but involve solutions which are not dilute but have solute concentrations of up to ten percent or more. With these systems, it is no longer reasonable to expect the existence of local inter-phase equilibrium or of independent linear binary isotherms and other basic assumptions of the equilibrium theory. It becomes necessary to allow for the effect of high concentrations of solute species which can create conditions in the system which include non-equilibrium and non-linear isotherms. These conditions and their effects on the mathematical model and the experimental system toluene-acetophenone-n-heptane on silica gel are covered in Chapter 4.

With this background on the performance of multi-component systems, the next logical step was to provide the means for scale-up and design and this is covered in Chapter 5. The dilute solution theory is used because the basic analytical equations needed for predicting separation exist for this theory and can be incorporated into relatively simple design equations and graphs ex-pressing the heating, cooling, and power requirements for the system components.

Before proceeding to the dilute solution theory, it is desirable to put the operation defined as "direct mode thermal parametric pumping" into its proper perspective as merely one subdivision of a very broad group of processes operating under the parametric pumping principle, to define that principle, and to describe some of the other processes operating under that general principle.

CHAPTER 2

BACKGROUND

Parametric pumping is the forcing of a desired con-
centration effect by synchronizing a cyclic change in a
parametric variable with an oscillating field--actually
pumping to a desired concentration level by utilizing
energy from a cyclic parameter change.

In the field of physics, parametric pumping is the
formation of a laser beam by "coupling electromagnetic
waves (light) with quantum mechanical electronic fields
of atoms" (Wilhelm, 1966). In the field of biology,
parametric pumping is associated with Na^+ transport in
membranes (Wilhelm, 1966). In the field of chemical
technology, parametric pumping achieves a separation by
forcing the migration of fluid species in desired direc-
tions by coupling an oscillating change in pH, temperature,
pressure, or other state variable with the cyclic flow of
a fluid phase past a stationary phase.

Conventional separation processes involve two phases
in close proximity, the unidirectional movement of one phase
relative to the other, an equilibrium function relating the
compositions of the two phases, and steady state operation
with state variables such as pressure or temperature held
constant. Parametric pumping represents a whole new approach

to separation and differs from the conventional processes in that the relative motion of the two phases is reciprocal rather than unidirectional and the key state variable is not held constant but is caused to oscillate between fixed levels and is coupled to the reciprocating flow.

The first known application of the parametric pumping principle was heatless or pressure-swing adsorption (Skarstrom, 1959). A solute from a gas stream was adsorbed at high pressure and then purged from the adsorbent bed at low pressure using a fraction of the high pressure product stream. Two columns were used, one for the high pressure adsorption and the other for the low pressure desorption. After each half-cycle, the flows were switched and the operation repeated, restoring the beds to their original condition and completing the cycle. The process worked because, during the high pressure period, the solute concentration in the gas phase was high and the driving force was from the gas to the adsorbent bed. When the bed was exposed to the solute-depleted low pressure gas, the direction of the driving force was reversed and the solute desorbed from the bed. Heat was not required because the cycles were very short and the heat from the adsorption remained in the bed and was available for the desorption.

Skarstrom's invention was used commercially for drying air over a silica gel bed. Other uses of heatless

adsorption were the purification of hydrogen (Alexis, 1967), and the production of oxygen-rich gas from air (Lee and Stahl, 1972). In these operations the numbers of beds and the cycles were changed but the basic principles remained the same. An excellent review of these and other parametric pumping operations was given by Wankat (1974).

Despite the commercial success of heatless adsorption, the process was complicated and difficult to model. A mathematical model by Shendalman and Mitchell (1972) incorporated the assumptions of local equilibrium, linear adsorption isotherms, and no axial dispersion as did the equilibrium theory of Pigford et al (1969). This model showed the importance of a high purge to feed ratio and was in reasonable agreement with experimental results at high ratios. When mass transfer was taken into account, the prediction was conservative.

A semicontinuous modification of Skarstrom's basic process by Turnock and Kadlec (1971) and Kowler and Kadlec (1972) involved the admission of high pressure feed followed by feed shut-off and exhaustion of the column at the feed end. Product was withdrawn continuously from the other end. The basis of the separation was the same as before--adsorption of solute from the high pressure gas and purging the solute from the bed with a portion of the solute-depleted gas as exhaust, the remainder of the

solute-depleted gas leaving the other end of the column as a steady product stream. The mathematical model, based on the assumptions of local equilibrium, no axial dispersion, and a Freundlich isotherm was in good agreement with the experimental data. Reasons for the good agreement could be the assumption of a non-linear isotherm and the inclusion of the depressurization and repressurization steps in the mathematical model.

Another form of parametric pumping is pH parametric pumping based on a change in chemical potential. The work of Sabadell and Sweed (1970) was in the recuperative mode because the H^+ and OH^- ions could not be impressed on the packed bed through the walls of the column but travelled through the bed with the reciprocating fluid flow. The closed end of the bed was maintained at a low pH by titration with concentrated HCl. When the flow to the column is from the acidic closed end, H^+ ions are carried into the bed to release the Na^+ and K^+ ions attached to the resin. On the next half-cycle, the feed solution carries OH^-, Na^+, and K^+ ions into the bed. The OH^-ions neutralize the H^+ ions attached to the resin and the Na^+ and K^+ ions attach themselves to the sites on the resin made available due to the neutralization reaction. The excess Na^+ and K^+ ions move towards the closed end of the column and accumulate at this acidic end of the column.

The neutralization that occurs in the alkaline downflow half-cycle is the source of energy for the separation. This energy is supplied externally by the addition of HCl to maintain the low pH at the acidic end of the column.

No mathematical model was developed for pH parametric pumping but the model for recuperative thermal parametric pumping was suggested as a starting basis. The efficiency of the separation was poor but the principle of the separation was clearly demonstrated. pH parametric pumping may have applications in the separation of biological materials because it has been associated with Na^+ transport in membranes (Wilhelm, 1966) since the K^+, Na^+ equilibrium on proteins is known to be pH sensitive.

Miscellaneous applications of parametric pumping were liquid-liquid extraction parametric pumping (Wankat, 1973), thermal parametric pumping as a chemical reactor (Apostolopoulos, 1975), and the effects of parametric pumping on chemical reactions (Kim and Huburt, 1971). The range of possible applications of the parametric pumping principle is very large and more applications may be expected in the future.

The most widespread use of the parametric pumping principle has, thus far, been in the thermal field. Thermal parametric pumping has been effective because of the large

effect of thermal energy on forcing the migration of solute species in achieving a separation. Two methods of transferring heat to the packed bed have been used: the recuperative mode by Wilhelm et al (1966) in which the fluid entering the packed bed is heated and cooled by alternate half-cycles by external heat exchangers; and the direct mode developed independently by Wakao et al (1968) and by Wilhelm and Sweed (1968) in which the heat was transferred through the walls surrounding the packed bed. This direct process allowed isothermal operation during the hot and cold half-cycles and increased the efficiency of the separation, but tended to limit the diameter of the packed column due to heat transfer considerations.

The recuperative mode of thermal parametric pumping utilizes the moving fluid phase to transport the thermal energy as well as the solute species through the packed bed. The fluid is heated as it enters the top of the column and, as the thermal wave travels down the bed, the solutes are desorbed and move down the column with the flowing stream. The flow is then reversed and cold fluid enters the bottom of the column. The solutes are now adsorbed and held back as the solvent moves upwards. By repeating this pattern of hot and cold half-cyles, a concentration wave pattern is generated in the bed and, eventually, a cyclic steady state condition prevails; a dilute stream

leaves the top of the column and an enriched stream leaves the bottom.

Recuperative parametric pumping has been applied to both batch and open systems. The mathematical model (Wilhelm et al, 1968) (Rolke and Wilhelm, 1969) included mathematical expressions for equilibrium, rate, and continuity for both heat and mass transfer and were quite complicated. The equations were solved numerically and were in good agreement with the experimental results, but the separations were poor in comparison to those achieved by the direct mode. Sweed and Rigaudeau (1973) explained that good separations required that the thermal wave pass through the entire column. Since this would not normally happen (because the thermal wave travelled with the flowing fluid), it was proposed that in-bed heat exchangers be installed to advance the thermal wave beyond the concentration wave front. This was proposed as a means of successful scale-up of recuperative thermal parametric pumping (Sweed and Rigaudeau, 1973). The use of multiple bed units for scale-up via direct mode thermal pumping was described as undesirable due to column packing and operational difficulties.

The direct mode of thermal parametric pumping differs from the recuperative mode in that the transfer of heat is directly through the column walls. For this reason,

the operation is isothermal throughout each of the hot
and cold half-cyles and the separation is increased to
the maximum possible within a given temperature range.
The separation factors, at least for certain systems,
appeared to be limited only by the ability to analyze
the product solutions for trace quantities of solute.

In the typical direct mode of operation, the column
is heated and the solutes desorb and are carried upwards
toward the top of the column with the flowing fluid. Then
the flow is interrupted, the column is cooled, and the
flow is reversed. The solutes are adsorbed and held in
place while the cold solvent flows down the column. This
pattern of hot upflow and cold downflow is repeated and a
wave pattern is generated that leads to the migration of
the strongly adsorbed solutes to the top of the column and
the solvent and weakly adsorbed solutes to the bottom.
Depending on the operating conditions, any desired
separation split of the solutes between the top and bottom
effluent streams is possible, including a solute-free
bottom product.

The direct mode was first modeled by Wilhelm et al
(1968) for the batch operation in which the fluid was
pumped between two reservoirs located at the opposite
ends of the column. The system was loaded with feed
solution, operated for a required number of cycles, and

the top and bottom products were unloaded from the two reservoirs. The procedure was repeated until the desired amount of production was obtained.

The mathematical analysis of the batch pump was greatly simplified by the equilibrium theory originated by Pigford et al (1969) and generalized by Aris (1969). This equilibrium theory postulated that local interphase equilibrium exists with a linear distribution law having a temperature dependent coefficient and negligible axial diffusion. With these assumptions, it was possible for Pigford and his coworkers to solve the partial differential equations by the method of characteristics and to fit the analytical solution to the data of Wilhelm et al (1968). This equilibrium theory stimulated some additional work on batch systems which included a batch separation scheme for multicomponent mixtures (Butts, Gupta, and Sweed, 1972).

The equilibrium theory also led to the increased development of open systems. Gregory and Sweed (1970) presented mathematical models and analytical solutions for two open systems in which the feed and product flows occur during different portions of each cycle. The sequencing of the various flows is complex and can best be described as sequenced cyclic operations. In a later paper, Gregory and Sweed (1972) presented three additional open

systems and experimental verification for two systems.

Chen and Hill (1971) extended the equilibrium theory to batch, semicontinuous, and continuous systems with allowance for dead volume. The inclusion of dead volume increased the accuracy of separation prediction in the transient period prior to cyclic steady state operation. Details of the mathematical models, the analytical solutions, and the experimental verifications were presented by Chen et al (1972) for the continuous system and by Chen et al (1973) for the semicontinuous system. The semicontinuous operation differed from those of Gregory and Sweed in that the sequence of feed and product flows were basically simple--batch operation during the hot upflow half-cycle and continuous feed and product flows during the cold downflow half-cycle. For the continuous mode of operation, all flows were continuous and constant for all half-cycles. In a comparison between the sequenced cyclic operations of Gregory and Sweed (1970) and the semicontinuous operation of Chen and Hill (1971), it was pointed out (Chen et al,1973) that a sequenced cycle system with equal reservoir displacement for cold and hot cycles would correspond to a limiting case of no top product for the semicontinuous pump. It was further pointed out that both systems have the capability of infinite separation.

In their extended analysis of the equilibrium theory Chen and Hill (1971) showed that the basis of separation was the relationship of the penetration distances of the hot upflow and cold downflow wave fronts to each other and to the height of the packed column. To achieve maximum separation, it was necessary that the penetration distance of the cold downflow wave front never exceed either the penetration distance of the hot upflow wave front or the height of the column. Since these penetration distances were defined in terms of the column interstitial velocities and the adsorption isotherm parameters, it was simple to operate the column for maximum separation once these parameters were established.

Chen and his coworkers further extended their analysis to dilute multicomponent systems (Chen et al, 1973) which will be discussed in some detail in Chapter 3.

At this point, it would be pertinent to mention some of the chemical systems that have been investigated via direct thermal mode parametric pumping. The emphasis in the selection of most of the systems has naturally been oriented towards simple, easily analyzed, chemical systems that lend themselves to testing theories rather than systems whose separations have commercial significance.

Some of the binary liquid systems which have been
used experimentally in direct mode thermal parametric
pumping are toluene and n-heptane on silica gel (Wilhelm
and Sweed, 1968) (Chen et al, 1972, 1973); benzene and
n-hexane on silica gel (Wakao et al, 1968); sodium chloride
and water on ion retardation resin (Sweed and Gregory,
1970); urea and water on activated carbon (Goldstein, 1969)
(Bringhurst, 1970); sodium nitrate and water on ion re-
tardation resin (Chen and Manganaro, 1974).

Binary gas system separations have also been reported
despite some inherent problems with gas systems. Since
most systems would be operated at constant volume, the
high pressure corresponding to the high temperature during
the hot upflow half-cycle would tend to counteract the
normal desorption effect due to the temperature; and con-
versely, during the cold downflow half-cycle, the low
pressure would tend to counteract the normal adsorption
effect. A second major problem occurring with gas systems
would be the lag between the jacket and bed temperatures
due to the poor heat conduction of the gases. Despite
these disadvantages, some binary gas separations have
been reported and some may have commercial potential.
Some of these were ethane and propane on activated carbon
(Jenczewski and Myers, 1968); argon and propane on
activated carbon (Jenczewski and Myers, 1970); ethane

and propane on activated carbon (Jenczewski and Myers, 1970); sulfur dioxide and air on silica gel (Patrick et al, 1972); and boron trifluoride isotopes on boron trifluoride-dimethylsulfoxide complex (Schroeder and Hamrin, Jr., 1975).

Multicomponent mixture separations are a logical extension of binary separations. Chen et al (1974) applied the analytical expressions for the continuous binary parametric pump (Chen et al, 1972) to pairs of pseudo binaries and thus developed a mathematical basis for dilute multicomponent systems. Examples of multi-component systems studied thus far are glucose-fructose-water on Fullers earth (Chen et al, 1972); Na^+-H^+-K^+-H_2O on ion exchange resin (Butts et al, 1973); aniline-toluene-n-heptane on silica gel (Chen et al, 1974); and glucose-fructose-water on ion exchange resin (Chen and D'Emidio, 1975).

The multicomponent systems selected for study in this thesis are aniline-toluene-n-heptane on silica gel and a new system, acetophenone-toluene-n-heptane on silica gel. The latter system was selected because there were no solubility limitations that would interfere with an extension of the study to concentrated solutions. It is hoped that the dilute solution theory for multicomponent systems, the section on the effect of concentration, and

the equations for scale-up and design will stimulate interest that will result in the application of thermal parametric pumping on an industrial scale.

CHAPTER 3

MULTICOMPONENT SEPARATION OF DILUTE SOLUTIONS

This chapter comprises four sections: a review of
the basic model, a review of the equilibrium theory, adaptation of this previous work to multicomponent separation of
dilute solutions, and experimental verification of the dilute
solution theory.

Basic Model

The basic model equations for parametric pumping were
discussed in detail by Wilhelm et al. (1968). These equations
are:

The material balance equation

$$\epsilon \frac{\partial y_i}{\partial t} + \epsilon v \frac{\partial y_i}{\partial z} + (1-\epsilon)\rho_s \frac{\partial x_i}{\partial t} - \epsilon \mathcal{D} \frac{\partial^2 y_i}{\partial z^2} = 0 \qquad (1)$$

The interphase rate equation

$$\frac{\partial x_i}{\partial t} = \lambda (y_i - y_i^*) \qquad (2)$$

and the equilibrium expression

$$y_i^* = y_i^*(T, y_j^*, x_j^*) \text{ where } j = 1,2...., \text{ n including } i$$
$$(3)$$

where y_i is the fluid concentration of component i in
moles of i per unit volume of fluid, x_i is the moles of
i adsorbed per unit weight of adsorbent, y_i^* is the
equilibrium concentration of i in the fluid, v is the

interstitial velocity of the fluid, t is the time, z is
the axial distance along the packed bed, ρ_s is the density
of the solid adsorbent, ϵ is the void fraction of the ad-
sorbent, T is the absolute temperature, λ is the mass
transfer coefficient, and $\mathcal{D}$ is the axial diffusivity.

In this chapter, these equations are applied to con-
tinuous direct mode thermal parametric pumping for the
separation of dilute multicomponent solutions. The parti-
cular method followed was originally proposed by Chen and
Hill (1971) and developed for the toluene-aniline-n-heptane-
silica gel system by Chen et al. (1974). In Chapter 5,
this dilute solution theory is incorporated into the de-
sign equations for the scale-up of laboratory systems into
pilot plant and larger size parametric pumping systems.

The continuous parametric pump, characterized by a
steady flow of both feed and product streams during the
hot upflow and cold downflow half cycles, is shown in
Figure (1). Flow is upward during the hot half cycle
and downward during the cold half cycle. Each half cycle
is π/ω time units in duration and the reservoir displace-
ment volume is $Q\pi/\omega$ where Q is the reservoir displacement
rate. The pump has dead volumes V_T and V_B for the top and
bottom reservoirs, respectively. The feed is directed to
the top of the column at the flow rate $(\emptyset_T+\emptyset_B)_Q$. The top
product flow rate is $\emptyset_T Q$ and the bottom product flow rate
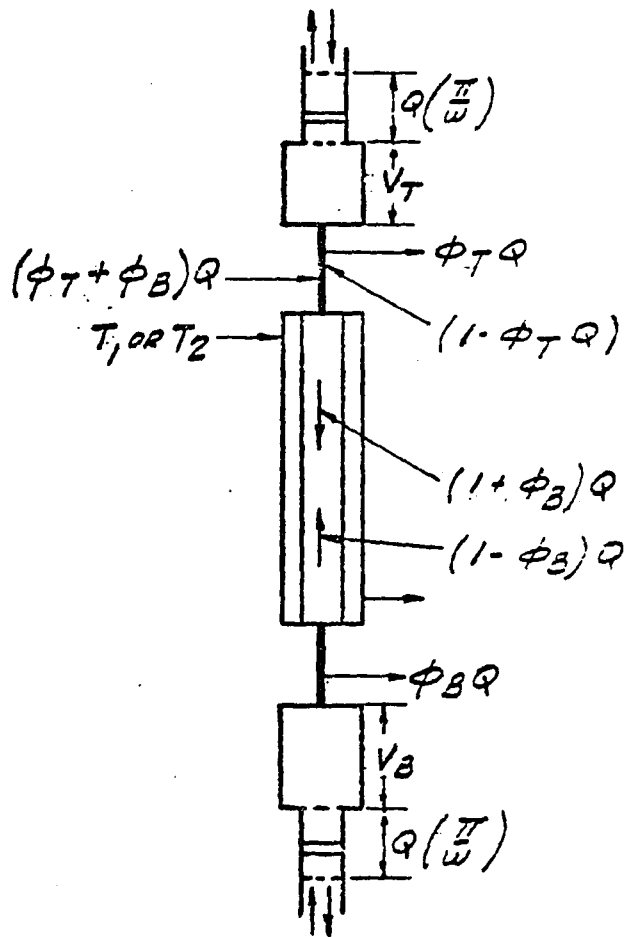
FIGURE (1)

Parametric Pump Schematic Diagram

is $\emptyset_B Q$ and $\emptyset_T$ and $\emptyset_B$ are the ratios of the top and bottom product rates to the reservoir displacement rate.

These parameters are involved in the mathematical development which requires: a mathematical description of the adsorption-desorption and flow processes occurring within the column (internal equations); material balances connecting the column to the reservoirs and all external streams; and a combination of these equations to produce the performance guidelines and concentration profiles which enable the researcher or designer to manipulate the parametric pumping separation to suit his particular needs.

Review of the Equilibrium Theory

First it is necessary to review the equilibrium theory originated by Pigford et al. (1969), generalized by Aris (1969), and extended to continuous direct mode parametric pumping by Chen and Hill (1971) and Chen et al. (1972).

Now in the case of the equilibrium theory, the following assumptions are made:

1. No axial dispersion ($\beta = 0$).

2. Instantaneous equilibrium ($y_i = y_i^*$).

3. Linear equilibrium adsorption ($x_i = M_i(T)y_i$).

4. Instantaneous temperature changes.

5. Plug flow (steady unidirectional flow of all fluid elements).

6. Constant fluid density (Total moles of fluid per unit volume of fluid is a constant. In the equations, the term y_i incorporates the fluid density term shown by Pigford et al. (1969) as ρ_f.)

With these simplifying assumptions, the material balance is:

$$\frac{\partial y_i}{\partial t} + v\frac{\partial y_i}{\partial z} + \frac{(1-\varepsilon)\rho_s}{\varepsilon}\frac{\partial x_i}{\partial t} = 0 \tag{4}$$

Now if the linear isotherm is differentiated

$$\frac{\partial x_i}{\partial t} = M_i(T)\frac{\partial y_i}{\partial t} + y_i\frac{\partial M_i(T)}{\partial T}\frac{\partial T}{\partial t} \tag{5}$$

And if

$$m_i = \frac{(1-\varepsilon)\rho_s M_i(T)}{\varepsilon} \tag{6}$$

Then

$$\frac{\partial m_i}{\partial T} = \frac{(1-\varepsilon)\rho_s}{\varepsilon}\frac{\partial M_i(T)}{\partial T} \tag{7}$$

And by substitution Equation (4) becomes

$$(1+m_i)\frac{\partial y_i}{\partial t} + v\frac{\partial y_i}{\partial z} + \frac{\partial m_i}{\partial T}\frac{\partial T}{\partial t} y_i = 0 \tag{8}$$

Then by the method of characteristics we get

$$\frac{dt}{1+m_i} = \frac{dz}{v} = \frac{-dy_i}{\frac{dm_i}{dT}\frac{dT}{dt}y_i} \tag{9}$$

which become

$$\frac{dz}{dt} = \frac{v}{1+m_i} \tag{10}$$

and

$$\frac{dy_i}{y_i} = \frac{dm_i}{1+m_i} \tag{11}$$

Considering the definitions of Pigford et al. (1969),

$$v = v_o sq(\omega t) \tag{12}$$

$$m_i = m_{oi} - a_i sq(\omega t) \tag{13}$$

$$u_{oi} = v_o/(1+m_{oi}) \tag{14}$$

$$b_i = a_i/(1+m_{oi}) \tag{15}$$

as the interstitial velocity (v), the dimensionless equilibrium constant (m_i), the wave front velocity (u_{oi}), and the dimensionless equilibrium parameter (b_i). The subscript (o) denotes the value at the mean of the two operating temperatures, the constant a_i denotes the deviation of m_i from the mean, and the sq(ωt) term denotes whether the deviation from the mean is positive or negative in sign.

With these definitions, Equation (10) becomes

$$\frac{dz}{dt} = \frac{u_{oi}\,sq\,(\omega t)}{1-b_i\,sq\,(\omega t)} \tag{16}$$

showing that in the z-t plane, the characteristic curves
are straight lines having slopes of $u_{oi}/(1-b_i)$ for hot
upflow and $-u_{oi}/(1+b_{oi})$ for cold downflow.

Now if Equation (16) is integrated between the limits
of $t = 0$ and π/ω, we get the wave front penetration dis-
tances for hot upflow and cold downflow, respectively,
which were first defined by Chen and Hill (1971) as follows:

$$L_{1i} = \frac{u_{oi}\,(\pi/\omega)}{(1-b_i)} = \frac{v_o\,(\pi/\omega)}{(1-b_i)\,(1+m_{oi})} \tag{17}$$

$$L_{2i} = \frac{-u_{oi}\,(\pi/\omega)}{(1+b_i)} = \frac{-v_o\,(\pi/\omega)}{(1+b_i)\,(1+m_{oi})} \tag{18}$$

Now from Figure (1), the flow rates in the column
during hot upflow and cold downflow are $Q(1-\emptyset_B)$ and $Q(1+\emptyset_B)$
and Equations (17) and (18) become

$$L_{1i} = \frac{v_o\,(1-\emptyset_B)\,(\pi/\omega)}{(1-b_i)\,[1+0.5\,(m_{1i}+m_{2i})]} \tag{19}$$

$$L_{2i} = \frac{v_o\,(1+\emptyset_B)\,(\pi/\omega)}{(1+b_i)\,[1+0.5\,(m_{1i}+m_{2i})]} \tag{20}$$

where m_{1i} and m_{2i} are the dimensionless equilibrium constants during hot upflow and cold downflow defined by Equation (6). The quantity b_i, defined by Equation (15), may be expressed as

$$b_i = \frac{0.5(m_{2i}-m_{1i})}{1+0.5(m_{1i}+m_{2i})} \tag{21}$$

Now

$$\frac{L_{1i}}{L_{2i}} = \frac{(1-\emptyset_B)}{(1+\emptyset_B)} \frac{(1+b_i)}{(1-b_i)} \tag{22}$$

Chen and Hill (1971) showed that the pump performance depends on the relative magnitudes of L_{1i}/L_{2i} and the height of the column, h. There are three possible regions of pump operations depending on L_{1i}/L_{2i} and h,

$$\text{Region 1, } \frac{L_{1i}}{L_{2i}} \geqslant 1 \text{ (or } \emptyset_B \leqslant b_i) \text{ and } L_{2i} \leqslant h \tag{23}$$

$$\text{Region 2, } \frac{L_{1i}}{L_{2i}} < 1 \text{ (or } \emptyset_B > b_i) \text{ and } L_{1i} \leqslant h \tag{24}$$

$$\text{Region 3, } L_{1i} \text{ and } L_{2i} > h \tag{25}$$

Equations (9) through (25) provide the operating guidelines for column performance. They were obtained by combining the column flow rates (external equations) with the internal equations (17, 18) that represent half of the analytical solution of Equations (1, 2, 3).

The other half of the analytical solution of Equation (9) leads to the concentration profiles. Equation (11) is combined with Equations (13, 15) and is integrated without definite limits (Pigford et al., 1969).

$$y_i(z,t) \left[1-b_i \, sq(\omega t) \right] = \text{integration constant} \qquad (26)$$

This means that $y_i(z,t)$ undergoes a change in value proportional to the ratio $(1+b_i)/(1-b_i)$ when the characteristic line passes from a cold region into a hot one. The reverse is true when passing from a hot to a cold region. Now if the change in $y_i(z,t)$ is followed for n cycles, the value of y_i <u>for the bottom of the column</u> is

$$\left\langle y_{B2i} \right\rangle_n = \left\langle y_{B1i} \right\rangle_n \frac{(1-b_i)}{(1+b_i)} = y_{oi} \left[\frac{1-b_i}{1+b_i} \right]^n \qquad (27)$$

where $\left\langle y_{B2i} \right\rangle_n$ is the concentration of the i component at the bottom of the column during the cold downflow half cycle, $\left\langle y_{B1i} \right\rangle_n$ is the concentration of the i component at the bottom of the column during the preceding hot upflow cycle, and y_{oi} is the concentration of the i component in the original or feed solution.

Chen and Hill (1971) modified Equation (27) to include the effect of dead volume in the reservoirs, which is always present in actual systems. With this correction for dead volume, Equation (27) becomes

$$\frac{\left\langle y_{BP2i} \right\rangle_n}{y_{oi}} = \frac{(1-b_i)}{(1+b_i)} \left[\frac{(1-b_i)/(1+b_i)+C_2}{1+C_2} \right]^{n-1} \qquad (28)$$

This correction for dead volume was made by solving the first part of Equation (27) simultaneously with an external material balance equation (Chen and Hill, 1971).

Chen and Hill also gave the bottom product-to-feed ratio for cyclic steady state, which for multicomponent systems is

$$\frac{\langle Y_{BP2i} \rangle_\infty}{Y_{oi}} = 0 \tag{29}$$

The equations for the top product stream were developed in the same manner as those for the bottom product stream, cycle by cycle to the nth cycle. But the top product stream is somewhat more complicated. The equations by Pigford et al. (1969) were generalized by Aris (1969) to apply to all batch pumps with no dead volume. Chen and Hill (1971) extended these equations to include batch, continuous, and semi-continuous pumps with dead volume and the transient equations were given for the continuous and semicontinuous pumps by Chen et al. (1972, 1973). The development of the equations for the continuous pump proceeds as follows:

As the progress of the concentration wave fronts is traced to the top of the column, it is found that after a certain number of cycles, a pattern develops--characteristic regions of constant concentrations from the bottom to the

top of the column. This pattern is established (for operation in Region 1) p_1+1 cycles after time zero, where

$$p_{1i} + q_{1i} = \frac{(h-L_{2i})}{(L_{1i}-L_{2i})} = \frac{(h-L_{2i})}{\Delta L_i} \qquad (30)$$

The internal equation for the average concentration of the effluent stream leaving the top of the column after $p_{1i}+1$ cycles, as given by Chen and Hill (1971) and adapted to multicomponent systems is

$$\langle y_{T1i} \rangle_n = \frac{L_{2i}}{L_{1i}} \frac{(1+b_i)}{(1-b_i)} \langle y_{T2i} \rangle_{n-1} +$$

$$\left[1 - \frac{L_{2i}}{L_{1i}} \right] \left[q_{1i} \langle y_{B1i} \rangle_{n-p_{1i}-1} + (1-q_{1i}) \langle y_{B1i} \rangle_{n-p_{1i}} \right]$$

$$(31)$$

and shows that the average concentration of component i in the top effluent stream after n cycles comprises contributions from three sources: the column bottom compositions from time zero and the first cycle, and the top composition from the previous downflow cycle.

This internal equation (31) must be solved simultaneously with the corresponding external equations around the top of the column. This was done by Chen and Hill (1971) for the binary system and the resulting transient equations were given by Chen et al. (1972) for the continuous column.

A total of ten equations for the concentration transients was given, including the binary system version of Equation (28). The equations present the concentration transients for the top and bottom product streams for operation in Regions 1, 2, and 3, and for ranges of time cycles from time zero ($n \geq 1$) to constant wave pattern development ($n \leq p_1+1$ for Region 1 and $n \leq p_2+1$ for Region 2) and beyond ($n \geq p_1+2$ for Region 1 and $n \geq p_2+2$ for Region 2). The equations for cyclic steady state ($n = \infty$) were previously given by Chen and Hill (1971). In the case of Region 3, there are no specific ranges of n to achieve constant wave front patterns because this mode of operation is characterized by wavefront breakthrough (L_{1i} and $L_{2i} > h$) on both hot upflow and cold downflow half cycles.

Most components found in normal multicomponent mixtures have exothermic heats of adsorption and the slopes of the isotherms, $M_i(T)$ and $m_i(T)$, are positive. Some of these components will be in Region 1 and some in Region 2, depending on their values of b_i and on the manner in which the column is operated (values of $\emptyset_B$ and $\emptyset_T$ selected by the operator). However, it is possible for some components in this same mixture to be in the Region 3 mode of operation, especially those with endothermic heats of adsorption and negative isotherm slopes.

Therefore, all three Regions of operation are possible and all the concentration transient equations are necessary in any given multicomponent system. The binary forms of the equations given by Chen et al. (1972) are simply applied to each pseudo binary pair in the multicomponent system.

Two of the equations applicable to the top product concentration profiles for operation in Region 1 are:

$$\frac{\langle y_{TP2i}\rangle_n}{y_{oi}} = - \frac{\phi_B + \phi_T}{1-\phi_T} + \frac{1+\phi_B}{1-\phi_T} \left[\frac{C_1 + (1-\phi_T)/(1+\phi_T)}{1+C_1}\right]^{n-1}$$

$$+ \frac{1+\phi_B}{1-\phi_T}\frac{1+\phi_T}{2\phi_T}\left[1 - \frac{1-\phi_T}{1+\phi_T}\frac{1-b_i}{1+b_i}\right]$$

(32)

$$\left[1 - \left(\frac{C_1 + (1-\phi_T)/(1+\phi_T)}{1+C_1}\right)^{n-1}\right] \quad \text{for } n \leq p_1+1$$

and

$$\frac{\langle y_{TP2i}\rangle_\infty}{y_{oi}} = 1 + \frac{\phi_B}{\phi_T} \quad \text{for } n = \infty$$

(33)

Multicomponent Separation of Dilute Solutions

The adaptation of the binary equations to multicomponent separations has been published (Chen, Lin, Stokes, and Fabisiak, 1974). The binary system equations are applicable to a multicomponent mixture if the multicomponent mixture is

treated as a series of independent pseudo-binary systems, each binary behaving as though the other systems were not present. Chen and Hill (1971) first suggested that multi-component separations could be predicted by existing mathematical expressions for binary systems (Chen et al., 1972, 1973), and Chen et al. (1974) used this procedure on the toluene-aniline-n-heptane silica gel system. Their derivations will not be repeated here, but note that they found that at steady state (n $\rightarrow \infty$) solute removal from the bottom product stream, $\emptyset_B Q$, was complete in Region 1 and only partially complete in Regions 2 and 3.

Now, consider a mixture containing s solutes, each with its own b_i and

$$b_i > b_2 >--- \quad b_k = \emptyset_B > b_{k+1} >---> b_s \tag{34}$$

where subscripts 1, 2, etc., refer to solutes 1, 2, etc. Furthermore,

$$L_{2i} \leq h \text{ when } i = 1, 2, --- k \tag{35}$$

$$L_{1i} \leq h \text{ when } i = k+1, --- \quad s \tag{36}$$

At steady state, the components, i = 1, 2, --- k, for which the operations are indicated in Region 1, would appear only in the top product stream, and the remaining components (k+1, --- s) would appear in both the top and bottom product

streams. In the extreme case where k = s, the bottom
product stream would consist only of pure solvent. By
proper adjustment of $\emptyset_B$ in Equation (26), a solute split
could be made which is analogous to that obtained by a
multicomponent distillation column.

Experimental Verification of the Dilute Solution Theory

The experimental verification of the theory has been
published (Chen, Lin, Stokes, and Fabisiak, 1974) and the
experimental details presented by Lin (1974). The experi-
mental apparatus and procedure was the same as that used
previously (Chen et al., 1972) and included two dual in-
fusion-withdrawal syringe pumps manufactured by the Harvard
Apparatus Co., one for the feed and one for the reservoirs.
The jacketed column was packed with 30 to 60 mesh chromato-
graphic-grade silica gel. Prior to each run, the column
and the bottom reservoir were filled with the feed mixture
of concentrations, y_{oi}. Hot and cold water baths were
connected to the column jacket and solenoid valves were
wired to a dual timer to insure that hot water was directed
to the column during upflow and cold water during downflow.
Feed was pumped continuously to the top of the column and
the continuous top and bottom product streams were throttled
by micrometer capillary valves to regulate flow and to im-
pose a small back pressure on the system. Samples were
taken at the end of each cycle and analyzed by ultraviolet
spectrophotometry.

Four runs were made. The experimental and model parameters are presented in Table (1) and the results in Figures (2) and (3).

Figure (2) illustrates the concentration profile of $\langle y_{BP2i}\rangle_n/y_{oi}$ versus n for both toluene and aniline in both binary and ternary systems. It can be seen that this ratio of bottom product to feed decreases as the number of cycles increases and, as indicated by Equation (29), approaches zero as n becomes large. The slope of log $(\langle y_{BP2i}\rangle_n/y_{oi})$ versus n of the solute in the binary mixture coincides with that in the ternary system. This means that for a given set of operating temperatures and dimensionless top reservoir dead volume, the value of b_i was essentially the same for the binary and ternary systems. Since b_i is a measure of the extent of adsorption and de-sorption of a solute between the two operating temperatures (Equation 21), the separation is increased by a large b_i and solute concentration in the bottom stream becomes smaller (see Equation 28). The b_i values in the present case were 0.15 for toluene and 0.31 for aniline.

Figure (3) shows the effects of the hot upflow and cold downflow wavefront penetration distances (L_{1i}, L_{2i}) and the height of the column (h) on product concentrations. As long as the wavefront penetration on cold downflow is less than or equal to that on hot upflow or the height of

TABLE 1

EXPERIMENTAL AND MODEL PARAMETERS

$\frac{\P}{\omega} = 1,200$ sec., $T_1 = 333°K$, $T_2 = 298°K$, $h = 0.9$ m, $\phi_T + \phi_B = 0.4$

	Y_{oi}		ϕ_B	C_1	C_2	b_i	$L_{1i}(m)$	$L_{2i}(m)$	Region
	Toluene	Aniline							
1. Toluene-n-heptane	0.025	0	0.07	0.12	0.13	0.15	0.51	0.43	1
2. Aniline-n-heptane	0	0.025	0.10	0.11	0.13	0.31	0.70	0.45	1
3. *Aniline-toluene-n-heptane	0.025	0.025	0.09	0.12	0.13				
a. Toluene-n-heptane						0.15	0.49	0.44	1
b. Aniline-n-heptane						0.31	0.71	0.45	1
4. *Aniline-toluene-n-heptane	0.025	0.025	0.22	0.12	0.13				
a. Toluene-n-heptane						0.15	0.42	0.49	2
b. Aniline-n-heptane						0.31	0.62	0.51	1

* Assume that a ternary system contains two pseudo-binaries.

$$\frac{<y_{BP2}>_n}{y_{01}}$$

$T_1 = 333°k$, $T_2 = 298°k$, $C_2 = 0.13$

	ϕ_B	b	Exp.
1. Toluene in n-Heptane	0.07	0.15	⊡
2. Aniline in n-Heptane	0.10	0.31	⊙
3a. Toluene in Aniline-n-Heptane	0.09	0.15	⊡
3b. Aniline in Toluene-n-Heptane	0.09	0.31	⊙
——— Calc.			

n
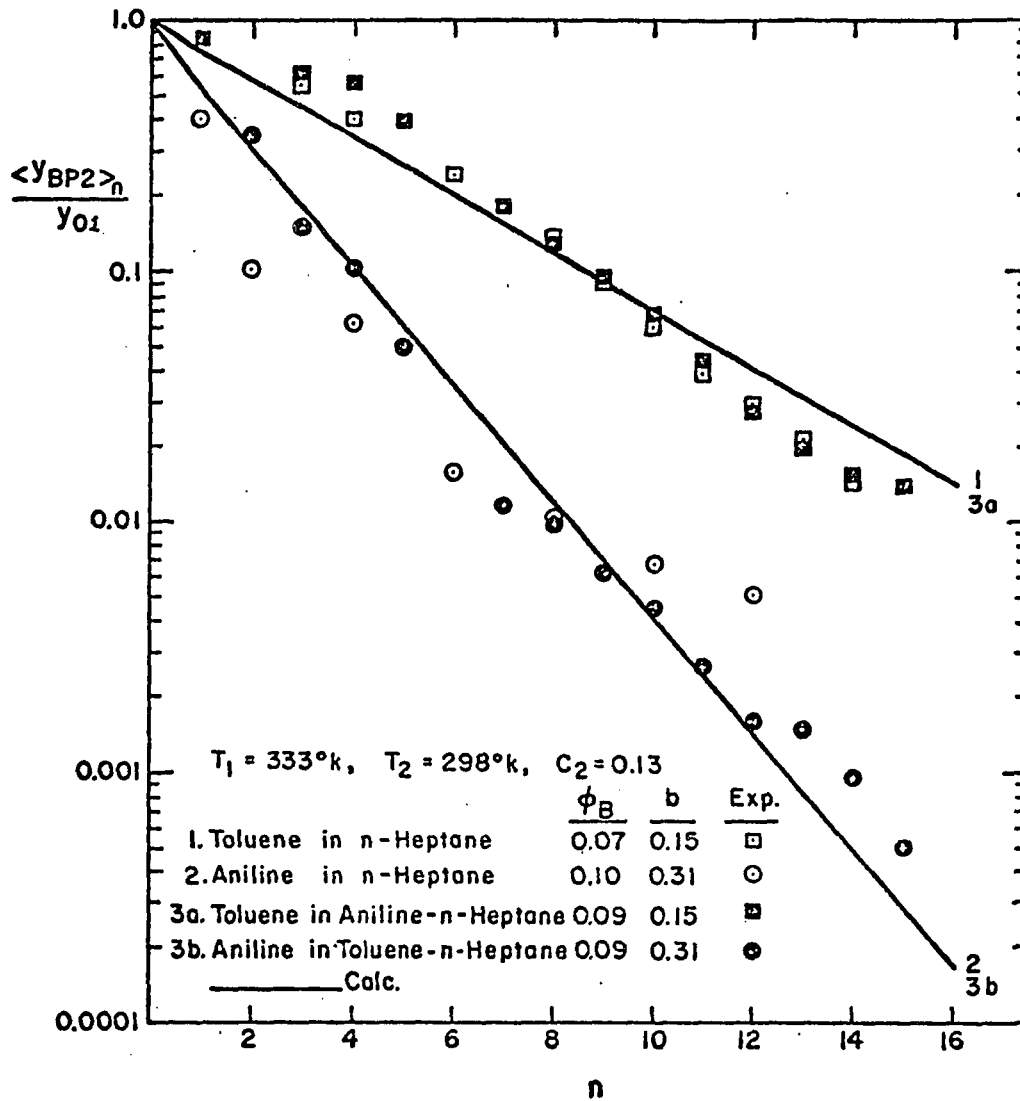
FIGURE (2)

Effect of b_i on Multicomponent Separation
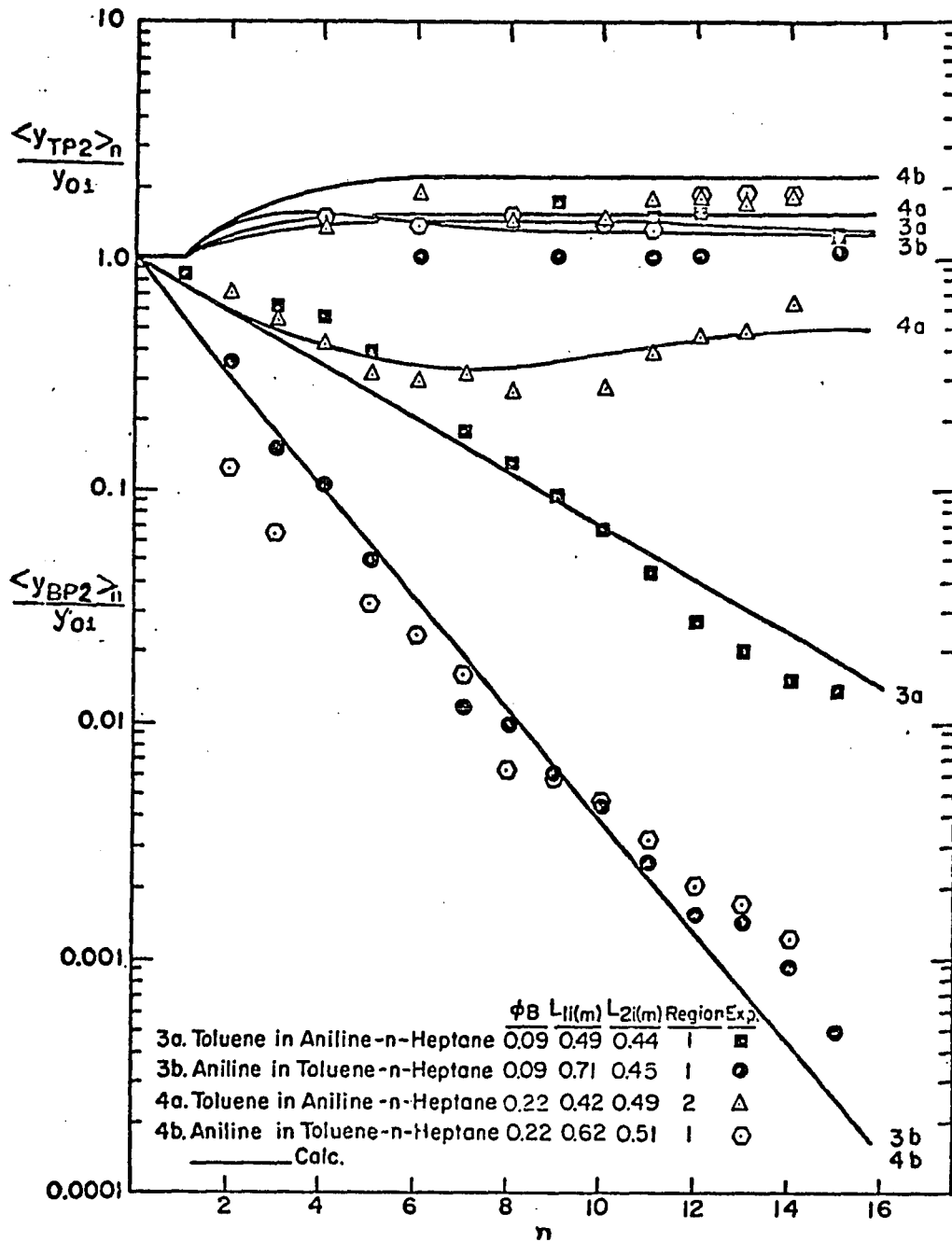
FIGURE (3)

Effect of ϕ_B on Multicomponent Separation

the column, the solute concentration in the bottom stream
approaches zero as n becomes large. But this steady state
behavior can abruptly change if pump operation moves out
of Region 1. If L_{2i} is increased until it exceeds h, or
if L_{1i} becomes less than L_{2i}, switching points are en-
countered which causes pump behavior to abruptly switch
from a mode in which solute is completely removed from the
bottom product stream to one in which solute removal is
incomplete. One may visualize crossing the boundary
L_{2i}=h as a result of increasing L_{2i} by increasing reservoir
displacement volume, $Q\pi/\omega$. Crossing of the boundary L_{1i}=L_{2i}
may be viewed as resulting from an increase of $\emptyset_B$ so that
$\emptyset_B > b_i$, or $L_{2i} > L_{1i}$. At $T_1 = 333^O K$ and $T_2 = 298^O K$, the
switching point for toluene corresponds to the condition
$\emptyset_B = b_{toluene} = 0.15$. In the case of aniline, the condition
is $\emptyset_B = b_{aniline} = 0.31$. Thus, when $\emptyset_B \leq 0.15$ (curves 3a
and 3b), the operation is in Region 1 for both toluene and
aniline, and solute removal from the bottom stream may be
complete as n approaches infinity. If $\emptyset_B$ is increased to
the interval range, $0.15 < \emptyset_B \leq 0.31$ (curves 4a and 4b),
the operation switches to Region 2 for toluene, remains in
Region 1 for aniline, and the bottom product could eventually
contain only toluene. If $\emptyset_B$ is further increased, $\emptyset_B > 0.31 =$
$b_{aniline}$, the operation is now in Region 2 for both toluene
and aniline, and both toluene and aniline would appear in
the bottom product stream as n approaches infinity. Note

that over the interval $\emptyset_B \leqslant b_i$ = switching point of solute i, the top concentration of i as n approaches infinity would be $\langle y_{TP2i} \rangle_\infty / y_{oi} = 1 + \emptyset_B / \emptyset_T$. Beyond the switching point, $\langle y_{TP2i} \rangle_\infty / y_{oi}$ can be expressed according to the equations by Chen and Hill (1971).

Figures (4) and (5) show the net direction of concentration fronts moving through the adsorption column as n increases. In Figure (4), the operation for both toluene and aniline is in Region 1, and in Figure (5) the operations are in Regions 1 and 2, respectively, for aniline and toluene. If the net direction of solute i is upward, $L_{1i}/L_{2i} \geqslant 1$, and complete removal of solute i from the bottom product may be obtained. If the net direction is downward, $L_{1i}/L_{2i} < 1$, and solute i removal from the bottom product will be incomplete. This net downward direction will occur if the bottom product flow becomes too large. However, it must be noted that even though the net direction is upward, a modest separation will occur if the reservoir displacement volume is excessive, if $L_{2i} > h$ (Region 3).

The method presented here is a means of predicting multicomponent separations by assuming that solutes do not interact with one another. In Chapter 4, the effect of higher concentrations and the competition for adsorption sites will be examined.

Toluene- Aniline- n-Heptane

with $\emptyset_B$= 0.09, h= 0.9meter

n	1	2	3	4	5	6	7	8	9
$\dfrac{\langle y_{TP2}\rangle_n}{y_0}$	1.00	1.19	1.31	1.37	1.41	1.43	1.44	1.45	1.4

$\dfrac{\langle y_{BP2}\rangle_n}{y_0}$	0.74	0.57	0.44	0.34	0.26	0.20	0.15	0.12	0.1
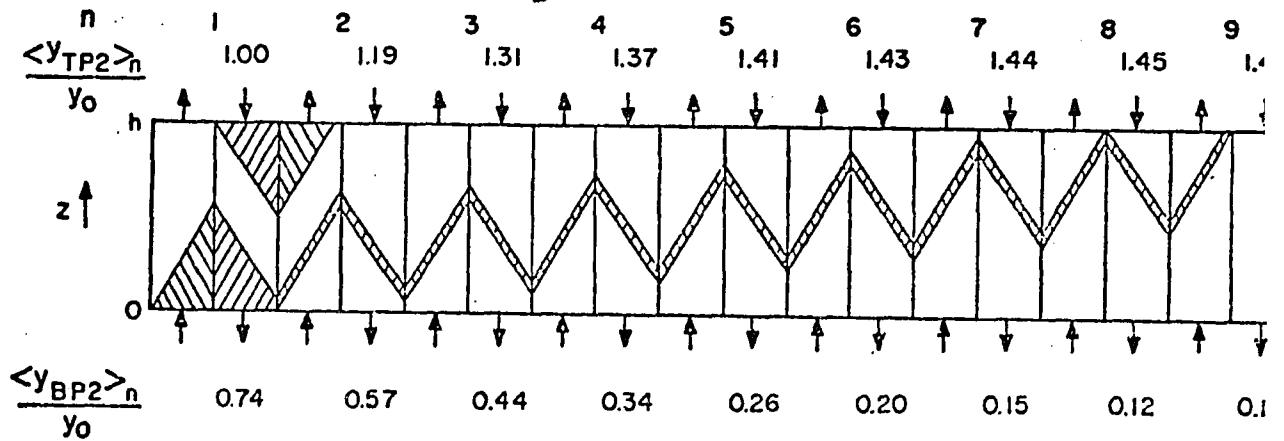
Toluene: b= 0.15, L_1= 0.49 meter

L_2= 0.44 meter

$\dfrac{\langle y_{TP2}\rangle_n}{y_0}$	1.00	1.35	1.53	1.55	1.51	1.46	1.41	1.37	1.35

$\dfrac{\langle y_{BP2}\rangle_n}{y_0}$	0.53	0.31	0.18	0.10	0.06	0.03	0.02	0.01	0.00
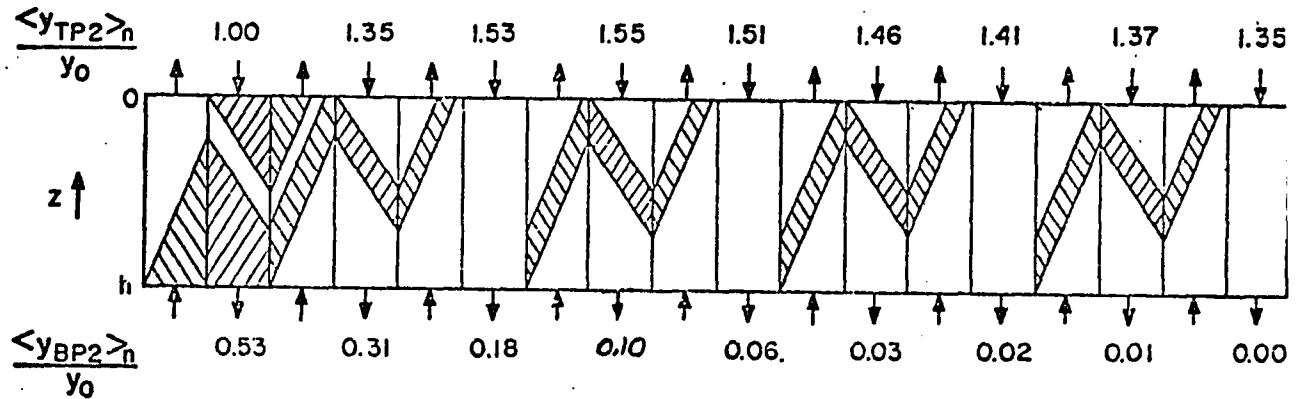
Aniline: b= 0.31, L_1= 0.71 meter

L_2= 0.45 meter

FIGURE (4)

Multicomponent Wave Fronts in Region 1 Operation

Toluene- Aniline- n-Heptane

with $\emptyset_B = 0.22$, h= 0.9 meter

n	1	2	3	4	5	6	7	8
$\dfrac{<y_{TP2}>_n}{y_o}$	1.00	1.20	1.34	1.43	1.48	1.52	1.54	1.56

$z \uparrow$

| $\dfrac{<y_{BP2}>_n}{y_o}$ | 0.74 | 0.59 | 0.49 | 0.42 | 0.38 | 0.34 | 0.32 | 0.34 |
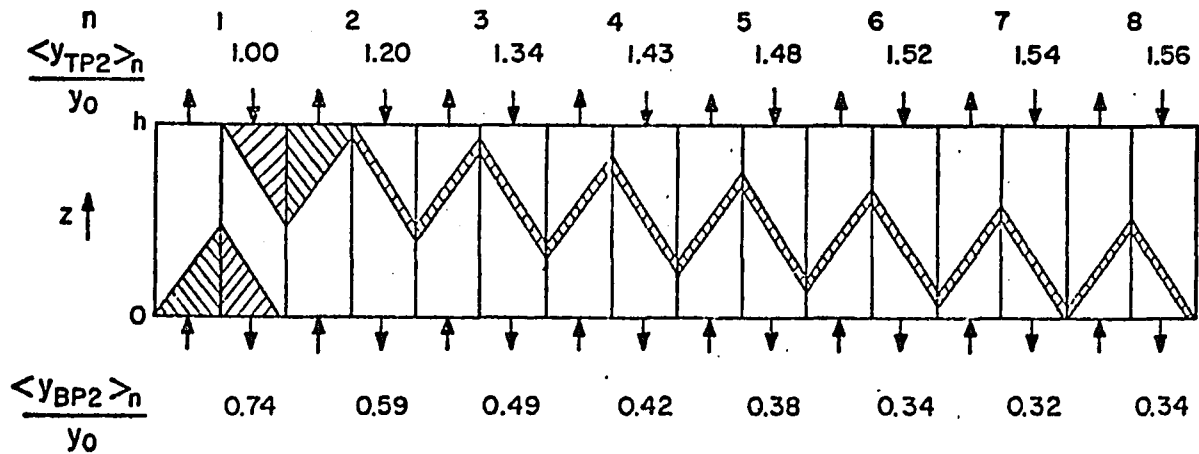
Toluene: b= 0.15, L_1= 0.42 meter

L_2= 0.49 meter

$\dfrac{<y_{TP2}>_n}{y_o}$	1.00	1.44	1.76	1.99	2.14	2.22	2.25	2.26

$z \uparrow$

$\dfrac{<y_{BP2}>_n}{y_o}$	0.53	0.31	0.18	0.10	0.06	0.03	0.02	0.01
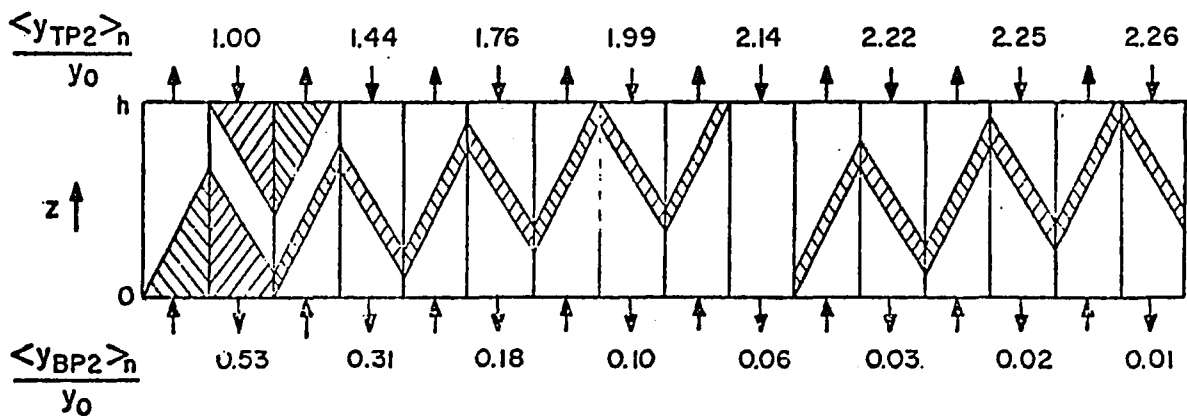
Aniline: b= 0.31, L_1= 0.62 meter

L_2= 0.51 meter

FIGURE (5)

Multicomponent Wave Fronts For Operation in

Regions 1 and 2

CHAPTER 4

EFFECT OF CONCENTRATION ON MULTICOMPONENT SEPARATION

Chapter 3 covered multicomponent separations for dilute solutions. The mathematical model for the dilute solution theory was made up of analytical solutions to the basic mass balance, equilibrium, and rate equations. In the case of more concentrated solutions, analytical solutions have not been possible because the necessary simplifying assumptions (Chapter 3) are not valid and it is necessary to resort to techniques such as the method of characteristics to reduce the partial differential equations to solvable ordinary differential equations. But this method is far too tedious for hand calculations and a computer program is necessary. A suitable computer program developed recently (Kim, 1976) is used in this chapter to provide the required mathematical comparison for the experimental work described in this chapter.

This chapter is divided into three sections: the mathematical model, the experimental work, and the results and discussion section. In this way, the chapter covers the basic mathematical logic behind the behavior of concentrated multicomponent systems when exposed to parametric pumping separation. Also

covered in detail are the experimental and analytical procedures needed for verification. Finally, these are combined in the results where the experimental top and bottom product concentrations vs. time are compared with the mathematical predictions.

The results show that the transient and steady state product concentrations vary with feed concentration, bottom product product rate, and cycle time. The concentration of solute(s) in the bottom product stream is significantly reduced by decreasing the bottom product rate and increasing the cycle time. The computer program predicted the results with reasonable accuracy and could do so with systems other than the toluene-acetophenone-n-heptane system described. The results also show that the separation capability decreases sharply as total solute concentrations approach 40 vol. percent and the column tends to become saturated first with the least strongly adsorbed solute and then with the more strongly adsorbed solutes.

Mathematical Development

The basis for the mathematical development here is the same as for the dilute solution theory of Chapter 3: the material balance equation, the interphase rate equation, and the equilibrium expression.

$$\varepsilon \frac{\partial y_i}{\partial t} + \varepsilon v \frac{\partial y_i}{\partial z} + (1-\varepsilon) \rho_s \frac{\partial x_i}{\partial t} - \varepsilon \mathcal{D} \frac{\partial^2 y_i}{\partial z^2} = 0 \qquad (1)$$

$$\frac{\partial x_i}{\partial t} = \lambda_i (y_i - y_i^*) \qquad (2)$$

$$y_i^* = y_i^* (T, y_j^*, x_j^*) \text{ where } j = 1, 2, \ldots, n \text{ including } i \qquad (3)$$

If there is no axial dispersion, $\mathcal{D} = 0$; and if z/v is set equal to $\hat{z}$, then Equation (1) becomes

$$\frac{\partial y_i}{\partial t} + \frac{\partial y_i}{\partial \hat{z}} = - \frac{(1-\varepsilon) \rho_s}{\varepsilon} \frac{\partial x_i}{\partial t} \qquad (37)$$

In Equation (37), y_i is a function of $\hat{z}$ and t, and the total differential of y_i is therefore

$$\frac{dy_i}{d\hat{z}} = \frac{\partial y_i}{\partial \hat{z}} + \frac{\partial y_i}{\partial t} \frac{dt}{d\hat{z}} \qquad (38)$$

According to the method of characteristics (Acrivos, 1956), the choice of paths in the $\hat{z}$ - t plane is optional. The two paths in the present case are along the diagonal

$$\frac{dt}{d\hat{z}} = 1 \qquad (39)$$

and along the horizontal $\hat{z}$ = constant or

$$\frac{d\hat{z}}{dt} = 0 \qquad (40)$$

If Equation (39) is substituted into Equation (38), the left hand sides of Equations (37) and (38) are equal. Furthermore, if Equation (2) is substituted into the right hand side of Equation (37), then Equation (37) becomes the ordinary differential equation (ODE) along the characteristic path defined by Equation (39) or

$$\frac{dy_i}{d\hat{z}} = - \frac{(1-\varepsilon)\rho_s}{\varepsilon} \lambda_i(y_i - y_i^*) \qquad (41)$$

A second ODE along the other characteristic path defined by Equation (40) is derived in the following manner. In Equation (37), if y_i is a function of $\hat{z}$ and t, then x_i is also a function of these variables and the total differential of x_i with respect to t is

$$\frac{dx_i}{dt} = \frac{\partial x_i}{\partial \hat{z}} \frac{d\hat{z}}{dt} + \frac{\partial x_i}{\partial t} \qquad (42)$$

Since the path to be followed is defined by Equation (40), $\partial x_i/\partial t$ becomes equal to dx_i/dt and Equation (2) becomes

$$\frac{dx_i}{dt} = \lambda_i (y_i - y_i^*) \tag{43}$$

which is the other ODE required, this time along the path in the $\hat{z}$ - t plane defined by Equation (40).

According to the method of characteristics, Equations (41) and (43) will be used to calculate fluid and adsorbent phase concentrations in the $\hat{z}$ - t plane along the characteristic paths defined by Equations (39) and (40) respectively. The starting points for these calculations are the initial conditions and the boundary conditions at the top and bottom of the adsorption column.

The initial conditions are, at t = 0 and $\hat{z} \geq 0$,

$$y_i = y_{oi}(\hat{z}) \tag{44}$$

and

$$x_i = x_i(\hat{z}) \tag{45}$$

The boundary conditions at the bottom of the column for hot upflow are, at $\hat{z} = 0$ and $t \geq 0$,

$$y_i = \langle y_{B1i} \rangle \tag{46}$$

for the fluid phase concentration and

$$\frac{dx_i}{dt}\bigg|_{\hat{z} = 0} = \lambda_i (\langle y_{B1i} \rangle - y_i^*)$$ (47)

for the solid phase concentration.

For cold downflow at the top of the column, the boundary conditions are, at $\hat{z} = h/v_2$ and $t = 0$,

$$y_i = \langle y_{T2i} \rangle$$ (48)

for the fluid phase concentration and

$$\frac{dx_i}{dt}\bigg|_{\hat{z} = h/v_2} = \lambda_i (\langle y_{T2i} \rangle - y_i^*)$$ (49)

for the solid phase concentration

The next step is to calculate the concentration profiles in the $\hat{z}$ - t plane (along the packed column with time) along the characteristic paths (Equations 39 and 40). For this purpose, the plane will be divided into equal increments, Δt and Δz, along the horizontal and vertical axes respectively as shown in Figure (37). Let

$$\Delta z/v = \Delta \hat{z} = \Delta t = \delta$$ (50)

Now the concentrations will be calculated from

point to point along the characteristic lines and the
finite difference equations needed for this are obtained
by integrating Equations (41) and (43) between the
limits of $\hat{z}$ and $\hat{z}_o$ and t and t_o to give

$$y_i \langle \hat{z} \rangle = y_i \langle \hat{z}_o \rangle - \frac{(1-\varepsilon)\rho_s}{\varepsilon} \lambda_i \int_{\hat{z}_o}^{\hat{z}} (y_i - y_i^*) \, d\hat{z} \qquad (51)$$

and

$$x_i \langle t \rangle = x_i \langle t_o \rangle + \lambda_i \int_{t_o}^{t} (y_i - y_i^*) \, dt \qquad (52)$$

Now, as previously mentioned and as shown in
Figure (6), the calculations for y_i will be made step
by step along the diagonals $\hat{z} = t$ (Equation 39) and the
calculations for x_i will be made along the horizontal
lines, $\hat{z}$ = constant (Equation 40). The position at the
junction of the characteristic lines is designated by
(i,j). Thus calculations for y_i at (i + 1, j + 1) will
be made by adding the increment of y_i [from (i,j) to
(i + 1, j + 1)] to the value of y_i at (i,j). Values
for x_i at (i + 1, j + 1) will be calculated by adding
the increment (from (i + 1, j) to (i + 1, j + 1) to the
value of x_i at (i + 1, j). In this fashion the concen-
tration profiles are calculated along the axis of the
column and time.
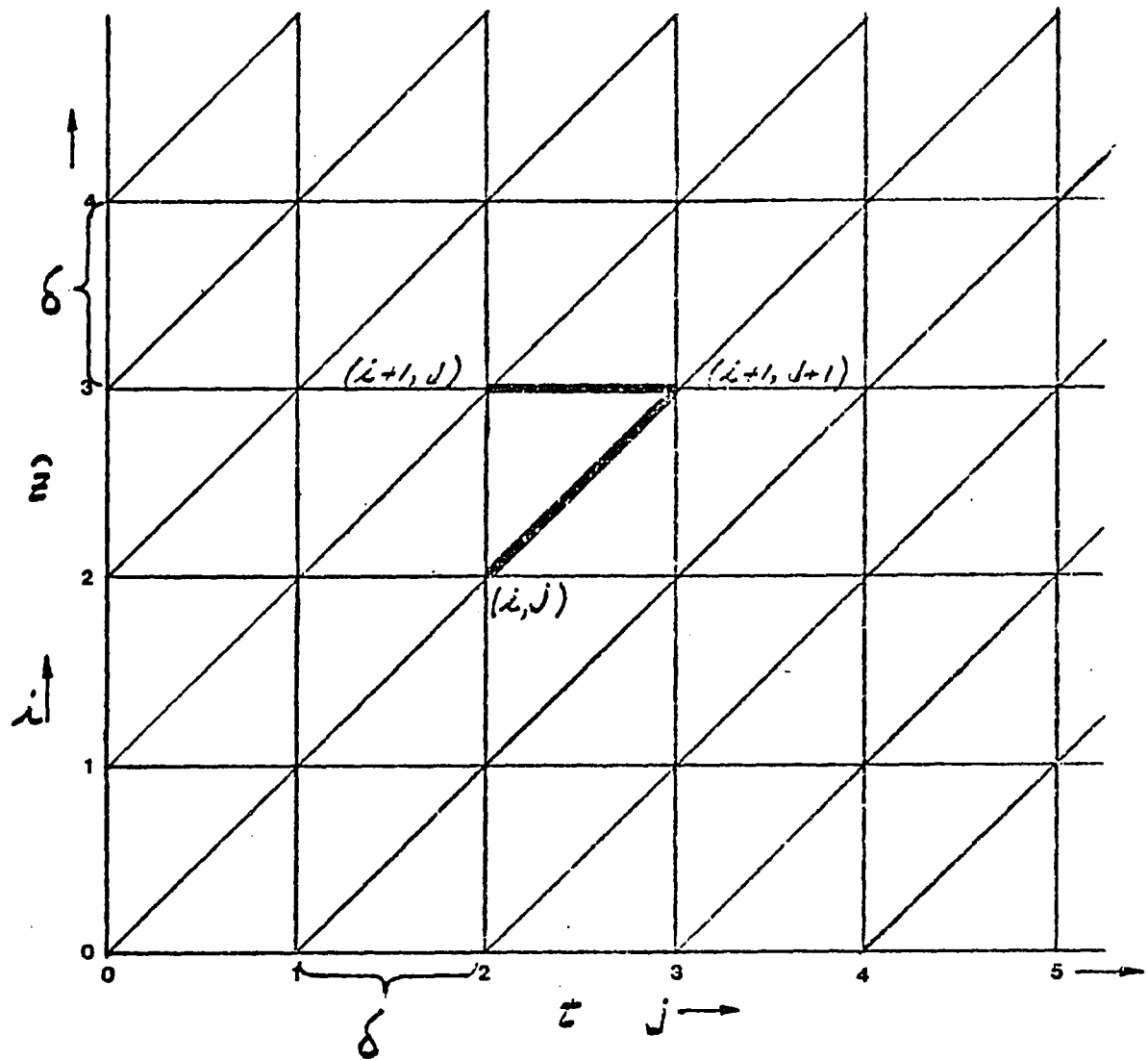
FIGURE (6)

Characteristic Calculation Paths in the ẑ-t Plane

If the intervals ($\delta = \Delta\hat{z} = \Delta t$) in Equation (50) and Figure (6) are small enough, then Equations (51) and (52) become

$$y_i(i+1,j+1) = y_i(i,j) - \frac{(1-\varepsilon)\rho_s}{\varepsilon} \frac{\lambda_i \delta}{2} \left[y_i(i+1, j+1) \right.$$
$$\left. -y_i^*(i+1,j+1) + y_i(i,j) - y_i^*(i,j) \right] \tag{53}$$

$$x_i(i+1,j+1) = x_i(i+1,j) + \frac{\lambda_i \delta}{2} \left[y_i(i+1,j+1) \right.$$
$$\left. -y_i^*(i+1,j+1) + y_i(i+1,j) - y_i^*(i+1,j) \right] \tag{54}$$

At the beginning of the first hot upflow half cycle, the entire column is filled with feed solution and $y_i = y_{oi}$ at $t = 0$ and $\hat{z} = 0$ to h/v. All corresponding values of x_i are equal to zero. Values of y_i and x_i at the end of the half cycle are calculated for various points along the column from Equations (53 and 54). The values of y_i and x_i at the end of the column ($\hat{z} = h/v$) are then combined with external material balance equations (Chen and Hill, 1971) to account for the effect of the feed, product, and reservoir streams at the top of the column.

These external equations (Chen and Hill, 1971) are
rearranged and modified for multicomponent systems. For
the top of the column

$$\left\langle y_{TP1i} \right\rangle_n = \frac{(\emptyset_T + \emptyset_B) y_{oi} + (1-\emptyset_B)\left\langle y_{T1i} \right\rangle_n}{1+\emptyset_T} \qquad (55)$$

$$\left\langle y_{TP2i} \right\rangle_n = \frac{Q\pi/\omega\left\langle y_{TP1i} \right\rangle_n + V_T\left\langle y_{TP1i} \right\rangle_{n-1}}{V_T + Q\pi/\omega} \qquad (56)$$

$$\left\langle y_{T2i} \right\rangle_n = \frac{(\emptyset_T + \emptyset_B) y_{oi} + (1-\emptyset_T)\left\langle y_{TP2i} \right\rangle_n}{1+\emptyset_B} \qquad (57)$$

The value of $\left\langle y_{T1i} \right\rangle$ from Equation (53) is substi-
tuted in Equation (55) to get the value of $\left\langle y_{TP1i} \right\rangle$. This
hot cycle top product concentration is then used in
Equation (56) to obtain the cold cycle top product con-
centration $\left\langle y_{TP2i} \right\rangle$ which is used for plotting the top
product vs. time graph shown in later in the chapter.
It is also used in Equation (57) to obtain the value
$\left\langle y_{T2i} \right\rangle$ which is used in the boundary condition equations
for the top of the column (Equations 48 and 49). These
equations give the values of y_i and x_i at the top of the
column for the cold downflow half cycle. Then, Equations
(53 and 54) are again used, this time to calculate the
concentration profiles in the column during the cold
downflow half cycle. The value of y_i at the bottom of

the column ($\hat{z} = 0$) is $\langle y_{B2i} \rangle$ and is used along with other known values in an external equation around the bottom of the column (Chen and Hill, 1971) rearranged for multi-component systems.

$$\langle y_{B1i} \rangle_n = \frac{Q\pi/\omega \langle y_{B2i} \rangle_{n-1} + V_B \langle y_{B1i} \rangle_{n-1}}{Q\pi/\omega + V_B} \tag{58}$$

Now $\langle y_{B2i} \rangle$ is equal to $\langle y_{BP2i} \rangle$ since both streams come from the same source. For the same reason, $\langle y_{BP1i} \rangle$ equals $\langle y_{B1i} \rangle$.

This value is used with the boundary equations at the bottom of the column (Equations 46 and 47) to give the values of y_i and x_i at the beginning of the next hot upflow half cycle. And Equations (53 and 54) are again used to calculate the concentration profile in the column for the second hot upflow half cycle.

This procedure is repeated for every cycle and the resulting top and bottom product concentrations calculated by the computer program are plotted along with the experimental data in the graphs presented in this chapter. The details of the computer program (including the incorporation of the external equations into the program) are given by Kim (1976).

Calculation of λ_i. Values of λ_i, the mass transfer coefficient, vary with temperature and solute concentration and must be calculated at every point in the column. The equations presented here were developed (Kim, 1976) for the particular system (toluene-acetophenone-n-heptane on silica gel) used for the experimental section of this thesis. The equations were generalized for multicomponent systems and may be used to extend the ternary system to additional solute contents.

$$\lambda_i = (A_p)(J_D)(v)(\varepsilon)(Sc)^{-2/3} \tag{59}$$

where

$$J_D = \alpha(Re)^{-0.78} \text{ for laminar flow} \tag{60}$$

$$Re = \frac{D_p v \rho_f \varepsilon}{\mu_f(1-\varepsilon)} = \text{Reynolds No. for flow in packed beds} \tag{61}$$

$$Sc = \frac{\mu_f}{\rho_f D_f} = \text{Schmidt No.} \tag{62}$$

$$A_p = a_p/\rho_s = \text{interfacial area/unit weight of adsorbent}$$

$$v\varepsilon = \text{superficial column velocity}$$

$$= v_1\varepsilon = (1-\emptyset_B)Qa_t \text{ for hot upflow}$$

$$= v_2\varepsilon = (1+\emptyset_B)Qa_t \text{ for cold downflow} \tag{63}$$

$$\rho_f = \Sigma_{n=1}^{n} \; y_i M_i \tag{64}$$

$$\mu_f = \Sigma_{n=1}^{n} \; y_i \mu_i / \Sigma_{n=1}^{n} \; y_i \tag{65}$$

where y_i (moles i/unit vol. solution) varies at each point in the column and μ_i varies with temperature (T_1, T_2).

α varies with the solute and the solute concentration (Kim, 1976), but usually becomes a single constant for all solutes at low concentrations.

D_f is the solute-solvent diffusivity which varies with the solute and with the temperature (Kim, 1976).

$$D_{fi} = \frac{7.4 \times 10^{-8} (60) (\psi_s M_s)^{0.5} T}{\mu_f V_{Mi}^{0.6}} \tag{66}$$

where

$T \; = T_1$ for hot upflow

$T \; = T_2$ for cold upflow

$\psi_s \; = 1.0$ for n-heptane

$M_s \; = 100.2$ for n-heptane

$V_{Mi} = 119$ for toluene (molecular volume)

$\quad = 161$ for acetophenone

Calculation of y^*. y_i^* is the fluid concentration of solute in equilibrium with the adsorbent. In the present type of system, the equilibrium should be determined from a Langmuir type of isotherm (Wilhelm et al, 1968). The particular form of the Langmuir isotherm was originally proposed by Sweed (1969). In the present nomenclature, this isotherm is:

$$x_i^* = \frac{A_i y_i}{1 + B_i y_i / \rho_i} + D y_i \qquad (67)$$

or (Kim, 1976),

$$y_i^* = \frac{-(A_i + D - B_i x_i / \rho_i) + [(A_i + D - B_i x_i / \rho_i)^2 + 4 B_i D x_i / \rho_i]^{1/2}}{2 B_i D} \qquad (68)$$

where A_i and B_i are constants

	toluene		acetophenone	
	343°K	298°K	343°K	298°K
A_i	1.46	8.65	0.10	40.0
B_i	18.47	66.97	50.00	10.0

and

$$D = 0.29 \text{ cm}^3 \text{ pores/gm dry silica gel}$$

Experimental

The experimental apparatus is shown in Figure (7).
The equipment consists of a jacketed glass column 1.0 cm
in diameter and 90 cm long packed with 30-60 mesh chroma-
tographic grade silica gel. The reservoirs for the top
and bottom of the column were two 50 cc glass syringes
operated by a dual infusion-withdrawal pump manufactured
by the Harvard Apparatus Co. A micro-switch was wired
into the pump circuit to automatically reverse the
syringes at the end of each cycle.

The jacket was heated and cooled on alternate half
cycles by water pumped from constant temperature hot
and refrigerated baths kept at 343 and 298°K respectively.
The baths were connected to the column and to recycle by
solenoid valves wired to a timer so that hot water was
always supplied to the jacket during the upflow half
cycle and cold water during the downflow half cycle.

Feed solution was fed to the top of the column
from a 50 cc syringe mounted in a second Harvard
Apparatus Co. pump. Pump operation was interrupted
to refill the syringe approximately every third cycle.
The top and bottom product streams were regulated with
micrometer capillary valves which also served to impose
a slight back pressure on the column to exclude air
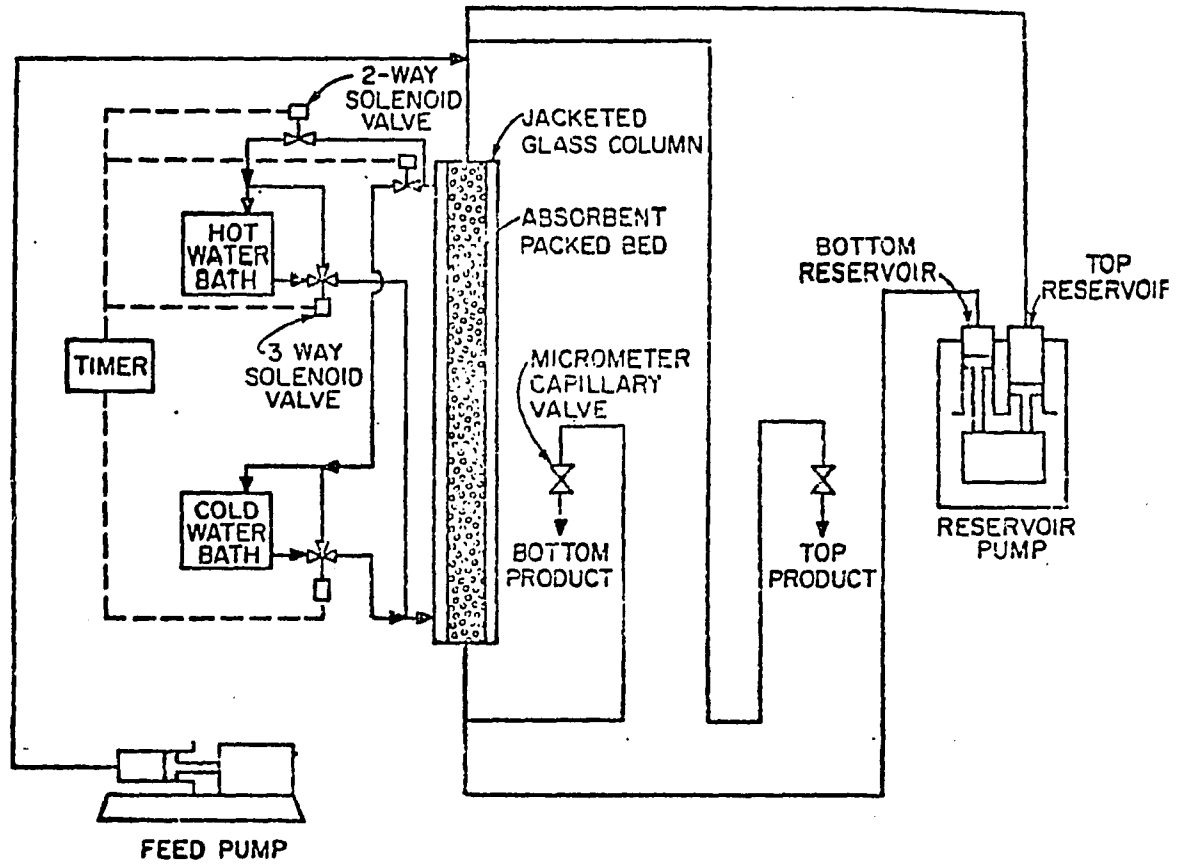
FIGURE (7)

Laboratory Parametric Pump

which could enter the system due to a small amount of thermal expansion and contraction of the process fluid.

In preparation for each run, the column was carefully packed with silica gel and feed solution so as to eliminate all air from the column. The reservoir and feed pumps and all connecting lines were filled with feed solution at ambient temperature. The reservoir syringes were set for the specified delivery with a dead volume of approximately 3 cc.

The run was started by switching on the syringe pumps and activating the timer. The bottom reservoir pumped fluid into the bottom of the column and, at the same time, the hot water bath pump supplied hot water to the column jacket. At the end of the hot half cycle, the microswitch reversed the action of the reservoir pump and the solenoid valves put the hot water bath system on recycle and supplied cold water to the jacket of the column. The top and bottom flow rates were adjusted to allow for thermal expansion so that the average rates for the complete cycle were correct.

The top and bottom products were collected for both hot and cold half cycles. The cold downflow product samples were analyzed by vapor phase chromatography.

A Hewlett Packard Model 5710A Chromatograph coupled with an electronic area integrator was used. For very low peaks, beyond the lower detection limit of the integrator, the areas were measured manually at one half the peak height. The helium rate was set at 86 cc/minute with a soap bubble flow meter. The temperatures of the injection port, the conductivity detector, and the oven were maintained automatically at constant values of 250, 250, and 205 degrees C respectively. The detector current was set at a constant 160 milliamps and the chart speed at 0.2 inches per minute. Dual columns were used made of 0.25 inch o.d. copper tubing 6 feet long and packed with "Pennwalt 223 on 4% KOH" from Applied Science Laboratories, Inc. Under these conditions, the approximate peak times for n-heptane, toluene, and acetophenone were 1.1, 2.2, and 10.1 minutes respectively. A few peaks from most of the runs were checked with an F & M Model 810-29 Chromatograph with the same columns and approximately the same running conditions. Sample injections were all 5 microliters from a 10 microliter Hamilton syringe.

In the chromatograph calibration runs for this
system, the area percent of the component peaks was only
approximately equal to the weight percent of the corre-
sponding component in solution. A better correlation is
shown in Figure (8) which gives the area of the component
peaks versus the actual volume (microliters) of the
component injected into the chromatograph, either as a
solution or as the pure material. This linear relation-
ship of chart peak area to injection volume is fundamental
to vapor phase chromatography and Figure (8) demonstrates
its applicability to the present system.

With this calibration, the ratios of the areas of
the component peaks in any given product sample to the
areas of the corresponding peaks in the feed sample give
the desired product/feed concentration ratios directly.

$$\langle y_{BPi} \rangle_n / y_{oi} = \frac{\text{area of the component peak in the product}}{\text{area of the component peak in the feed}}$$

Of course the same relationship applies to top
product sample components. These concentration ratios
apply equally well to volume, weight, or mole ratios
because any conversion factors from volume to other
units automatically cancel themselves out. To eliminate
errors from variations due to the equipment or analytical
techniques, feed and product samples are run the same day.
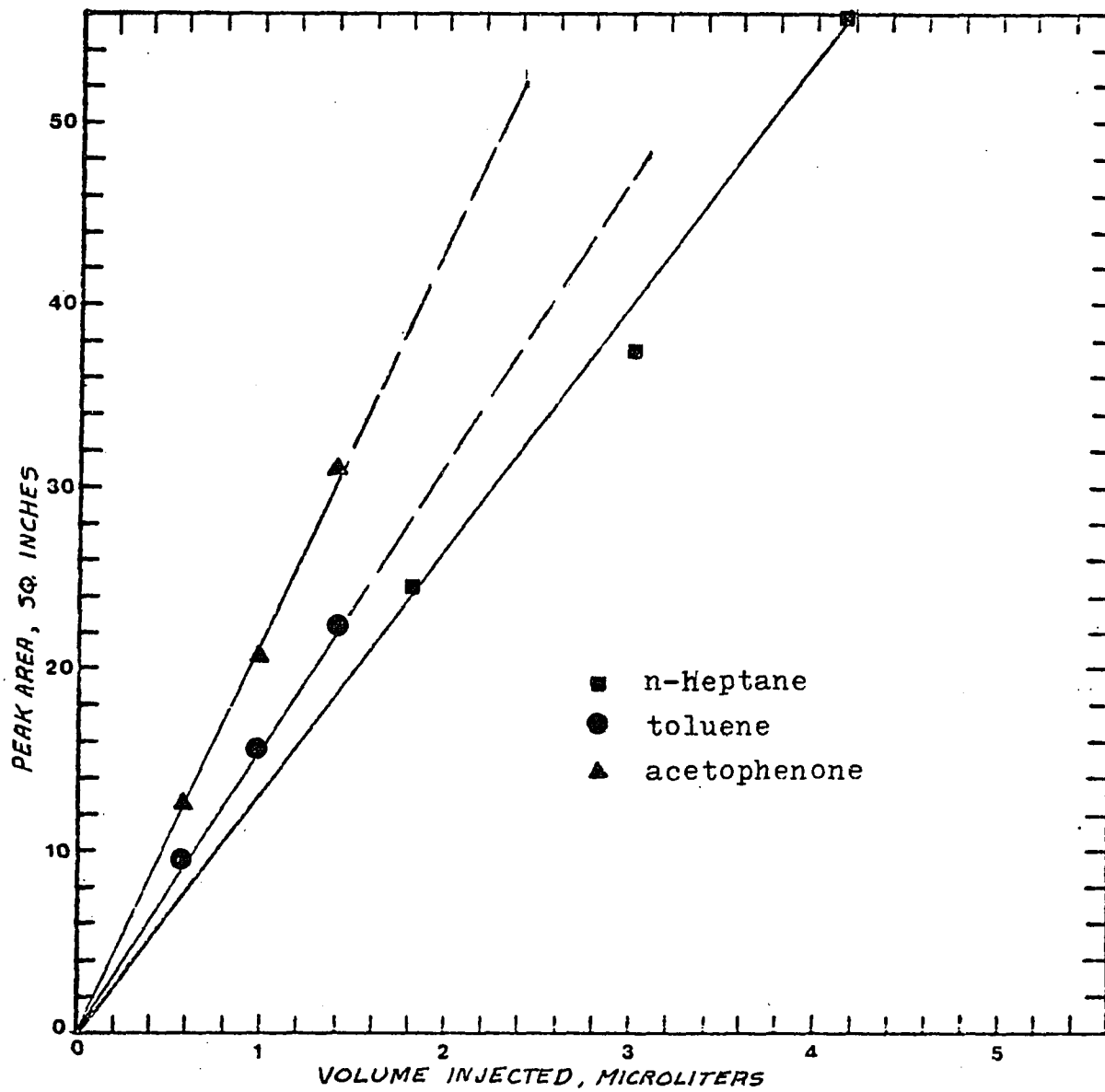
FIGURE (8)

Calibration: Solute Volume vs Peak Area

The chromatographic peak analysis, as previously mentioned, was by area integration. The large peaks as shown in Figure (9) were automatically integrated by the attached electronic integrator. For very small peaks (very low solute concentrations), it was necessary to calculate the area by hand as indicated in Figure (10). The results are presented as area or concentration ratios in the experimental data tables in Appendix I.

FIGURE (9)

CHROMATOGRAPHIC PEAK ANALYSIS (EXAMPLE)

Hewlett Packard Model 5710A, "Pennwalt 223+ 4% KOH" Packing,
He = 86 cc/min, T.C. Detector, 160 ma current, Oven 205 C.
I.P. 250 C., Detector 250 C., Col- ¼"o.d.x 6' copper.
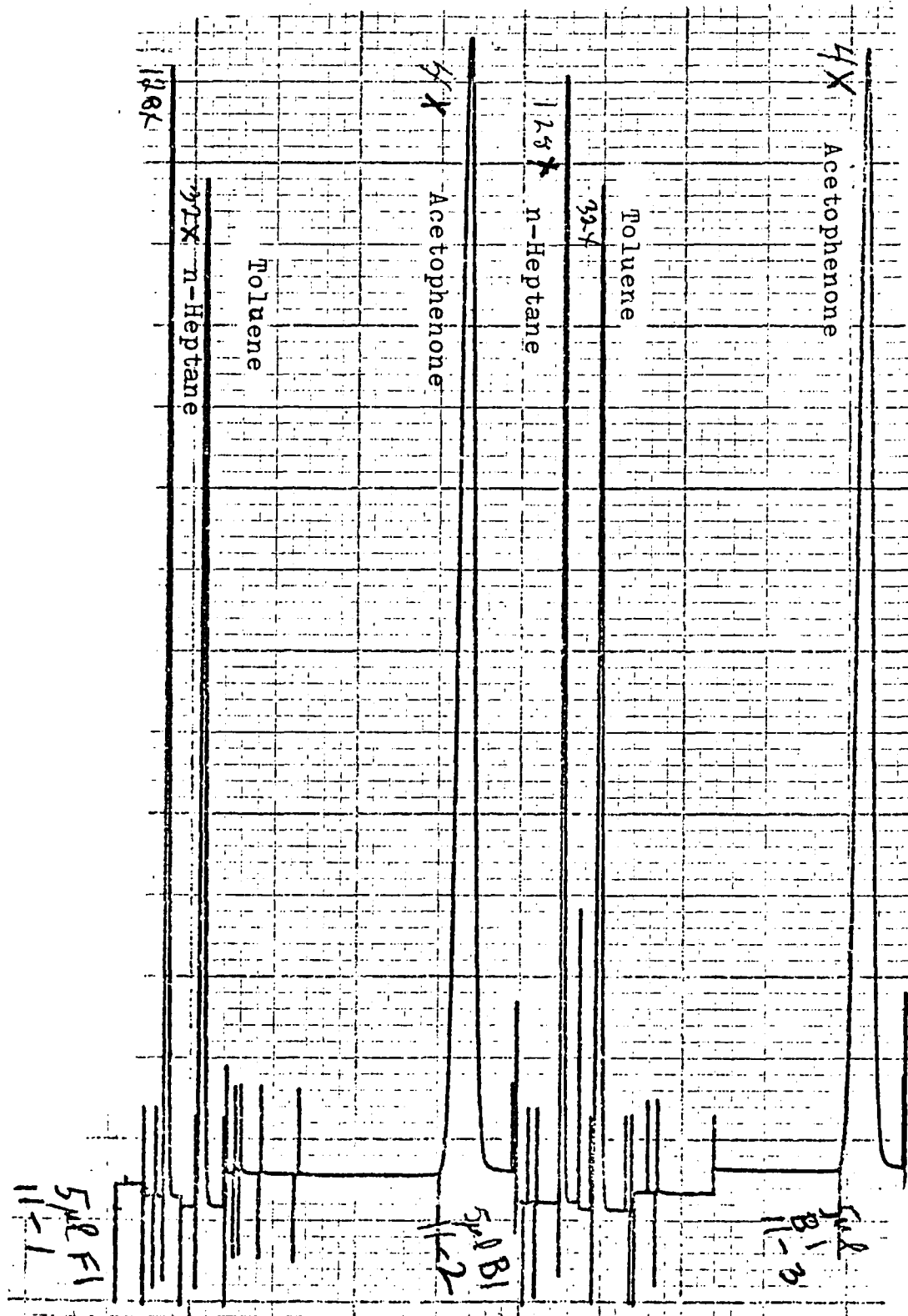
FIGURE (10)

CHROMATOGRAPHIC PEAK ANALYSIS (EXAMPLE)

(Small Solute Peaks)

Hewlett Packard Model 5710A
"Pennwalt 223+4% KOH" Packing
He = 86 cc/min
T.C. Detector
Current= 160 ma
Oven = 205 C.
Injection Port= 250 C.
Detector = 250 C.
Col.- ¼"o.d.x 6' copper
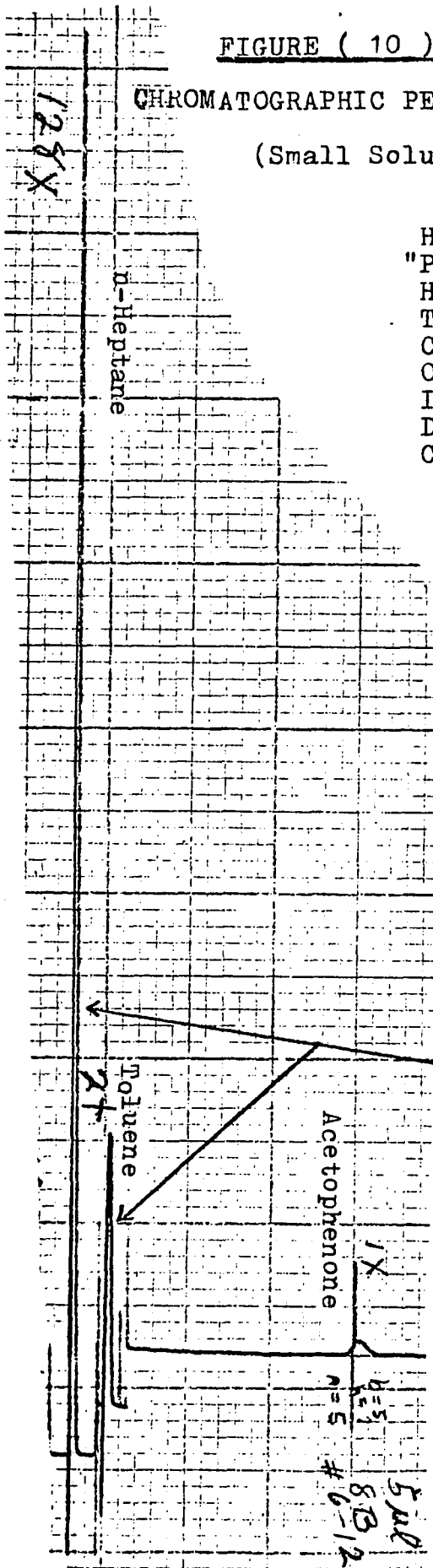
peak areas by electronic
integrator

manual peak area calculation

Results and Discussion

Ten runs corresponding to various solute concentrations, cycle times, and bottom product rates were carried out. The experimental parameters are shown in Table (2). The complete experimental data are shown in tabular form in Appendix I. The data are plotted as product/feed solute concentration ratios vs. time (cycle number) in Figures (11) to (20) inclusive. In all cases, the hot upflow temperature was 343°K (70°C), the cold downflow temperature was 298°K (25°C), the ratio of the feed to reservoir volume was 0.4, and the top and bottom reservoir dead volumes were 5 cm.^{3} Also, the column height and diameter were 90 cm. and 1.0 cm. for all runs.

Dilute solution runs. The runs with 2.5 volume percent toluene and acetophenone in n-heptane are shown in Figures (11,12,13). As pointed out in Chapter 3, the dilute solution theory applies to these low solute concentrations, and the dimensionless equilibrium parameter has special significance in predicting column performance. This parameter, b, depends only on the particular binary system and the two operating temperatures, T_1 and T_2. The value for toluene-n-heptane was 0.22 for 277° and 343°K (Chen et al, 1972, 1973) and 0.15 for 298° and 333°K (Chen et al, 1974). For the present temperatures, 298° and 343°K, the value of b

TABLE 2

EXPERIMENTAL PARAMETERS - CONCENTRATION EFFECT

Hot upflow half cycle temperature, $^\circ K$	343
Cold downflow half cycle temperature, $^\circ K$	298
Feed volume/reservoir ratio, $\emptyset_T + \emptyset_B$, dimensionless	0.400
Column height, h, cm.	90
Column diameter, d_1, cm.	1.0
Top reservoir dead volume, V_T, cm.^{3}	5.0
Bottom reservoir dead volume, V_B, cm.^{3}	5.0

Specific Run Data

Run No.	Fig. No.	Feed Composition, vol. %		$Q\pi/\omega$ cm.^{3}	$\emptyset_B$		Cycle time π/ω, min.	
		Toluene	Aceto-phenone		Exp.	Calc.	Exp.	Calc.
1	-	2.5	0	20	0.15	0.15	20	20
2	-	0	2.5	35	0.10	0.10	20	20
3	11	2.5	0	35	0.035	0.035	20	20
4	12	0	2.5	35	0.035	0.035	20	20
5	15	10.0	10.0	25	0.25	0.25	20	20
6	13	·2.5	2.5	25	0.25	0.30	20	20
7	16	10.0	10.0	25	0.035	0.085	20	20
8	17	10.0	10.0	25	0.035	0.035	10	15
9	18	10.0	10.0	25	0.035	0.035	5	10
10	20	20.0	20.0	25	0.035	0.035	10	10
11	19	20.0	10.0	25	0.035	0.035	10	10
12	14	0	10.0	35	0.035	0.035	20	20
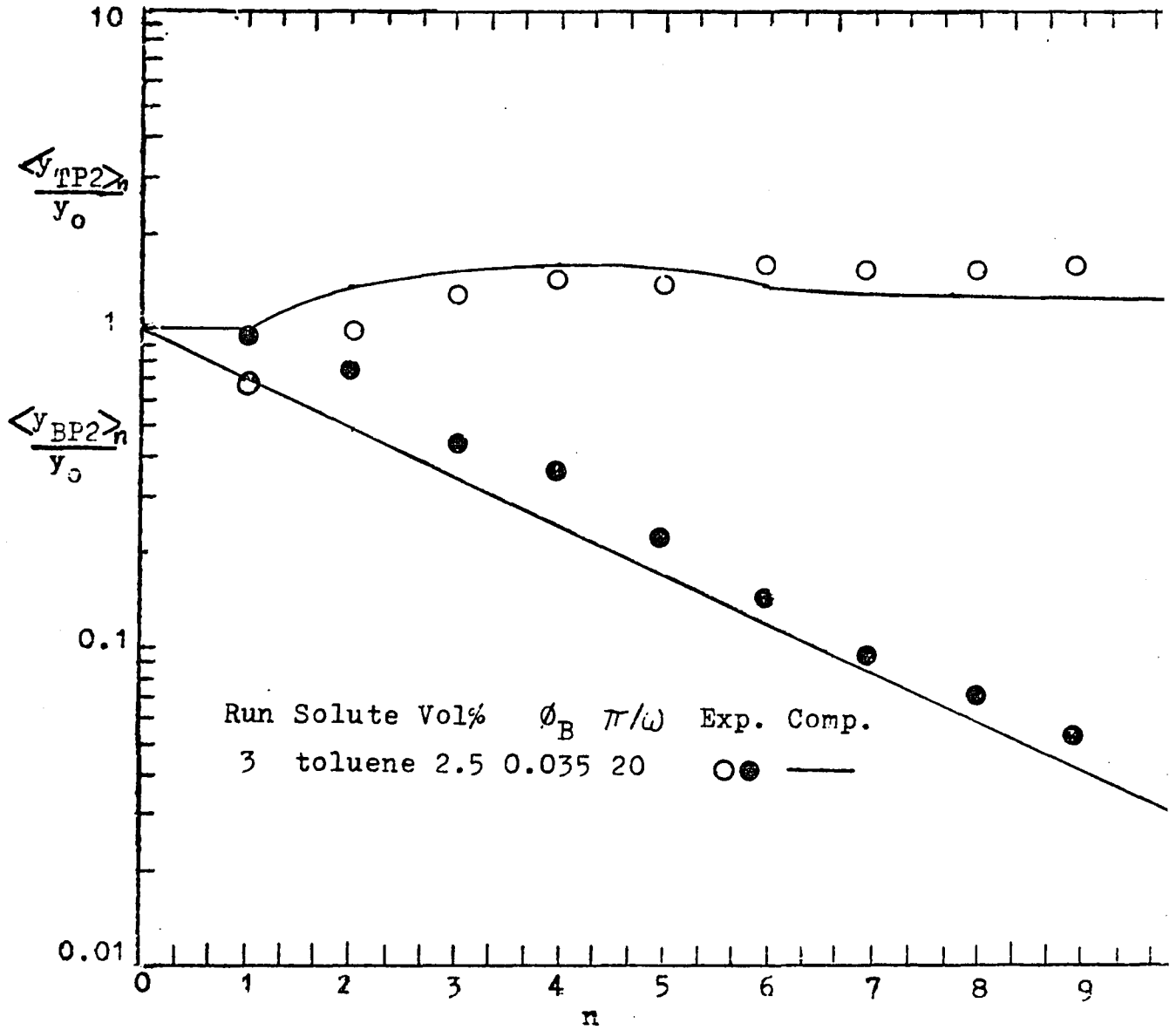
FIGURE (11)

Dilute Binary System: 2.5% Toluene in n-Heptane
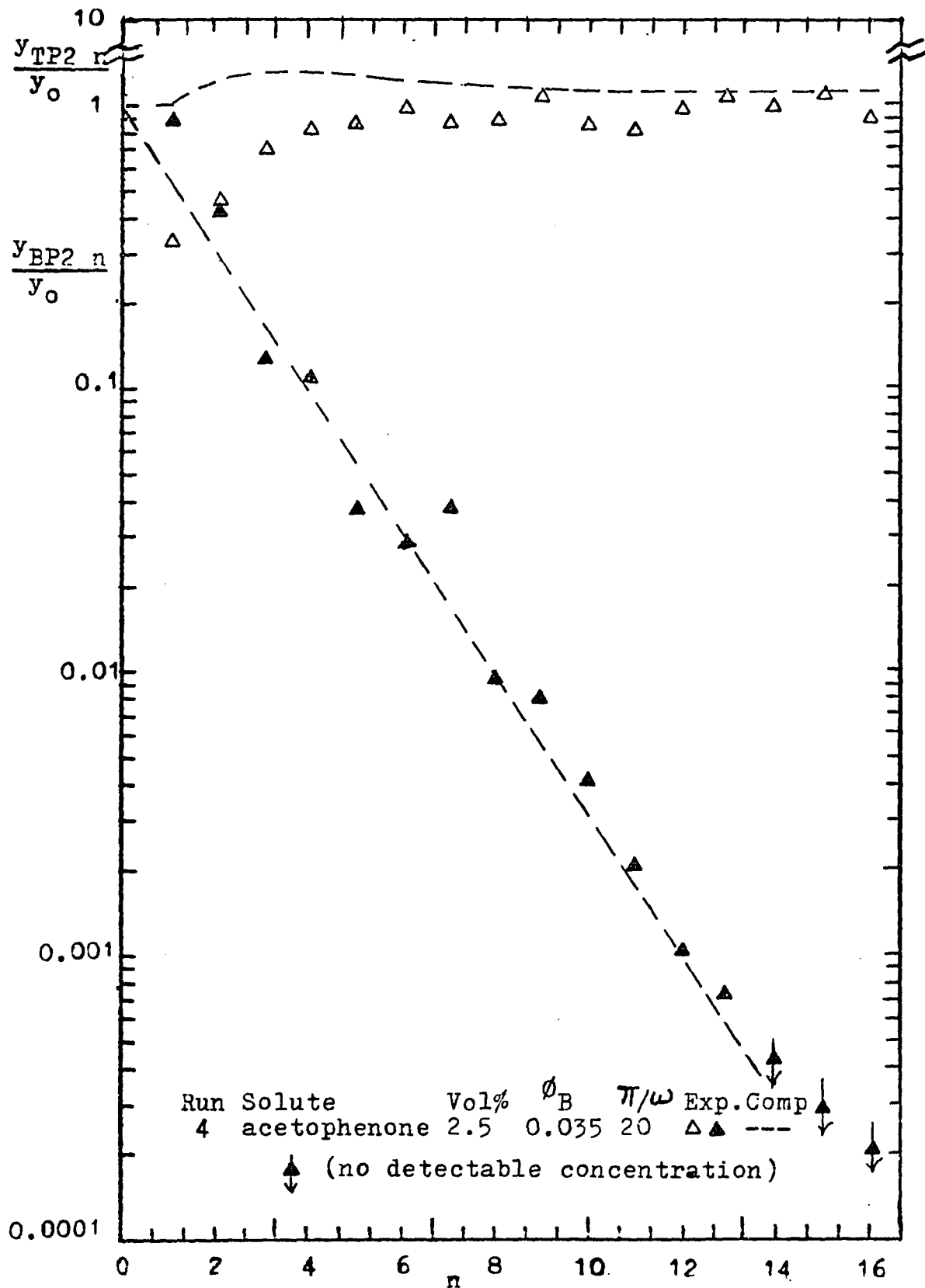
FIGURE (12)

Dilute Binary System: 2.5% Acetophenone in n-Heptane
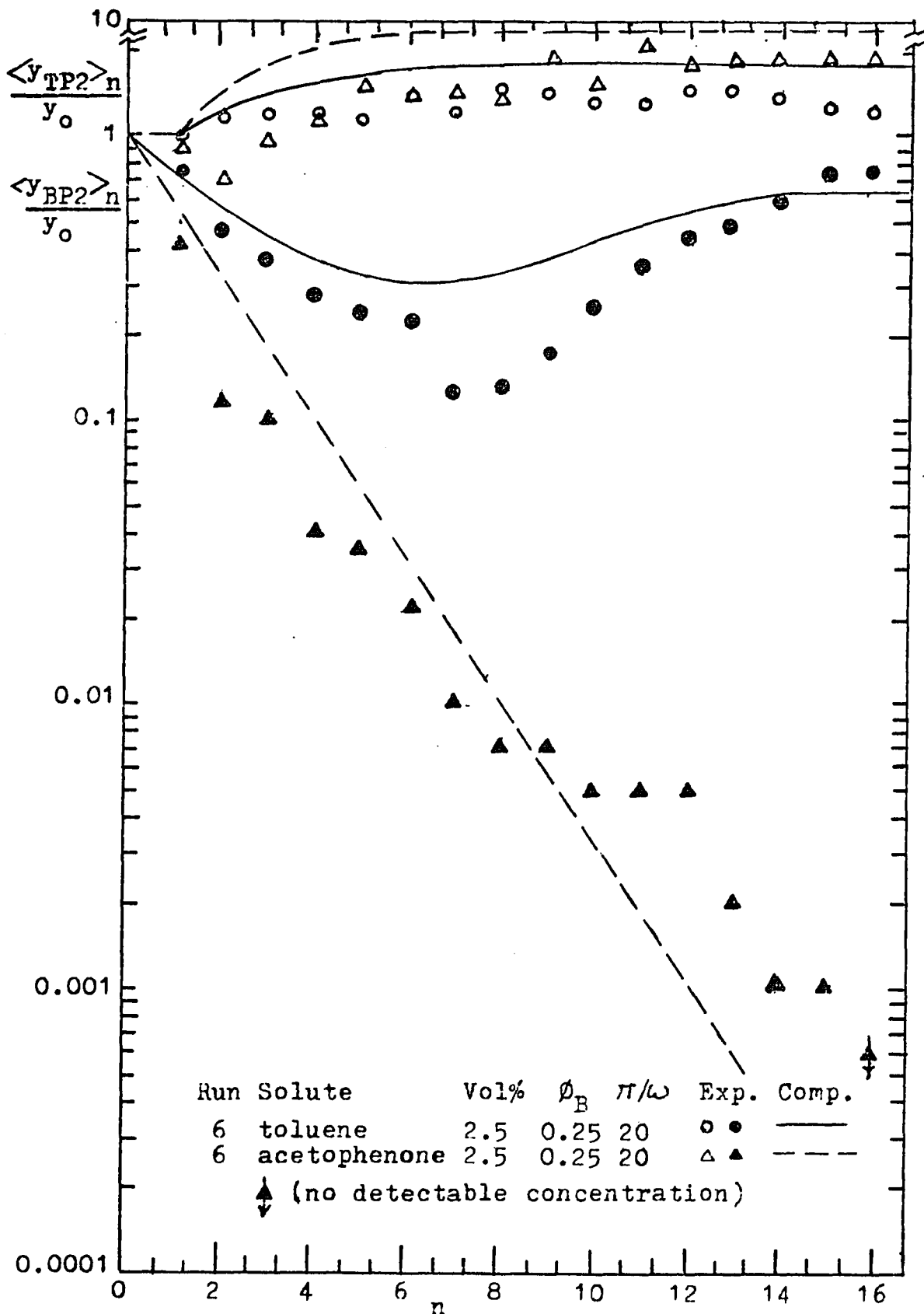
FIGURE (13)

Dilute Ternary System: 2.5% Toluene and Acetophenone in n-Heptane

for toluene-n-heptane was estimated at 0.20 from the bottom product curve in Figure (11) by the method of Chen et al (1972). The value of b for acetophenone was estimated at 0.33 by the same method from the bottom product curves for both the binary system (Figure 12) and the acetophenone toluene-n-heptane ternary (Figure 13). This is further proof (over that given in Chapter 3 for the toluene-aniline-n-heptane system) that the value of the parameter b is independent of the system for dilute multicomponent solutions. With these values of b (0.20 for toluene and 0.33 for acetophenone), the bottom product/reservoir ratio ($\emptyset_B$) was set at 0.25 for run no. 6, and acetophenone was separated from toluene in the bottom product stream (Figure 13). This result is easily predictable from the dilute solution theory of Chapter 3.

Figure (14) shows the product concentration profile for 10% acetophenone in n-heptane. This is comparable to the 10% toluene in n-heptane binary (Chen et al, 1972) in that it may be considered dilute since the 10% refers to total concentration. Actually, the bottom product profile was fitted better by the mathematical model for concentrated solutions and this model was used to compute the profile shown in Figure (14).
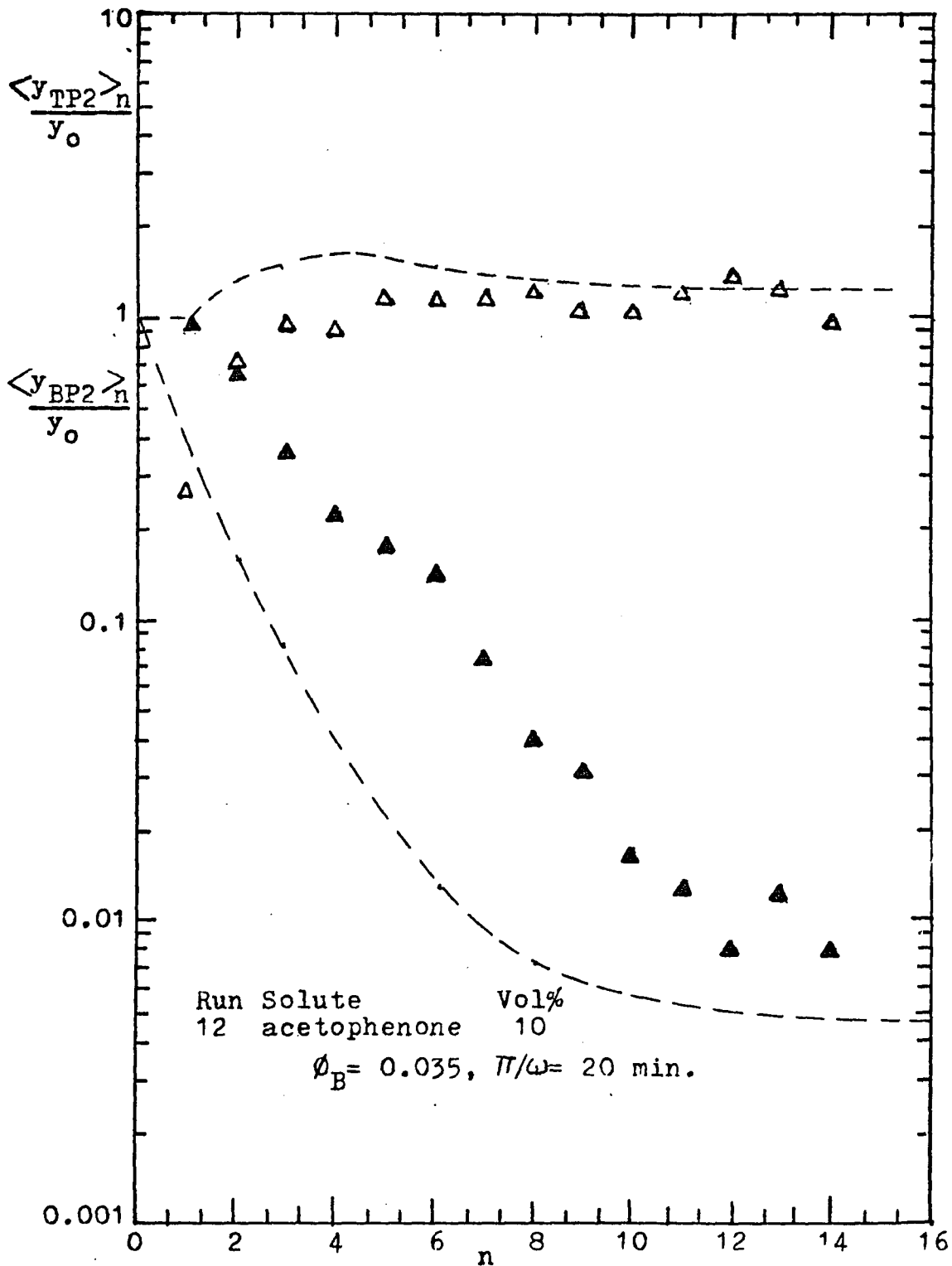
FIGURE (14)

10% Binary System: Acetophenone in n-Heptane

<u>Concentrated solution runs</u>. When the feed concentration was increased to 10 vol. percent for acetophenone and toluene, and the value of $\emptyset_B$ was held at 0.25, there was only a modest separation of acetophenone from toluene in the bottom product stream as shown in Run No. 5 (Figure 15). The initial downward slope of the acetophenone bottom product stream extends to the eighth cycle and is followed by a sharp turn upwards to the twelfth cycle and a levelling off after cycle no. 12. This dip in the bottom product curve is quite sensitive to the value of $\emptyset_B$ input to the computer program, the bulge tending to disappear at values of $\emptyset_B$ less than 0.20. Experimentally, this is shown in Run no. 7 (Figure 16) in which the dip disappears completely at a $\emptyset_B$ of 0.035. One physical interpretation of this phenomenon is that the acetophenone is rapidly adsorbed from the solution initially saturating the entire column and the dilute n-heptane solution is displaced down the column by the main stream until the normal acetophenone concentration wave front breaks through the bottom of the column at cycle 8. The bottom column effluent is then rapidly saturated with acetophenone until the acetophenone wavefront is no longer diluted by the residual n-heptane and assumes its steady state value as shown in Figure (15). Of course, the larger the value of $\emptyset_B$, the

sharper the bulge of the bottom product concentration curve.
The same phenomenon is shown with toluene in the same run
(No. 5), but the bulge is smaller because toluene is less
strongly adsorbed.

The transient effect described above is interesting
but less important than the steady state separation effect
which is small (y_{BP2}/y_o = 0.8) for the concentrated solu-
tion run and large (y_{BP2}/y_o = 0) for the dilute solution run.

The computed curves tend to level out above the experi-
mental points, indicating that the experimental separation
is better than that predicted by the computer program. This
usually occurs when the bottom product concentration is low
(y_{BP2}/y_o) is 0.01 or less. The analytical results at this
point tend to be inaccurate because the acetophenone peaks
on the chromatographic charts are very small, cannot be de-
tected by the electronic integrator and, if they show up at
all, must be integrated by hand. The analytical results at
this level are generally very uncertain and the data tend to
scatter. Therefore, the levelling out trend indicated by
the computer is not necessarily contradicted by the experi-
mental data.
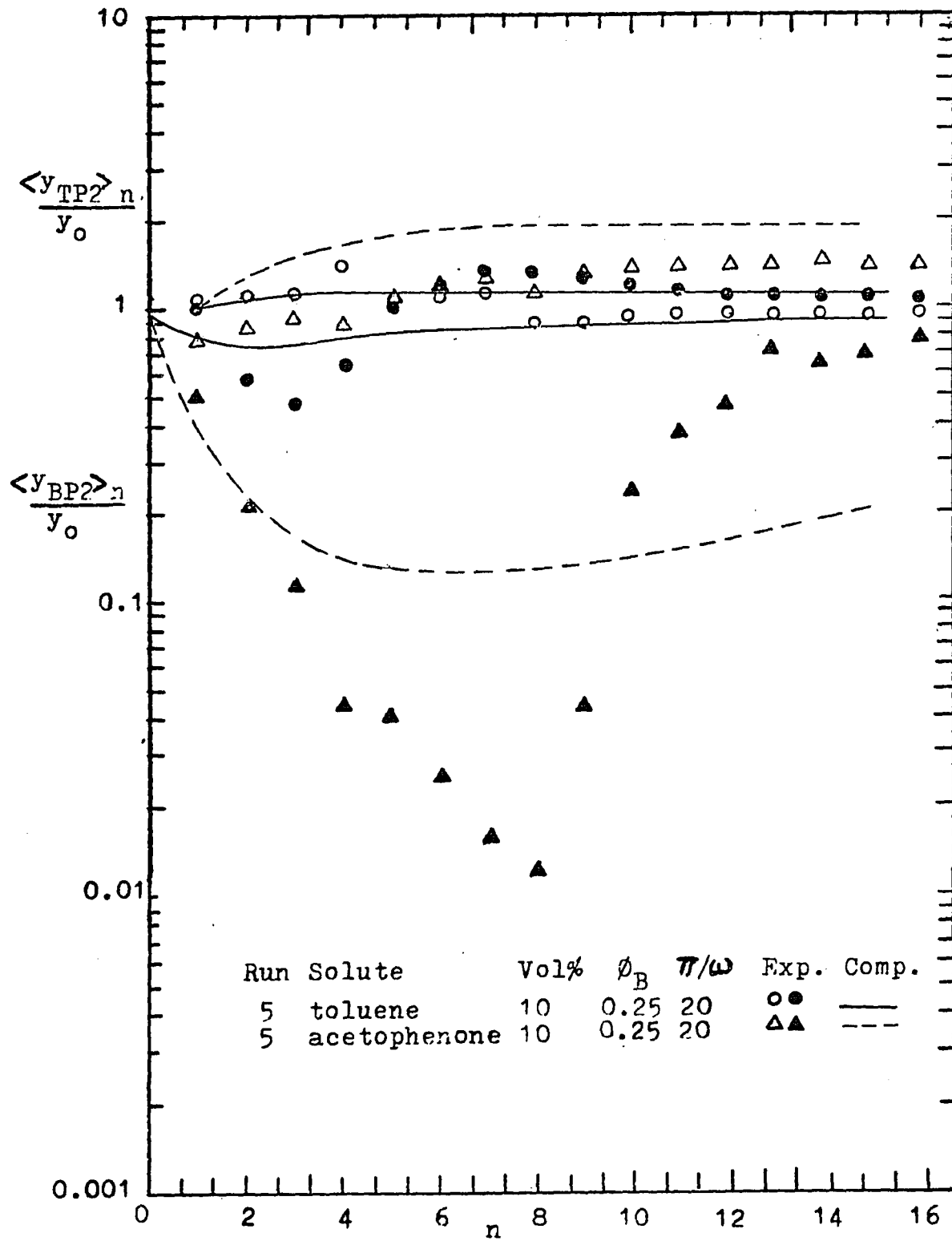
FIGURE (15)

Concentrated Ternary System: 10% Toluene and Acetophenone in n-Heptane
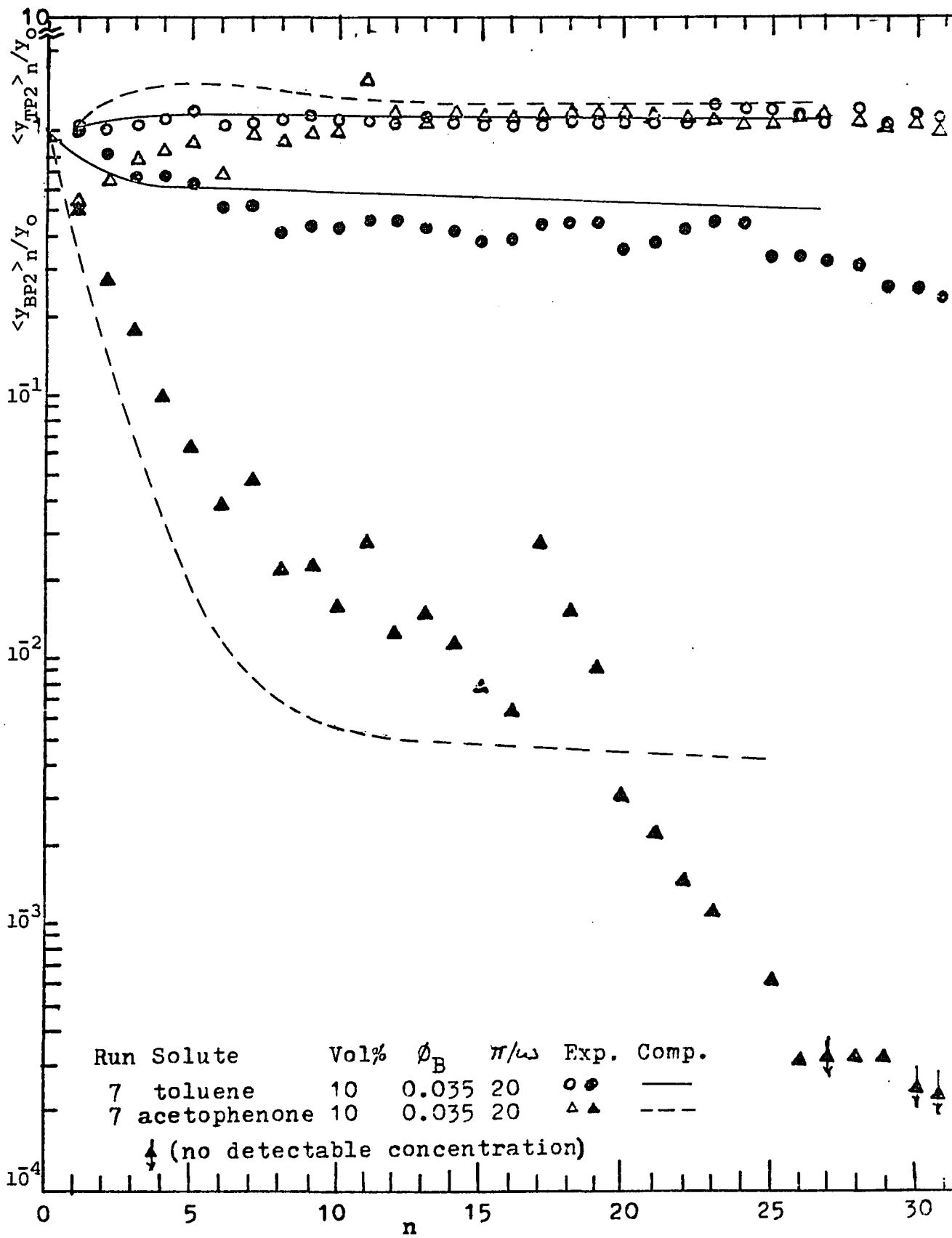
FIGURE (16)

10% Ternary System: Effect of Reducing $\emptyset_B$

Effect of cycle time. The length of the cycle affects the separation by changing the approach to equilibrium. In the mathematical logic and in the computer program, the cycle time shows up in the column velocity and in the mass transfer coefficients which are automatically computed for every point in the column and incorporated into the calculated concentration profiles. The net result is shown in Runs 7, 8, and 9 (Figures 16, 17,18) for half cycle times (π/ω) of 20, 10, and 5 minutes.

Experimentally, the net effect of reducing the cycle time and decreasing the approach to equilibrium appears to be a tendency of the bottom product concentration to level out at increasingly higher solute concentrations. For 10 vol. percent feed solutions with dimensionless bottom product rates ($\emptyset_B$) of 0.035, the bottom product concentration ratios (y_{BP2}/y_o) appear to level out at values of 0.0003, 0.001, and 0.008 for the respective half-cycle times of 20, 10, and 5 minutes. As previously mentioned, the analytical accuracy in this concentration range is uncertain and the computed results should show the actual trends.
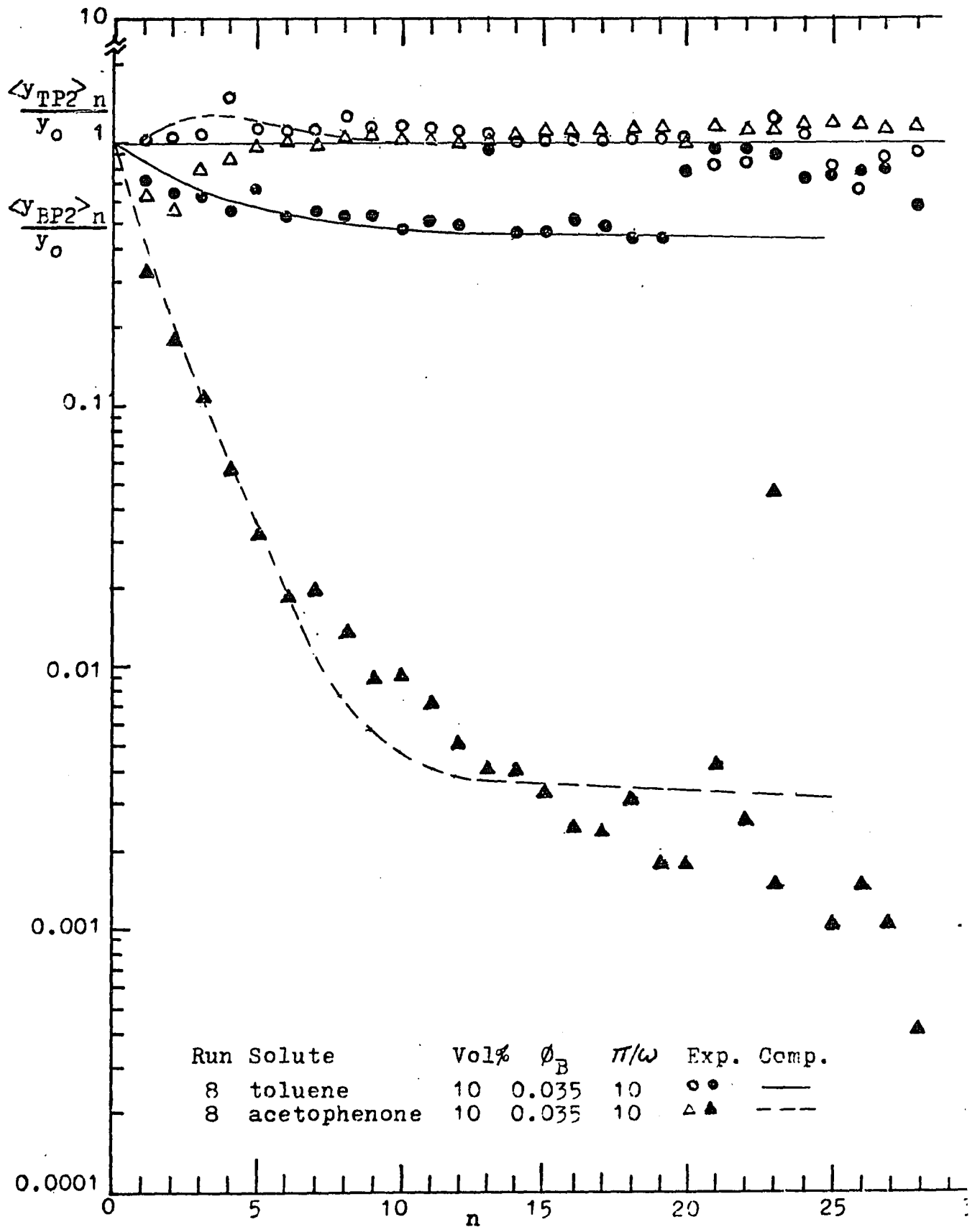
FIGURE (17)

10% Ternary System: Effect of Increasing Separation Rate by 100%

Run	Solute	Vol%	ϕ_B	π/ω	Exp.	Comp.
9	toluene	10	0.035	5	O ●	——
9	acetophenone	10	0.035	5	△ ▲	— — —
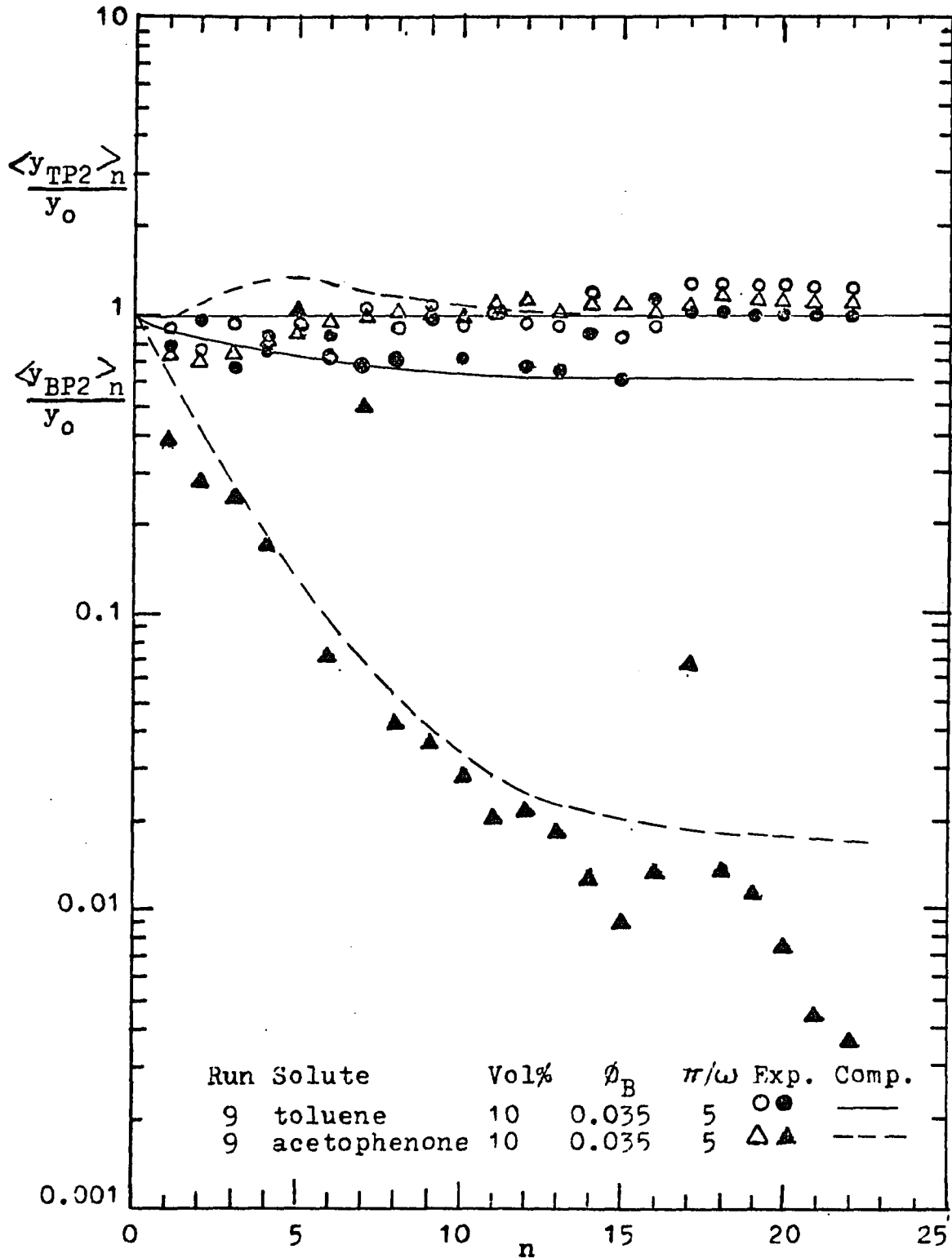
FIGURE (18)

10% Ternary System: Effect of Increasing Separation Rate by 400%

Effect of high solute concentrations. The effect
of going from dilute (2.5 vol. %) solute concentrations
to higher concentrations (10 vol. %) has been described
as a changeover from the dilute solution theory of
Chapter 3 to the concentrated solution mathematical
model of this chapter. The effect of increasing solute
concentrations to 20 vol. percent can now be considered.
If two solutes are involved, the total concentration is
40% and proceeding beyond this point is not warranted
unless the solvent is redefined.

Runs 8, 10, and 11 (Figure 17,19,20) show the
effect of varying solute concentration in the concentrated
solution range (above that of the dilute solution theory).
All of these runs used the same value of $\emptyset_B$ (0.035) and
a half cycle time (π/ω) of 10 minutes. In Run 8, the
concentrations of toluene and acetophenone were 10 volume
% each. The toluene concentration was increased to 20%
in Run 11 and both solute concentrations were increased
to 20% in Run 10.

In all three runs, the concentrations of toluene
and acetophenone in the top product stream were almost
identical and the same as the feed concentration. In
Run 8, there was some separation of toluene in the
bottom product stream (y_{BP2}/y_o = 0.5) and acetophenone

was separated to a greater extent $(y_{BP2}/y_o = 0.002)$.
When the toluene concentration of the feed was increased
to 20 vol. %, the toluene concentration in the bottom
product relative to the feed rose to 0.9 and the
acetophenone bottom product concentration rose to 0.009.
When the feed concentration of acetophenone was also
increased to 20 vol. % (Run no. 10), the toluene concen-
tration in the bottom product was actually greater than
that of either the feed or the top product. The concen-
tration of acetophenone in the bottom product rose to a
steady state value of approximately 0.1 relative to that
of the feed.

Thus the overall effect of increasing the solute
concentration in the feed is to decrease the separation
of the solutes in the bottom product. In the case
where both toluene and acetophenone feed concentrations
were 20%, the column behaved as though it were completely
saturated with toluene and no separation was possible.
Acetophenone was still separable, but the separation
was relatively poor and it is doubtful that the column
could handle a more concentrated feed unless the feed
rate was reduced.
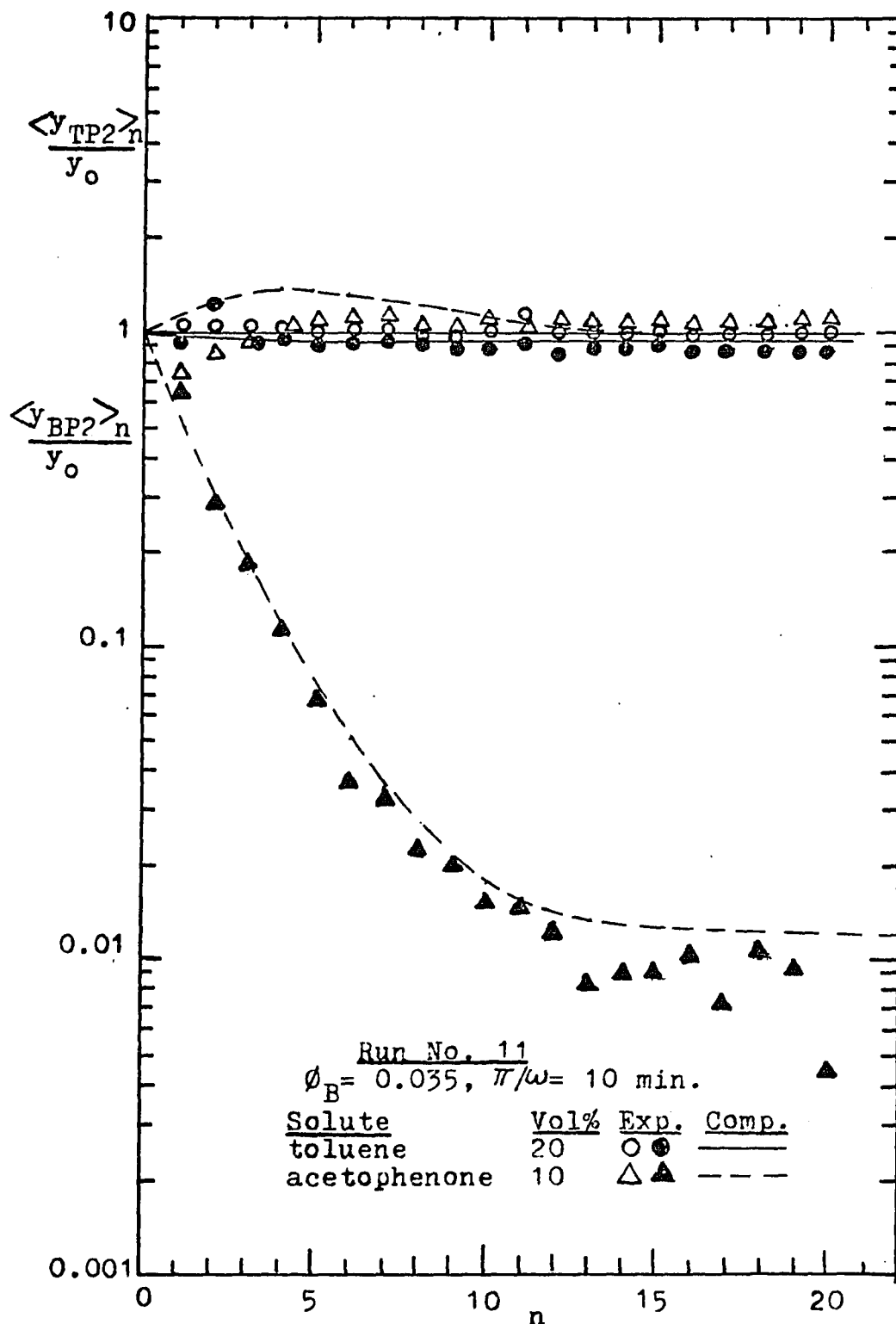
FIGURE (19)

Concentrated Ternary System: Effect of Increasing
Concentration of One Solute (Toluene) to 20%
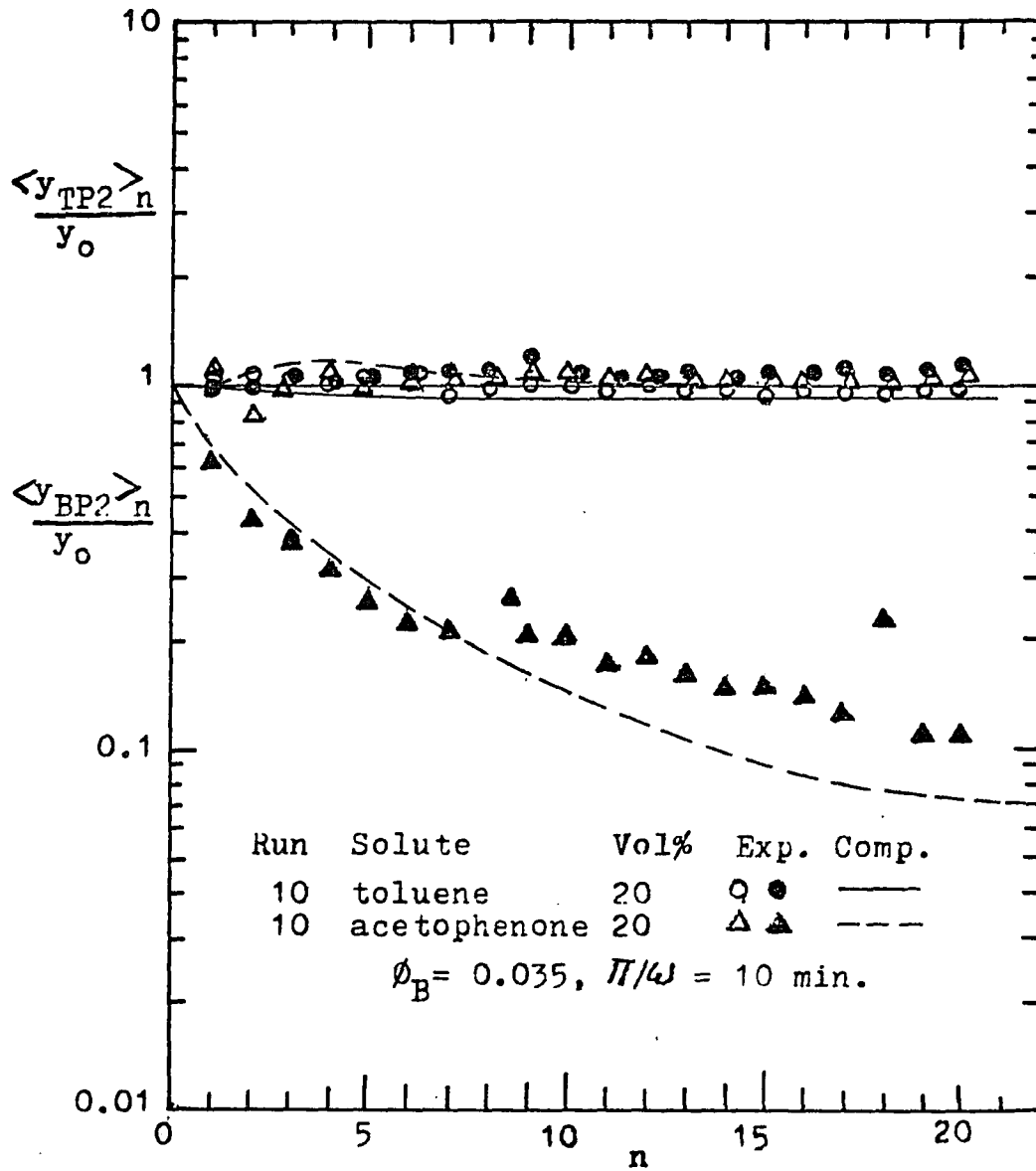
FIGURE (20)

Effect of Increasing Concentration of Both
Solutes to 20%

CHAPTER 5

APPLICATION OF THE DILUTE SOLUTION THEORY TO

SCALE-UP, DESIGN, AND ENERGIES

In this chapter the dilute solution theory of Chapter
3 is applied to the scale-up, design, and energies of para-
metric pumping systems. The four main sections of the
chapter are: the basic design concepts and equations; a
process design example to illustrate the use of these con-
cepts in the design of a separation system for toluene-n-
heptane-silica gel; a further expansion of the equations
and concepts to correlate process energy and product purity
requirements with equipment size and key operating para-
meters; and a description of a full scale parametric pump-
ing system with the associated equipment and instrumenta-
tion.

It is hoped that this information will encourage the
development of the parametric pumping separation technology
into industrial processes. Gregory (1974) contributed
towards this goal in his comparison of parametric pumping
with conventional adsorption. Gregory's comparison dealt
with the recuperative rather than the direct mode, but is
generally valid for both approaches. The broad conclusion
was that the parametric pumping process can handle larger
volume feed streams than conventional adsorption processes

for equivalent separations. But, because of the frequent temperature changes, the energy requirements will, in general, be higher than those of conventional adsorption.

The energy requirements are highly significant in process separations, especially in an era of rising fuel costs. Nevertheless, the overall process must be considered and it is quite possible that the higher volumes processed by the parametric pumping system will outweigh any higher energy costs on a unit volume basis. In the section describing the full scale plant operation, methods are proposed to minimize energy requirements. And the section on energies predicts what those requirements would be for different size plants.

A series of four graphs relate equipment size and product draw-off rate to separation efficiency and to the energies required on both a BTU per operating cycle basis and a BTU per pound of product basis. As an example, a system with a 10 ft.^{3} reservoir and a 9 ft.^{3}/hr. draw-off rate could have a total minimum energy consumption of 171,000 BTU per cycle (heating, refrigeration, and pumping) for a product solute concentration reduced to 55% of the feed. For complete separation, the energy costs would rise to 237,000 BTU per cycle. The practical operating range of solute separations of 0-100%, required 540-900 BTU/lb. of product.

Design Concept and Equations

The dilute solution theory presented in Chapter 3 is well established for both the multicomponent systems and the binary systems, and therefore forms a reliable design basis for the present work. The design equations derived in Appendix III and summarized in this section are based on the dilute solution theory. Modifying these equations to account for the effect of solute concentration covered in Chapter 4 is beyond the scope of the present work.

In developing the design equations, as explained in Appendix III, the mathematic expressions for the binary or the multicomponent systems are identical and equally valid because the design is focussed on the separation of one particular solute. Whether that solute is the only one, as in a binary system, or only one of many, the design is the same because the equipment can produce only two product streams (as in a distillation column). Further separation of one or both streams requires another parapump for each separation and repetition of the design procedures described below.

Packed column diameter and switchover time. The basic configuration of a pilot plant or commercial parapump unit depends on a minimal switchover time

between hot and cold half-cycles. And the relationship between this switchover time and the column diameter or radius is (III-1)

$$t_{90} = 0.5 \ r^2/k \qquad (70)$$

in which t_{90} is the time required for the temperature at the axis of the column to reach 90% of the external fluid temperature, r is the column radius, and k is the thermal diffusivity. This equation, as explained in Appendix III, was first applied by Sweed (1969) to a single laboratory column to explain that the switchover time for laboratory size columns was sufficiently small to consider the switch-over "instantaneous" as required by the equilibrium theory.

In Appendix III, this equation was extended to (III-2,3)

$$t_1/t_2 = d_1^2/d_2^2 = N \qquad (71)$$

where d_1 is the diameter of one large column equal in cross section area (or capacity) to N small tubes of diameter d_2.

Therefore, if the equilibrium theory is to be applied and the temperature change is to be instantaneous by means of externally applied heating or cooling, the design must be based on multiple tubes in a heat exchanger configura-tion and the first scale up criteria is to use multiple tubes rather than a single large tube in which an internal

heat transfer device could interfere with the adsorption wave pattern and plug flow, also basic to the equilibrium theory.

Packed column length and capacity. The second scale-up concept relating to capacity is the length of the columns. As shown in the derivation in Appendix III, optimum separation is achieved when the ratio of the bottom product take-off rate to the reservoir flow rate is equal to or less than the value of the equilibrium separation parameter b. Theoretically, the capacity is at a maximum when this ratio is equal to b. Under these conditions, the penetration distance of the adsorption wavefront during the cold downflow is at a maximum and this penetration distance must be equal to or less than the length of the column. In terms of column length, h, and the superficial column velocity v, this relation was shown to be (III-9, 10)

$$h \geq K'v \tag{72}$$

where

$$K' = \frac{(1+\emptyset_B)(\pi/\omega)}{(1+b_i)(1+m_{oi})(\varepsilon)} \tag{73}$$

and $\emptyset_B$ is the ratio of the bottom product rate to the reservoir rate, b_i is a dimensionless equilibrium parameter, π/ω is the half cycle time, m_{oi} is a dimensionless

equilibrium parameter, and ε is the dimensionless void fraction of the adsorbent packing.

In terms of the column volumetric flow rate, the length of the column is (III-12, 13)

$$h \gtrsim K''Q/N \tag{74}$$

where

$$K'' = \frac{(1+\emptyset_B)(\pi/\omega)}{(1+b_i)(1+m_o)(\varepsilon)(a_t)} \tag{75}$$

and a_t is the cross section area of one tube, N is the number of tubes, and Q is the volumetric reservoir rate.

Now K' and K'' are, in fact, constants for a given system operating under a fixed set of conditions because b_i and m_{oi} are constants for any given system operating at specific temperatures for hot upflow and cold downflow, $\emptyset_B$ is a fixed ratio of the bottom product rate to the reservoir rate, π/ω is usually the minimum half cycle time required to give a separation, ε is the void fraction characteristic of the packing, and a_t is usually fixed.

Heat requirements during the hot upflow half cycle. The heat requirements may be divided into two sections as shown in the following equation derived in Appendix III (III-17).

$$q_1 = (w_t c_t + w_s c_s + w_f c_f) Nh (T_1 - T_2) n$$

$$+ Q(1 - \emptyset_B)(\rho_f c_f)(\pi/\omega)(T_1 - T_2) n \qquad (76)$$

The first half of the equation represents the heat required to raise the temperature of the tubes and tube contents from T_2 to T_1. The second half represents the heat required to raise the temperature of the fluid pumped through the column from T_2 to T_1. In this equation w_t, w_s, and w_f represent the mass per unit length of the tube wall, the solid adsorbent, and the fluid respectively, c_t, c_s, and c_f represent the respective heat capacities. T_1 and T_2 are the hot upflow and cold downflow temperatures, ρ_f the average fluid density, and n is the number of cycles or half-cycles for the operation under consideration.

In most cases, the duty for heating the tube and contents is roughly twice that for heating the fluid pumped through the column. Moreover, since the duration is only approximately 2 minutes as compared to roughly 20-30 minutes for a typical half cycle time, the _rate_ for heating the tubes and contents could easily be 20 times or more that of the average rate for the entire half cycle. To save the cost of a large heat generating plant (steam boiler), a hot water reservoir could be used to store the heat and the reservoir would be reheated during the cold half cycle.

Cooling requirements during the cold downflow half cycle.

$$q_2 = (w_t c_t + w_s c_s + w_f c_f) Nh \ (T_1 - T_2)_n$$

$$+ \ Q(1 + \emptyset_B)(\rho_f c_f)(\pi/\omega)(T_{2H} - T_2)n \qquad (77)$$

This equation (III-18) is the same as that for the heating half cycle except for the $(1 + \emptyset_B)$ term (which accounts for the additional column flow needed to supply the bottom product stream on cold downflow) and for the T_{2H} term which accounts for the heat effects of the feed and product streams on the fluid reentering the column. The equation for calculating T_{2H} is derived in Appendix III as Equation (III-14) from heat balances around the top of the column during hot upflow and cold downflow.

For design purposes, it is permissible to substitute T_1 for T_{2H} because T_{2H} is involved only in the portion of the cooling duty pertaining to the fluid flowing down the column during the cold downflow half cycle which is very small compared to the duty during the switchover period from the hot to the cold half-cycles. Furthermore, the substitution of T_1 makes the design more conservative because T_1 is generally higher than T_{2H} due to the cooling effect of the feed stream. For design purposes, Equation III-18 may be modified to the simplified form

$$q_2 = \left[(w_t c_t + w_s c_s + w_f c_f) Nh + Q(1+\emptyset_B)(\rho_f c_f)(\pi/\omega)\right] (T_1 - T_2) n$$

$$(78)$$

Finally, in the design, it would be preferable to provide a large cold water reservoir and a relatively small compressor rather than one large compressor for the high initial duty during the switchover period. The system could be regenerated during the hot half-cycle. Most refrigeration systems are designed this way wherever the plant layout provides sufficient space for the reservoir.

Pressure drop of the shellside heat transfer fluid.
As derived in Appendix III, the shellside pressure drop is (III-33)

$$\Delta p = \frac{1.525 \times 10^{-4} w^2 (2h-1)}{(0.005732 N^{.9474} - 0.001736 N)^2}$$

$$+ \frac{2.756 \times 10^{-4} w^{1.8} (0.07117 N^{.4737} - 0.0417)(2h)}{(0.03293 N^{.4737} - 0.01563)^{1.8}} \qquad (79)$$

where N is the number of tubes, w is the water rate in pounds per second, h is the tube length in feed, and Δp is the pressure drop in psi. The equation shown above was derived for water as the shellside fluid for heating or cooling. For other heat transfer media, the pressure

drop can be calculated from Equations (III-23 and III-28) in Appendix III.

Also, Equation (III-33) is for turbulent flow which is correct for most designs using water. For laminar flow, Equations (III-23 and III-29) may be used for fluids in general and Equation (III-34) for water.

The derivations in Appendix III include the complete sets of equations required with no limiting assumptions. The assumptions incorporated in Equation (III-33) are for a 6-inch baffle spacing, 25% baffle cutout, and a 1.375D triangular pitch with D equal to 1/2 inch outside diameter tubes.

The 1/2 inch 18 BWG tubes were chosen because they have approximately the same inside diameter as the packed columns used in research where switchover times were 2 minutes for aqueous systems (Sweed and Gregory, 1971), and 45 seconds for hydrocarbon systems (Sweed, 1969). Since typical half-cycle times are 20-40 minutes, the 0.75-2 minute switchover times are short enough to be considered "instanteous". Should shorter half-cycle times be necessary, smaller diameter tubes can be used and the pressure drop equations easily modified. Conversely, long half cycle times could utilize larger tubes and still operate according to the equilibrium theory, but to do so would extend the

operating time and lower the effective capacity of the equipment.

Pressure drop through the tubes. The basic equation chosen for pressure drop through the packed beds is the Blake-Kozeny equation for laminar flow. In Appendix III, the basic dimensionless form is rearranged to show the relationship between pressure drop and volumetric flow rate as usually expressed for parametric pumping. The equation is also expressed in terms of average column velocity and column length which is the most useful for the design example which follows in the next section. This is (III-20)

$$\Delta p = \frac{150(1-\epsilon)^2 \mu h v}{D_p^2 \, g_c \epsilon^3} \qquad (80)$$

where ϵ,h,v, have been previously defined, D_p is the average particle diameter, μ is the fluid viscosity, and g_c is the gravitational conversion factor.

Equation (III-20) is useful for the design of the parapump column assembly itself and is used for this purpose in the design example in the next section of this chapter. It should be pointed out that this pressure drop is only one of the considerations in the design of the feed and reservoir pumps that supply the necessary

pressure. The design of these pumps is discussed in some detail in Appendix III and also in the description of the parapump equipment later in this chapter.

Process Design Procedure

The n-heptane-toluene-silica gel system was used as an example because this system is a natural extension of previous work. As explained earlier, a binary system is adequate to illustrate the design procedure because the design "sees" only the two key components, regardless of the actual number of components present. The example will be developed in such a way as to show the relationship between capacity (determined as the reservoir rate Q) and the basic parameters of heat transfer and pressure drop. These relationships will be shown in the form of graphs from which the optimum process design can be selected.

The following general assumptions will be made:

1. The insulation is adequate to insure adiabatic operation and restrict the heating and cooling requirements to the process fluid, the adsorbent, and the tube walls.

2. A control system will be used which places the feed and one product stream on flow control. The product and the reservoir streams will be under a back pressure

imposed on the effluent product stream. The entire system will thus be under a constant pressure during both cold downflow and hot upflow half cycles. If liquid thermal expansion is neglected, the minimum pressure imposed will be that calculated for the cold downflow half-cycle.

3. The heat transfer fluid will be water which will be indirectly heated by steam and indirectly cooled by brine or chilled water refrigeration.

4. The heat transfer fluid (water) densities and specific heats, as indicated in Appendix IV, may be assumed equal to one. The viscosity varies from 0.5 to 1.5 over the operating temperature range but, since the viscosity is raised to the 0.2 power, the range is effectively narrowed to 1.08 to 0.88 and the assumption of a uniform value of 1 would be adequate for the present design.

5. A temperature rise of 15.2° F. in the water temperature will be used for design. Fixing this temperature rise automatically ties the heat transfer fluid (water) rate and the water pressure drop to the process reservoir rate Q through a heat balance. Fixing the Δt for the heat transfer fluid is therefore necessary if all the basic design parameters are to be related to the process reservoir rate (capacity parameter).

6. A switchover time of 2 minutes will be assumed for the toluene-heptane system. Sweed (1969) reported an experimental time of 45 seconds and a calculated time of 2 minutes. The two minute time is sufficiently conservative and accurate for engineering purposes.

7. The hot upflow and cold downflow temperatures will be 70° and 5° centigrade respectively.

Column length versus superficial velocity and capacity. In the equation

$$h \geq K'v \tag{72}$$

where

$$K' = \frac{(1+\emptyset_B)(\pi/\omega)}{(1+m_O)(1+b)(\varepsilon)} \tag{73}$$

and from Chen et al (1972), the values are $\varepsilon = 0.38$, $\emptyset_B = 0.15$, $\pi/\omega = 1200$ seconds or 0.333 hours, $b = 0.22$, $L_2 = 0.44$ meters, $h = 0.90$ meters, and $m_O = 1.88$. Then $K' = 0.2868$ and (III-9A)

$$h \geq 0.2868v \tag{81}$$

Also, since (from Appendix III, Equation 11)

$$v = (Q/(a_t/N)$$

and since $a_t = 8.81 \times 10^{-4}$ feet, $v = 1135 \, (Q/N)$ and

$$h \gtrsim 326 \, Q/N \qquad\qquad (82)$$

Equation (III-11A) is plotted in the graph, Figure (21) as Q vs. h with lines of constant values of N corresponding to the number of tubes available in various commercial shell sizes.
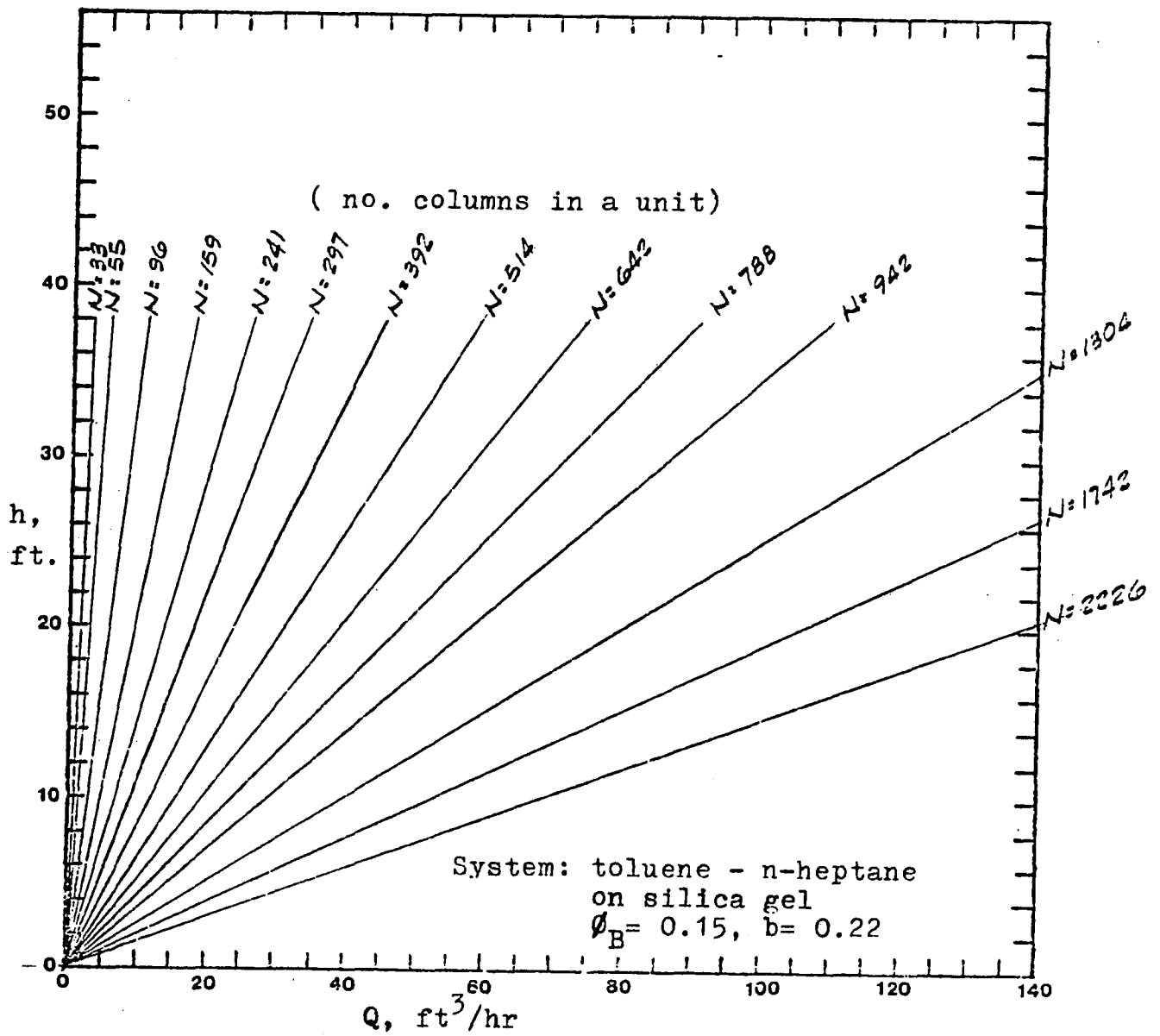
FIGURE (21)

EQUIPMENT SIZE vs RESERVOIR RATE

Column pressure drop. The pressure drop equation is

$$\Delta p = \frac{150(1-\varepsilon)^2 \mu h v}{D_p^2 \varepsilon^3 g_c} \tag{80}$$

where $\varepsilon = 0.38$, $D_p = 13.2 \times 10^{-4}$ feet, $g_c = 4.17 \times 10^8 lb_m/hr^2/ft$ (ft^2/lb_f), and the viscosity is 0.53 centipoise for a solution of 20% toluene in n-heptane at $5^O C$ and 0.28 cp for the same solution at $70^O C$. To convert the viscosity to $lb_m/hr/ft$, the required conversion factor is 2.42. The simplified equation is, for cold downflow,

$$\Delta p_2 = 1.855 \ h v_2 \tag{83}$$

If the control system described previously is used, only the cold downflow pressure drop need be considered. The hot upflow pressure drop would be 0.28/0.53 times that of the cold downflow, provided the fluid density is assumed constant and the correct velocity is used.

The pressure drop may also be described in terms of the reservoir flow rate Q. For cold downflow,

$$v_2 = (1+\emptyset_B) \ v = 1.15v \tag{84}$$

Since $\quad h = 0.2868v \tag{81}$

$$v = 1135 \ Q/N \tag{85}$$

then $\Delta p_2 = 2.133 \ hv = 0.6118 \ v^2 = 7.88 \times 10^5 (Q/N)^2$

$$\tag{86}$$

Similarly, for hot upflow

$$v_1 = (1-\phi_B)v = 0.85v \tag{87}$$

then

$$\Delta p_1 = 1.855(.28/.53)hv_1 = .833hv = .2389v^2 = 3.078 \times 10^5 (Q/N)^2 \tag{88}$$

The pressure drop to be considered for design is
that for cold downflow and this pressure would have to
be developed by the top reservoir pump as a miminum.
This would also be the pressure at the point where the
feed enters the column and would have to be developed
by the feed pump as a minimum. This subject is discussed
at greater length in the next section in this chapter.

Equation (86) is plotted in Figure (22) as the reser-
voir rate Q vs. the pressure drop in psi with lines of
constant values of N corresponding to the number of tubes
available in various commercial shell sizes.
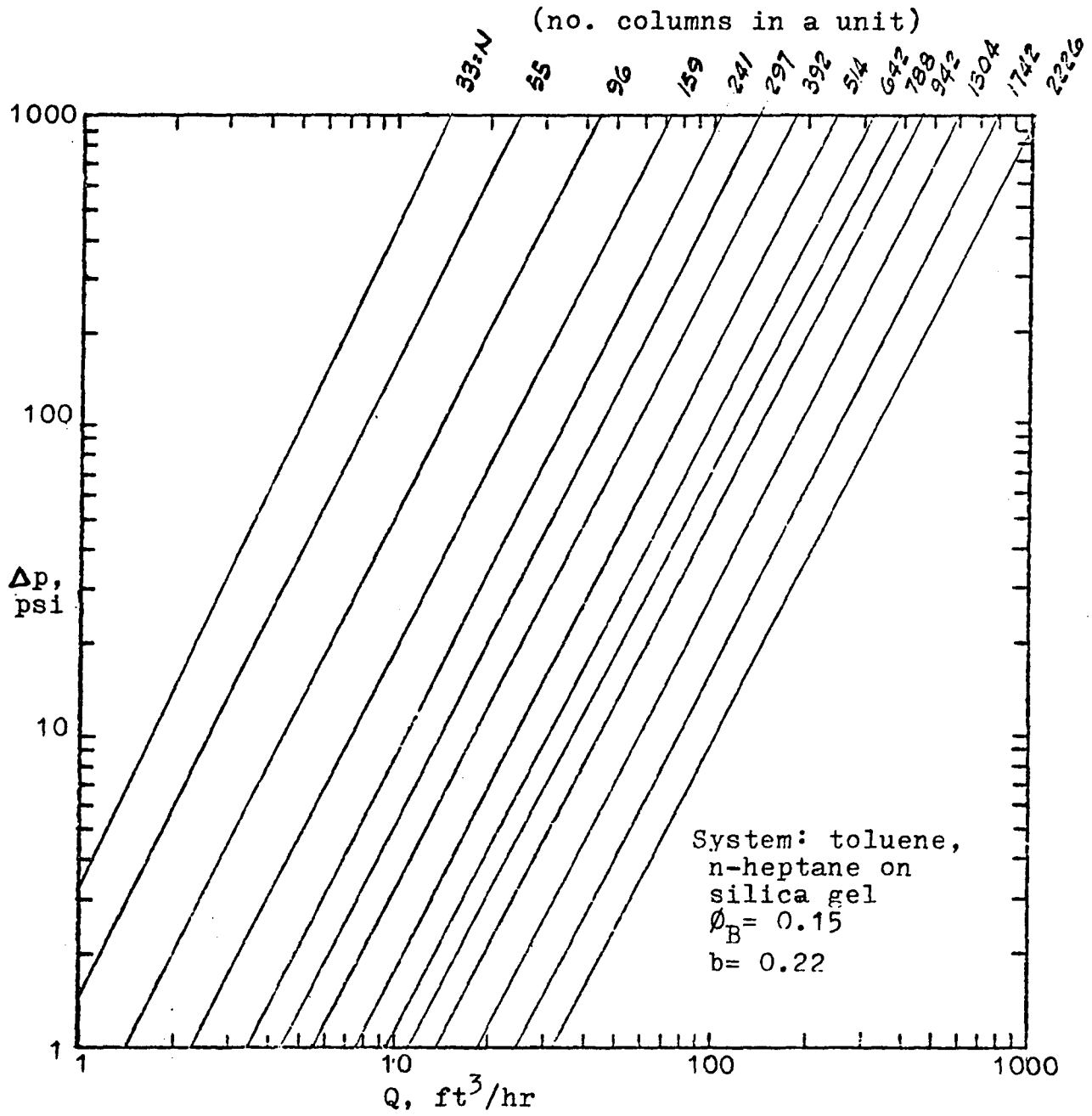
FIGURE (22)

COLUMN PRESSURE DROP vs RESERVOIR RATE

Heat transfer during hot upflow. The basic heat transfer equation given previously is

$$q_1 = \left[(w_t c_t + w_s c_s + w_f c_f) Nh + Q(1-\emptyset_B)(\rho_f c_f)(\pi/w)\right](T_1-T_2)n$$

(76)

where, from the data in Appendix IV, the quantity $(w_t c_t + w_s c_s + w_f c_f)$ is equal to 0.0874 BTU/^{O}K/ft of tube length, $\emptyset_B = 0.15$, $\rho_f = 0.72 \times 62.3 = 44.9$ lb/ft^3, $c_f = 0.53$ BTU/lb/^{O}F = 0.972 BTU/lb/^{O}K, $\pi/\omega = 0.333$ hr, $T_1 = 70^O$C$=343^O$K, $T_2 = 5^O$C $= 278$ ^{O}K, and n = number of cycles under consideration = 1. Now, substituting these quantities in Equation (76),

$$q_1 = 5.681\ Nh + 803Q$$

or since $Q = vNa_t = 8.81 \times 10^{-4}\ vN$ where v is the average tube velocity,

$$q_1 = 5.681\ Nh + 0.707\ vN$$

or

$$q_1/N = 5.681\ h + 0.707\ v \qquad (89)$$

Another way of expressing Equation (89) may be developed by combining it with Equations (82 and 85) to get the expression for q_1 as a minimum

$$q_1/N = 5.681 \times 326\ (Q/N) + 0.707 \times 1135\ (Q/N)$$

or

$$q_1\ (minimum) = 2651\ Q \qquad (90)$$

Now it should be pointed out that, according to Equation (90), the percent of heat transferred during the switchover time is 69.8% of the total and that this heat is transferred in a maximum of two minutes. The rate of heat transfer during the switchover period is therefore

$$\Delta H_1 = 1852Q/(2/60) = 55,560 \ Q \ BTU/hr$$

This rate is roughly seven times the overall heat transfer rate and this load could be provided by either instantaneous steam heating or by the temperature drop of a large reservoir. In the latter case, the regenerative heat rate would be 7935 BTU/hr, the regeneration occurring during the cold downflow half cycle.

Heat transfer during cold downflow. The basic heat transfer given previously is

$$q_2 = (w_t c_t + w_s c_s + w_f c_f)(Nh)(T_1 - T_2)n$$
$$+ Q(1 + \phi_B)(\rho_f c_f)(\pi/\omega)(T_{2H} - T_2)n \qquad (77)$$

As previously explained, T_{2H} may be replaced by T_1 for purposes of design (Equation 78). Substituting the quantities previously given,

$$q_2 = 5.681 \ Nh + 1086 \ Q$$

The remaining equations are developed in a manner identical to those for hot upflow and they are

$$q_2 = 5.681 \ Nh + 0.957vN$$

or

$$q_2/N = 5.681 \ h + 0.957v \qquad (91)$$

As was the case for hot upflow, Equation (91) may be combined with Equations (82 and 85) to give the expression for q_2 as a minimum

$$q_2/N = 5.681 \times 326 \ (Q/N) + 0.957 \times 1135 \ (Q/N)$$

or

$$q_2 \ (minimum) = 2936 \ Q \qquad\qquad (92)$$

Similar to the case for hot upflow, the percent of heat transferred during the switchover period is 62.9% of the total. Now the switchover rate would still be 55,560 BTU/hr but the regenerative rate would now be 8928 Q due to the higher total duty.

The Equation (92) for cold downflow and also Equation (90) for hot upflow, along with the switchover and regenerative rates are given in Figure (23).
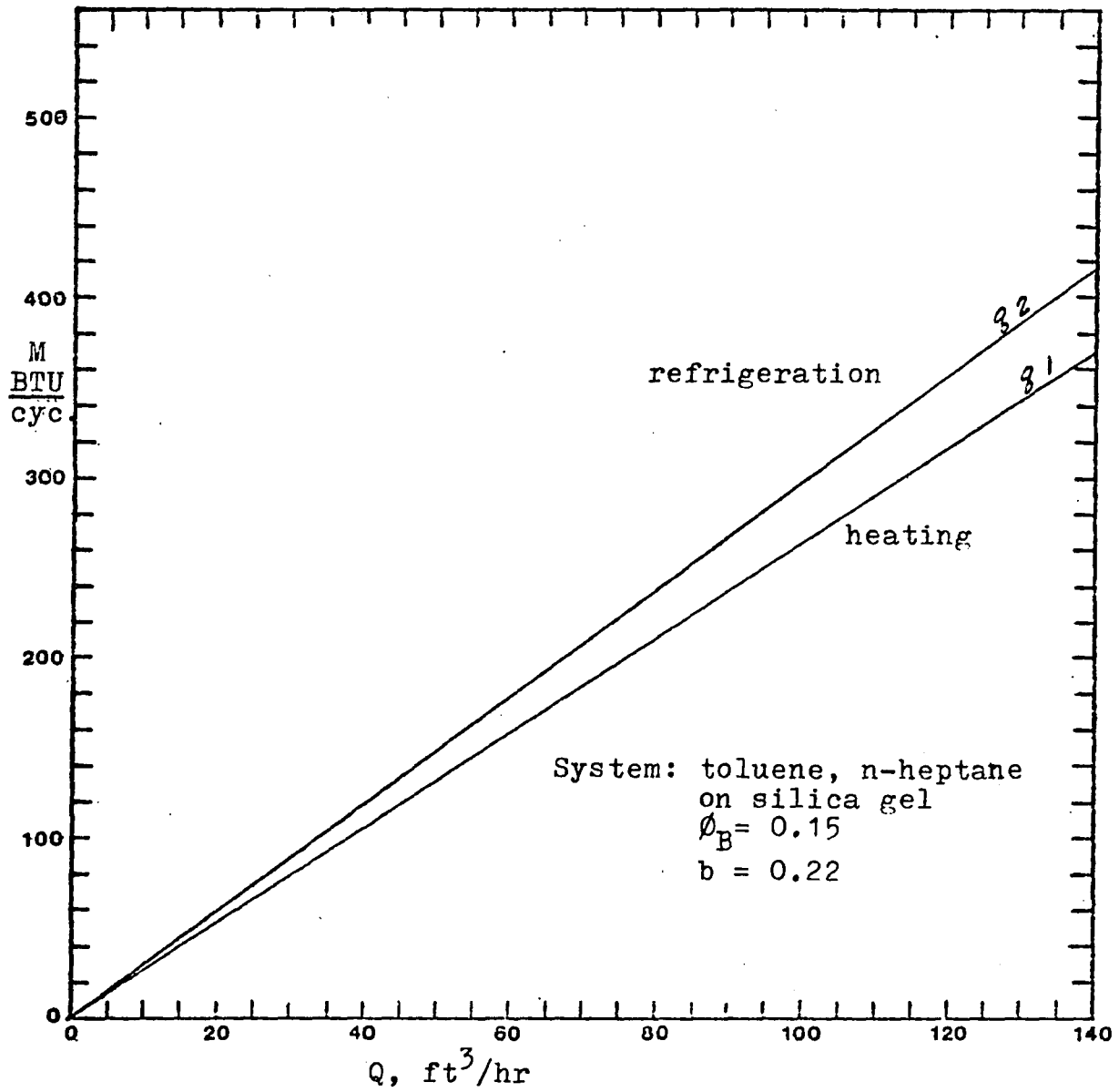
FIGURE (23)

HEAT TRANSFER DUTIES vs RESERVOIR RATE

Heat transfer fluid (water) rate vs. column length

and capacity. By definition

$$wc\Delta T + q_t/\tau \tag{93}$$

where w is the water rate in lb/sec, c is the heat capacity
of water equal to 1 BTU/lb/^{O}F, ΔT is the water temperature
rise fixed at 15.2^{O}F, q_t is the duty during the switchover
period in BTU equal to 5.681 Nh and τ is the time of the
switchover period fixed at 120 seconds.

Now rearranging Equation (93) and substituting the
quantities,

$$w/N = 3.115 \times 10^{-3} h \tag{94}$$

The use of q_t was limited to the switchover period
because the heat transfer rate is highest during this
period.

Also, since $h \geq 326$ (Q/N), $\qquad\qquad$ (82)

w(minimum) = 1.014 Q $\qquad\qquad$ (95)

Equation (94) is shown in Figure (24)

w= 1.014 Q

  w= lb/sec heat transfer
     fluid

  Q= ft^3/hr reservoir
     rate
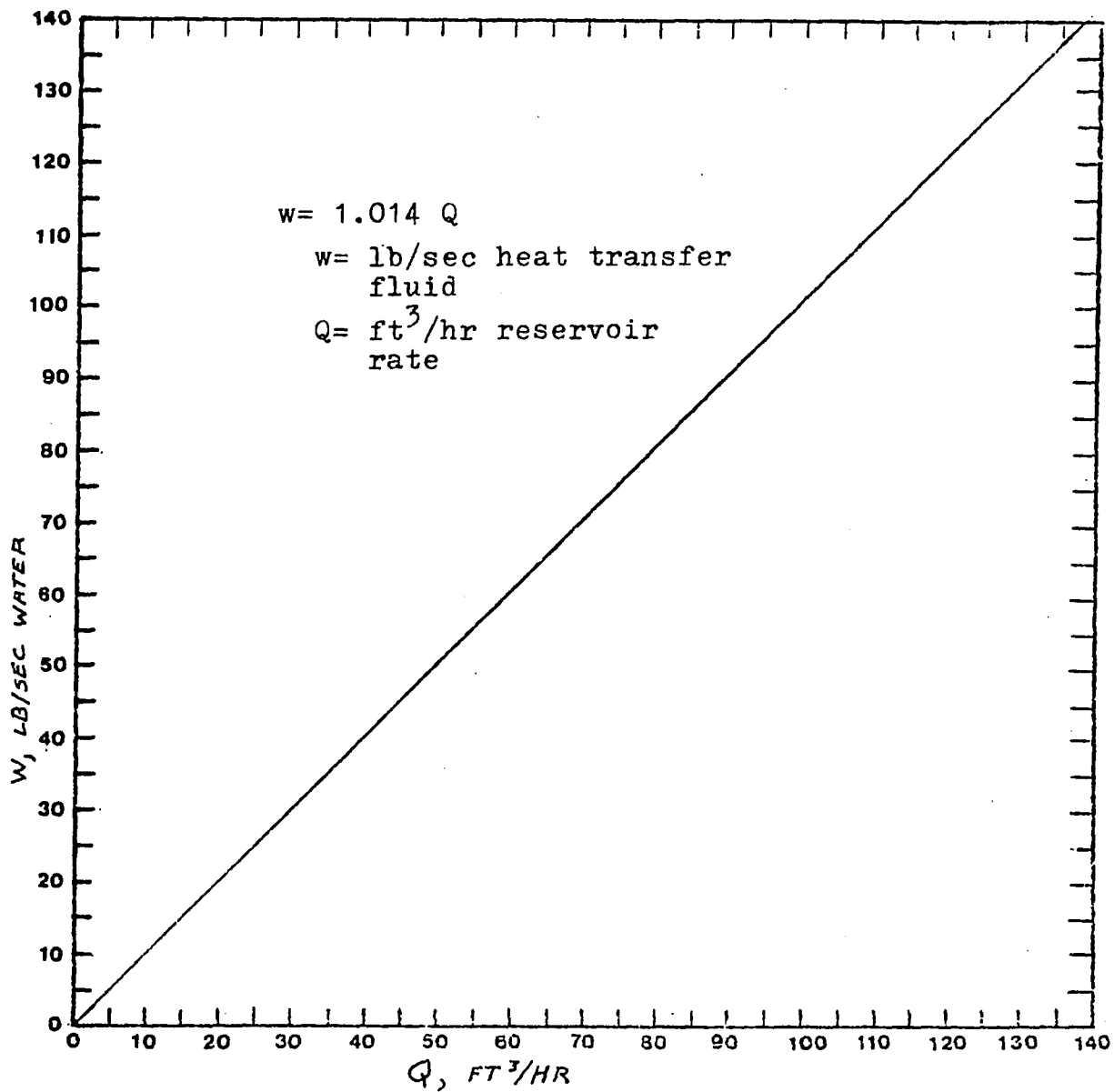
FIGURE (24)

Heat Transfer Fluid Rate vs Reservoir Rate

Shellside (heat transfer fluid) pressure drop. The
basic equation previously given is

$$\Delta p = \frac{1.525 \times 10^{-4} w^2 (2h-1)}{(0.005732 N^{.9474} - 0.001736 N)^2}$$

$$+ \frac{2.756 \times 10^{-4} w^{1.8} (0.07117 N^{.4737} - 0.0417)(2h)}{(0.03293 N^{.4737} - 0.01563)^{1.8}}$$

(79)

In this case it is not possible to get a simple
relationship with N, but the equation can be simplified.

$$\Delta p = F_{N1} w^2 (2h-1) + F_{N2} w^{1.8} (2h) \qquad (96)$$

Now since

$$w = 1.014 Q \qquad (95)$$

and

$$h \geq 326 \; Q/N \qquad (82)$$

then

$$\Delta p = F_{N1} (670 \; Q^3/N - 1.028 Q^2) + F_{N2} (670 \; Q^{1.8}/N)$$

(97)

where F_{N1} and F_{N2} may be obtained from Table (3).

TABLE 3

SHELLSIDE PRESSURE DROP FACTORS

Shell Diam., inches	N (no. tubes)	F_{N1} x 10^6	F_{N2} x 10^4
5	33	15220	25.60
6	55	5967	20.85
8	96	2153	16.72
10	159	856	13.72
12	241	400.8	11.67
14	297	273.9	10.76
16	392	165.2	9.663
18	514	100.9	8.703
20	642	67.36	7.988
22	788	46.43	7.383
24	942	33.58	6.893
28	1304	18.62	6.085
32	1742	11.03	5.446
36	2226	7.077	4.959

An alternative to Equation (96) is a similar equation which includes the term for baffle spacing. This may be useful for very large units where the six inch spacing would lead to unacceptably high pressure drops.

$$\Delta p = F_{N1}w^2(h/B_s-1) + F_{N2}(0.5/B_s)^{2.8}(2h)w^{1.8}$$

$$(98)$$

An examination of the derivations in Appendix III will show that F_{N2} is related to the resistance to the flow across the tube banks and that F_{N1} is related to the resistance through the baffle openings. Generally, as the number of tubes increases, the resistance due to flow through baffle openings remains relatively constant while that across the tube banks increases steadily and, with large numbers of tubes, accounts for practically all the resistance. The significance of this is that for large numbers of tubes, say 800 or more, the effect of dropping the first term of the equation would be small.

The shellside pressure drop with varying tube lengths and numbers of tubes has been calculated, based on water rates corresponding to a 15.2 $^{\circ}$F temperature change. The results are presented in Table (4).

Equation (97) is plotted in Figure (25) as the reservoir rate Q vs. the pressure drop in psi with lines of constant N.

TABLE 4

SHELLSIDE PRESSURE DROPS CORRESPONDING TO A 15.2°F TEMPERATURE CHANGE

h \ N	2	4	6	8	10	12	14	16	18	20
33	.003	.022	.077	.183	.359	.622	.989	1.48	2.10	2.88
55	.003	.028	.096	.227	.443	.763	1.21	1.80	2.56	3.22
96	.005	.040	.134	.314	.606	1.04	1.63	2.42	3.43	4.67
159	.008	.061	.200	.463	.888	1.51	2.36	3.49	4.91	6.68
241	.012	.093	.300	.687	1.31	2.21	3.45	5.07	7.12	9.64
297	.016	.117	.375	.857	1.63	2.74	4.27	6.26	8.78	11.9
392	.022	.162	.516	1.17	2.22	3.73	5.78	8.47	11.8	16.0
514	.031	.226	.716	1.62	3.05	5.13	7.94	11.6	16.2	21.9
642	.042	.300	.946	2.14	4.02	6.74	10.4	15.2	21.2	28.6
788	.055	.392	1.23	2.78	5.22	8.74	13.5	19.8	27.5	37.0
942	.070	.497	1.56	3.51	6.59	11.0	17.0	24.8	34.6	46.6
1304	.109	.770	2.41	5.42	10.2	17.0	26.2	38.1	53.1	71.4
1742	.163	1.15	3.58	8.04	15.0	25.1	38.7	56.4	78.5	106
2226	.230	1.61	5.02	11.3	21.1	35.2	54.2	78.8	110	148

FIGURE (25)

SHELLSIDE PRESSURE DROP vs RESERVOIR RATE
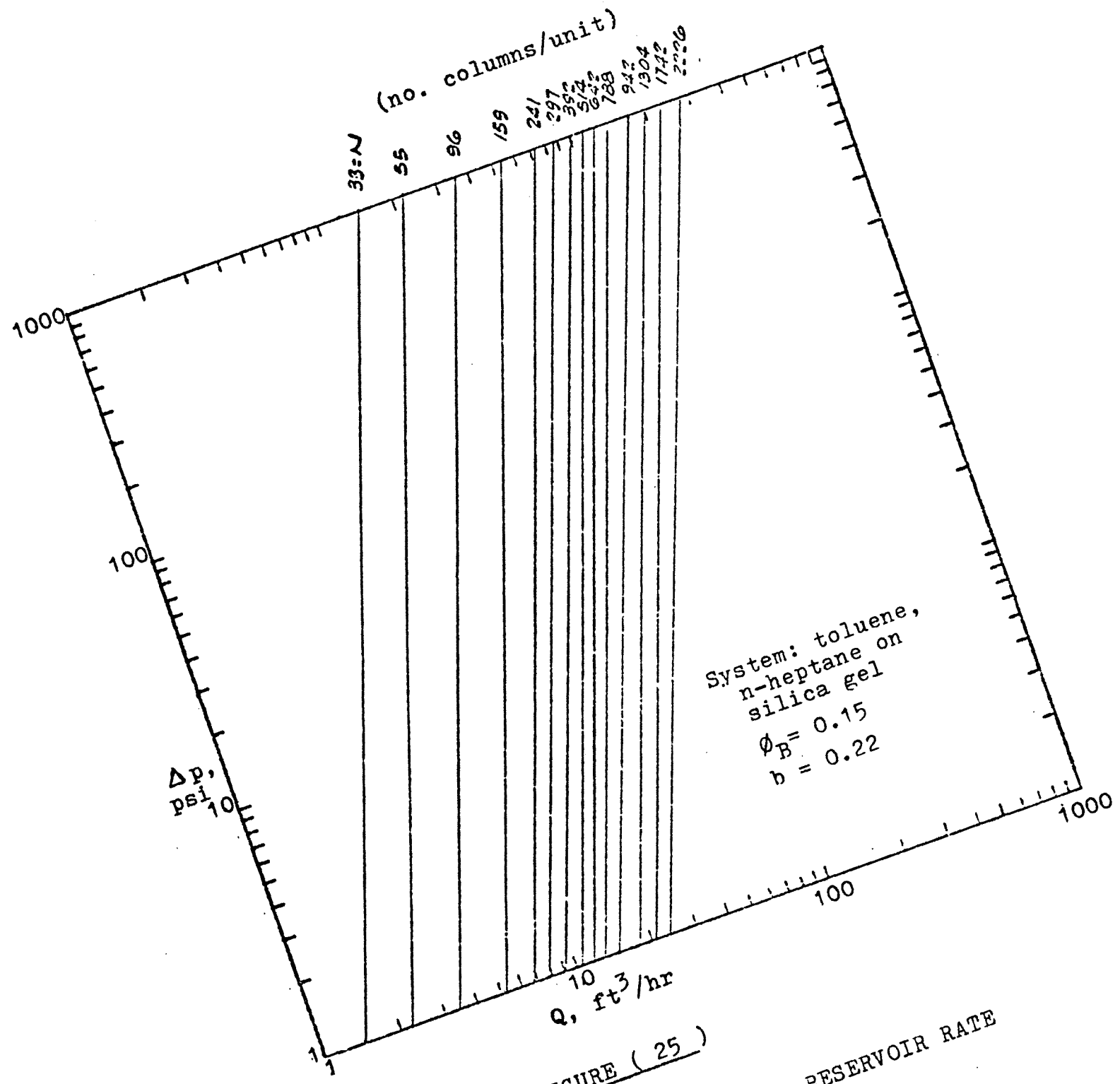
Process design from the tables and graphs. The graphs
and tables were developed for the toluene-heptane-silica
gel system. Similar charts and graphs could be developed
for any other system of interest and could be used to
determine the optimum design based on any two parameters
of interest.

As can be seen in the equations and graphs, the design
parameters are the number of tubes (N), the reservoir
rate (Q), the tube length (h), the velocity (v), the column
pressure drop, the shellside pressure drop, the heating
and cooling capability (q_1, q_2), or the available heat
transfer media (water) flow capacity (w). With the selec-
tion of any two key parameters, it is possible to deter-
mine the remaining parameters and complete the process
design. It should be emphasized that this design would
be optimum and that safety factors would have to be in-
corporated into any actual design.

A few typical designs are shown in Table (5). In-
cluded in the table is a typical laboratory operation
for purposes of comparison. Such a comparison will make
it obvious that a practical scale-up design incorporates
the use of higher column and shellside pressures as well
as larger equipment.

TABLE 5

TYPICAL PARAMETRIC PUMP PROCESS DESIGNS

	Lab Column	Single Tube	Pilot Plant	Plant
Rates, lb./hr. (ρ_f = 44.9 lb./ft.^{3})				
Feed, $Q(\emptyset_T + \emptyset_B)\rho_f$	0.0383	0.767	46.7	1796
Bot. Prod., $Q\emptyset_B\rho_f$	0.0143	0.288	17.5	674
Top Prod., $Q\emptyset_T\rho_f$	0.0240	0.479	29.2	1122
Reservoir, $Q\rho_f$	0.0956	1.917	116.7	4490
Solute conc., y/y_0				
Bot. Prod.	0	0	0	0
Top Prod.	1.6	1.6	1.6	1.6
Cycle time, min.				
Switchover	2	2	2	2
Half cycle, π/ω	20	20	20	20
Energies, BTU/lb. bottom product				
Heating				
Switchover	412	412	412	412
Half cycle	590	590	590	590
Refrigeration				
Switchover	412	412	412	412
Half cycle	662	662	662	662
Pumping (Total)	0.609	0.609	0.609	0.609
Equipment size				
No. tubes, N	1	1	55	2226
Length, h, ft.	3.28	13.9	15.4	14.8
Heat transfer fluid				
Rate, lb./sec.	0.00216	0.0433	2.64	101.4
Pressure drop, psi				
Column	0.025	10	10	10
Shell	neg'l	neg'l	1.6	60

Energy versus Equipment Size and Productivity

Energy equations relating heating, cooling, and pumping requirements to process parameters were developed in Appendix III from basic equations and from the process design concepts presented in the first two parts of this chapter. These equations relate energy (on a common BTU basis) to the reservoir displacement ($Q\pi/\omega$) for equipment size, to the bottom product/reservoir ratio ($\emptyset_B$) for productivity, to cycle time (π/ω), to reservoir displacement rate (Q), and to N, the number of tubes or columns in a parapump assembly. The length of these tubes (h) is indirectly included in the equations by a separate equation relating it to the column flowrate or tube velocity.

The key parameters are size ($Q\pi/\omega$) and productivity ($\emptyset_B$). The remaining parameters are usually fixed or directly tied to one of these through mathematical expressions. Equipment size ($Q\pi/\omega$) is related to energy on a BTU/cycle basis through Equations (III-45,50,52,57, 62,66, and 70). Productivity ($\emptyset_B$) is related to energy on a BTU/lb of bottom product basis through Equations III-47,51,53,58,63,67, and 71). Both sets of equations, in the case of pumping, were developed via equations for pressure drop and horsepower and these equations are also presented in Appendix III.

All of the equations in Appendix III are presented in full algebraic form and are thus applicable to any system. Since only the toluene-heptane-silica gel system will be discussed in this section, the Appendix III equations will immediately be simplified by assigning the following variables pertinent to the system and to water as the heat transfer fluid.

a_t, tube crossflow area, ft^2/tube   0.000881

b, dimensionless equilibrium parameter   0.22

c_f, process fluid heat capacity, BTU/lb/$^\circ$K   0.972

c_{HTF}, heat transfer fluid heat capacity

    BTU/lb/$^\circ$K   1.8
    BTU/lb/$^\circ$R   1.0

D_i, i.d. of the pipelines external to the column, ft   0.0833

D, outside diameter of each column, ft   0.0417

D_p, adsorbent particle diameter, ft 13.2×10^{-4}

g_c, gravitational conversion factor, lb_mxft to lb_fxhr^2 4.17×10^8

m_o, equilibrium constant, dimensionless   1.88

T_1, hot upflow temperature, $^\circ$K   343

T_2, cold downflow temperature, $^\circ$K   278

$(w_t c_t + w_s c_s + w_f c_f)$, heat capacity of column wall, the solid adsorbent, and the fluid calculated from Appendix IV data,

    BTU/$^\circ$K/ft of column height (h)   0.0874

ε, packed bed voidage, dimensionless   0.38

ΔT_w, temperature rise of heat transfer
    fluid, $^\circ R$ 15.2

τ, switchover time, seconds   120

ρ_f, process fluid density, lb/ft^3 44.9

ρ_{HTF}, heat transfer fluid density,
    lb/ft^3 62.3

μ_1, process fluid viscosity at T_1,
    $lb_m/hr/ft$ 0.678

μ_2, process fluid viscosity at T_2,
    $lb_m/hr/ft$ 1.283

μ_{BP}, bottom product viscosity $= \mu_2$

μ_{TP}, top product viscosity $= \mu_1$

μ_F, feed viscosity $= \mu_1$

From the above data, the value of K_h (Eq. III-48a) was found to be 850, and the value of K_w (Eq. III-54a), 2.65. Most data was from Appendix IV. Values of b, m_o, T_1, T_2, and ε, were given by Chen et al (1972).

The energy equations, simplified by use of the data presented above, are listed below. After each equation is the number of the original equation in Appendix III (to serve as a reference), and the new number of the simplified equation.

Heating duty (steam)(III-45, 47)

$$q_1 = Q\pi/\omega \quad \left[4830(1+\phi_B) + 2837(1-\phi_B)\right] \quad \text{BTU/cycle} \tag{99}$$

$$\frac{q_i}{P_B(2\pi/\omega)} = 53.78 \frac{1+\phi_B}{\phi_B} + 31.59 \frac{1-\phi_B}{\phi_B} \quad \text{BTU/lb BP} \tag{100}$$

Cooling duty (refrigeration)(III-52, 53)

$$q_2 = 7667 \; (Q\pi/\omega)(1+\phi_B) \quad \text{BTU/cycle} \tag{101}$$

$$\frac{q_2}{P_B(2\pi/\omega)} = 85.4 \frac{1+\phi_B}{\phi_B} \quad \text{BTU/lb BP} \tag{102}$$

Heat content of the shellside fluid (III-50, 51)

$$q_s = Q\pi/\omega)(1+\phi_B)(27,900N^{-0.0526}-8455)\text{BTU/cycle} \tag{103}$$

$$\frac{q_s}{P_B(2\pi/\omega)} = \frac{1+\phi_B}{\phi_B} \; (311N^{-0.0526}-94.2) \quad \text{BTU/lb BP} \tag{104}$$

Heat transfer fluid pump (III-57, 58, 54b)

$$q_{HTF} = 56.6(Q\pi/\omega)(\pi/\omega)(1+\phi_B)(\Delta p_{HTF}) \quad \text{BTU/cycle} \tag{105}$$

$$\frac{q_{HTF}}{P_B(2\pi/\omega)} = 0.63 \frac{1+\phi_B}{\phi_B} (\pi/\omega)(\Delta p_{HTF}) \quad \text{BTU/lb BP} \tag{106}$$

$$\Delta p_{HTF} = Q\frac{\pi}{\omega}^2 (1+\phi_B)^2 F_{N1} \left[\frac{11938}{N} Q\frac{\pi}{\omega}(1+\phi_B)-7\right] + \left[Q\frac{\pi}{\omega}(1+\phi_B)\right]^{2.8}$$

$$\left(\frac{9824F_{N2}}{N}\right) \tag{107}$$

Bottom reservoir pump (III-62, 63)

$$q_{BRP} = 1216 \ (1-\phi_B)^2 (1+\phi_B) \ (Q/N)^2 (Q\pi/\omega) \ (\pi/\omega) \ \text{BTU/cycle} \qquad (108)$$

$$\frac{q_{BRP}}{P_B(2\pi/\omega)} = 13.54 \ (1-\phi_B)^2 \ \frac{1+\phi_B}{\phi_B} \ (Q/N)^2 (\pi/\omega) \ \text{BTU/lb BP} \qquad (109)$$

Top reservoir pump (III-66, 67)

$$q_{TRP} = 2302 \ (1+\phi_B)^3 (Q/N)^2 (Q\pi/\omega) \ (\pi/\omega) \ \text{BTU/cycle} \qquad (110)$$

$$\frac{q_{TRP}}{P_B(2\pi/\omega)} = 25.63 \ (1+\phi_B)^2 \ \frac{1+\phi_B}{\phi_B} \ (Q/N)^2 (\pi/\omega) \ \text{BTU/lb BP} \qquad (111)$$

Feed pump (III-70, 71)

$$q_{FP} = 3.56 \times 10^{-4} (Q)(Q\pi/\omega) \ \left[(\phi_T + \phi_B)^2 + \phi_T^2 + 1.89\phi_B^2 \right]$$

$$+ \ 4594 \ (1+\phi_B)^3 (Q/N)^2 (Q\pi/\omega) \ (\pi/\omega) \ \text{BTU/cycle} \qquad (112)$$

$$\frac{q_{FP}}{P_B(2\pi/\omega)} = 3.96 \times 10^{-6} (Q/\phi_B) \ \left[(\phi_T + \phi_B)^2 + \phi_T^2 + 1.89\phi_B^2 \right]$$

$$+ \ 51.2 \ (1+\phi_B)^2 \ \frac{1+\phi_B}{\phi_B} \ (Q/N)^2 (\pi/\omega) \ \text{BTU/lb BP} \qquad (113)$$

Relative energy requirements. It is useful to know
the relative requirements for steam, refrigeration pumping,
and the residual heat content of the shellside fluid.
The various utilities can then be ranked as to their energy
requirements.

The most convenient method for presenting the relative
energy requirements is to use the equations for energy in
BTU/lb BP or cycle and reference them to the equation for
refrigeration. The equations listed below are therefore
in terms of BTU for the utility/BTU for refrigeration:

$$q_1/q_2 = 0.630 + 0.37(1-\phi_B)/(1+\phi_B) \tag{114}$$

$$q_s/q_2 = 3.64 \; N^{-0.0526} - 1.1 \tag{115}$$

$$q_{HTF}/q_2 = 0.00738 \; (\pi/\omega)(\Delta p_{HTF}) \tag{116}$$

$$q_{BRP}/q_2 = 0.159 \; (1-\phi_B)^2 (Q/N)^2 (\pi/\omega) \tag{117}$$

$$q_{TRP}/q_2 = 0.300 \; (1+\phi_B)^2 (Q/N)^2 (\pi/\omega) \tag{118}$$

$$q_{FP}/q_2 = 4.64 \times 10^{-8} \; Q/(1+\phi_B) \left[(\phi_T+\phi_B)^2 + \phi_T^2 + 1.89\phi_B^2\right]$$

$$+ 0.600 \; (1+\phi_B)^2 (Q/N)^2 (\pi/\omega) \tag{119}$$

Now if values are assigned to the variables in Equations (114) to (119), numerical ratios can be given. The values given for the process design example earlier in the chapter were 0.15 for $\emptyset_B$, 0.25 for $\emptyset_T$, and 0.333 hr for π/ω. For the 55 tube unit, values of Q and Δp_{HTF} of 2.6 ft^3/hr and 1.6 psi were given in Table (5) for the process design example. Eq. (107) also gave 1.6 psi. Substitution of these values gives the following numerical ratings:

steam	0.902
heat content of shellside fluid	1.85
heat transfer fluid pump	3.94×10^{-3}
bottom reservoir pump	8.57×10^{-5}
top reservoir pump	2.96×10^{-4}
feed pump	
line resistance	2.78×10^{-8}
column resistance	5.92×10^{-4}

Certain conclusions can be drawn from the ratings. The line resistances for the feed pump can be neglected (for the line sizes and flow rates chosen). The shell-side heat transfer fluid must be dumped to the appropriate reservoir at the end of each half cycle (an integral part of the design) or the energy requirements could be roughly tripled. Finally, in overall energy considerations, the pumps consume less than 1 percent of the total.

Energies versus reservoir displacement (equip. size).

The equations relating energies to reservoir displacement
$(Q\pi/\omega)$ (Eq. 99,101,103,105,108,110,112) were used with
values of 0.15 for $\emptyset_B$ and 0.333 hr for π/ω assigned as in
the case of the process design example presented earlier.
In the case of the pumping energies, it was necessary to
assign a pressure drop of 10 psi for the packed columns
during cold downflow. All other pressure drops for pumps
would have a lower pressure drop with the possible excep-
tion of the heat transfer pump (up to 60 psi for the
highest flow) and this can easily be lowered by a small
design change (see Eq. 98). Assigning this 10 psi pres-
sure drop allowed the values of Q and the corresponding
values of N to be selected from Figure (25). With these
values it was possible to include the pumping energies
along with those for heating and refrigeration in Fig.
(26).

Figures (26) and (27) give the energies and the
bottom product concentrations (purities) for any given
bottom product volume $(P_B 2\pi/\omega \text{ ft}^3/\text{cycle})$ and equipment
size $(Q\pi/\omega \text{ ft}^3$ of reservoir displacement). It is possible
to predict the equipment size, the amount of steam,
refrigeration, and pumping energies that will be needed
to produce a given volume of bottom product at a specified
purity.

For example, if a bottom rate of 3 ft^3/cycle and a product purity of $\langle Y_{BP} \rangle_\infty / Y_O$ of 0.55 is required, then a 10 ft^3 reservoir displacement is needed. The minimum energy requirements per cycle are 88,000 BTU for refrigeration, 80,000 BTU for heating, 3000 BTU equivalents for the heat transfer fluid pump, and 80 BTU equivalents for the feed and reservoir pumps. Now if the product purity must be increased to the maximum $\langle Y_{BP} \rangle_\infty / Y_O = 0$), the equipment size must be increased to 13.5 ft^3, and the energies to 120,000 BTU for refrigeration, 110,000 for heating, 6,000 BTU equivalents for the HTF pump and 110 BTU equivalents for the other pumps. Of course, the same purity could be achieved with the original equipment and energy requirements by reducing the product draw-off to 2.2 ft^3/cycle.

Thus the equipment and energy requirements can be predicted by specifying the product rate and purity. Conversely, the performance of existing equipment for a new application can also be predicted. It should be emphasized that the equipment and energy requirements need not be projected beyond the zero $\langle Y_{BP} \rangle_\infty / Y_O$ level unless it is desired to overspecify the system.
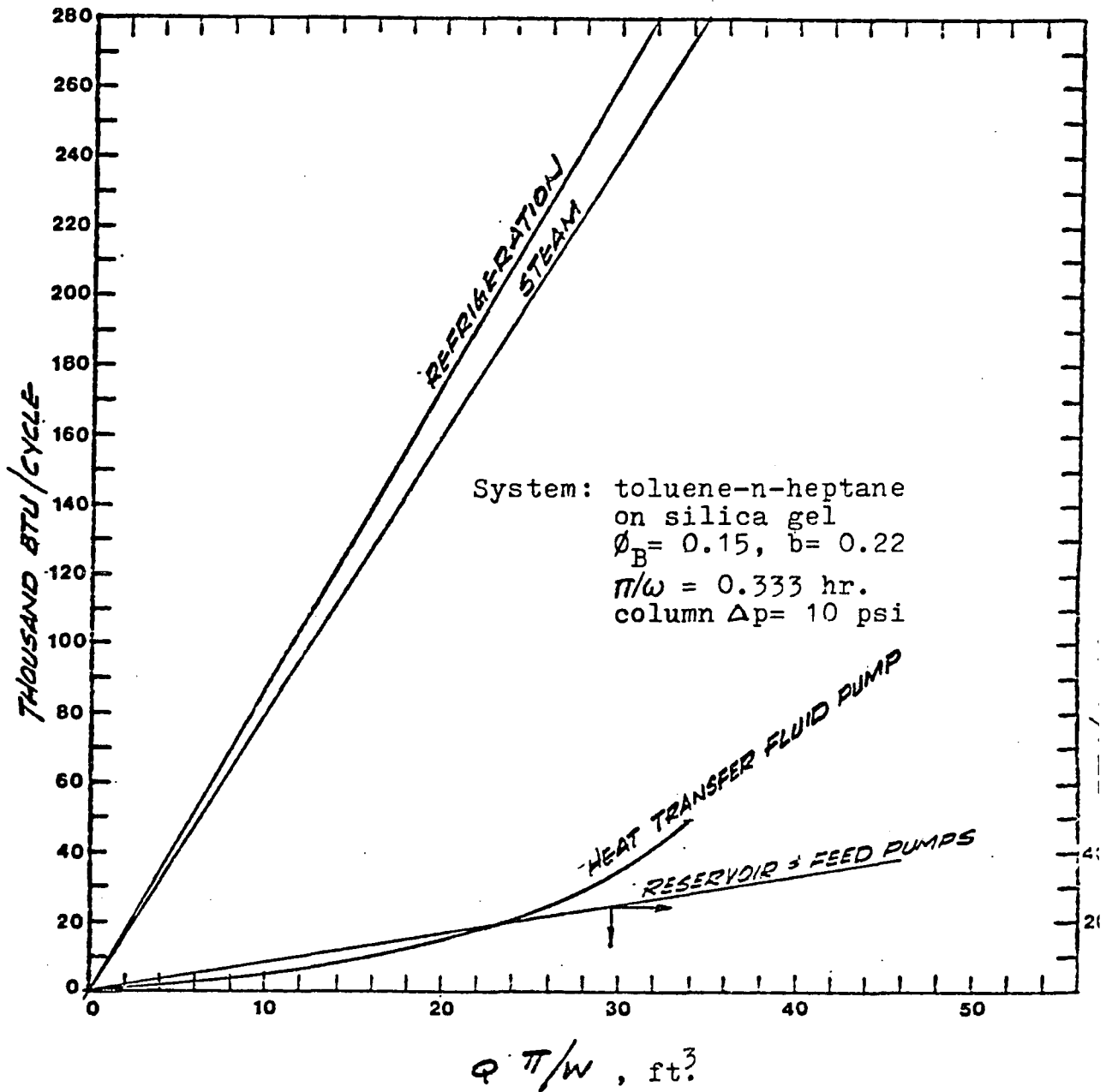
FIGURE (26)

Parametric Pumping Energies vs Reservoir
Displacement
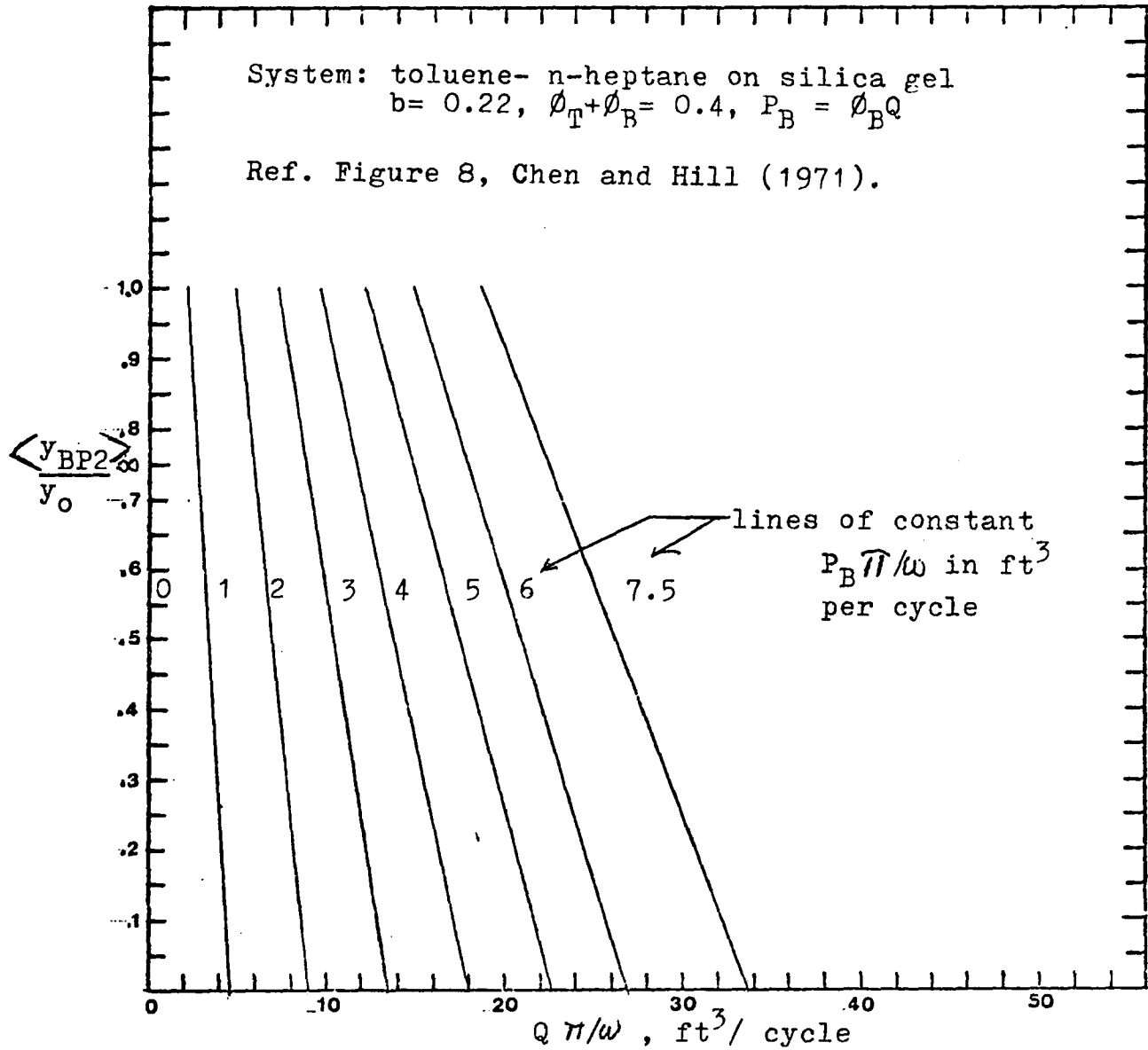
FIGURE (27)

Bottom Product Concentration vs Reservoir
Displacement

Energies versus bottom product/reservoir ratio.

The equations in this section (100,102,104,106,109,111, 113) relate the energies per pound of bottom product to the ratio of the bottom product take-off over the reservoir displacement ($\emptyset_B$). As before, the pressure drop in the packed columns was limited to 10 psi which, from Fig.(25) gave Q/N values of 0.0465 over the full range of reservoir displacements. This value of Q/N along with a value of 0.333 hr for π/ω was needed for the pumping energy equations. With these substitutions, the energy equations for the pumps were included in Figure (28), along with the energies for heating and refrigeration.

Figures (28) and (29) show how the key operating variable ($\emptyset_B$) can effect both the product quality and the energy consumption per pound of bottom product. As can be seen in Figure (29), the value of $\langle y_{BP} \rangle_\infty / y_O$ is zero (infinite separation) from a $\emptyset_B$ of zero (no bottom product take-off) to a value of 0.22, the value of b for the toluene in n-heptane (Chen et al, 1972). As explained by Chen and his co-workers, the pump is operating in the range of infinite separation when $\emptyset_B$ is less than b. When the bottom take-off is increased so that $\emptyset_B$ exceeds the value of b, solute appears in the bottom product stream and $\langle y_{BP} \rangle_\infty / y_O$ increases from zero to one as

$\emptyset_B$ is increased from 0.22 to 0.4. At 0.4, the volume of the bottom product stream is equal to that of the feed stream and, of course, there is no separation.

Figure (28) shows the corresponding effect on the energies. In the range of $\emptyset_B$ from zero to b (0.22), the energies in BTU/lb of bottom product decrease from infinity to finite values. Also, according to Figure (29), the solute separation is complete and there is no benefit derived from the higher energy consumptions. At $\emptyset_B$ = 0.22, the consumptions are 490 BTU/lb. of bottom product for refrigeration, 410 for heating, 2.2 BTU equivalents for the heat transfer fluid pump, and 0.5 BTU equivalents for the feed and reservoir pumps.

As the value of $\emptyset_B$ continues to increase, the energy consumptions decrease to the lower limits of 300 for refrigeration, 240 for heating, 2.0 for the heat transfer fluid pump, and 0.4 for the feed and reservoir pumps. Of course at this point, the separation is nil and there is no point in operating the column. It is up to the operator to select the operating level between $\emptyset_B$ of 0.22 and 0.4 that will give the required separation $\langle y_{BP}\rangle_\infty / y_o$ between zero and one, and to estimate the utility consumptions accordingly.

System: toluene- n-heptane on
        silica gel
        b= 0.22
        column pressure drop = 10 psi
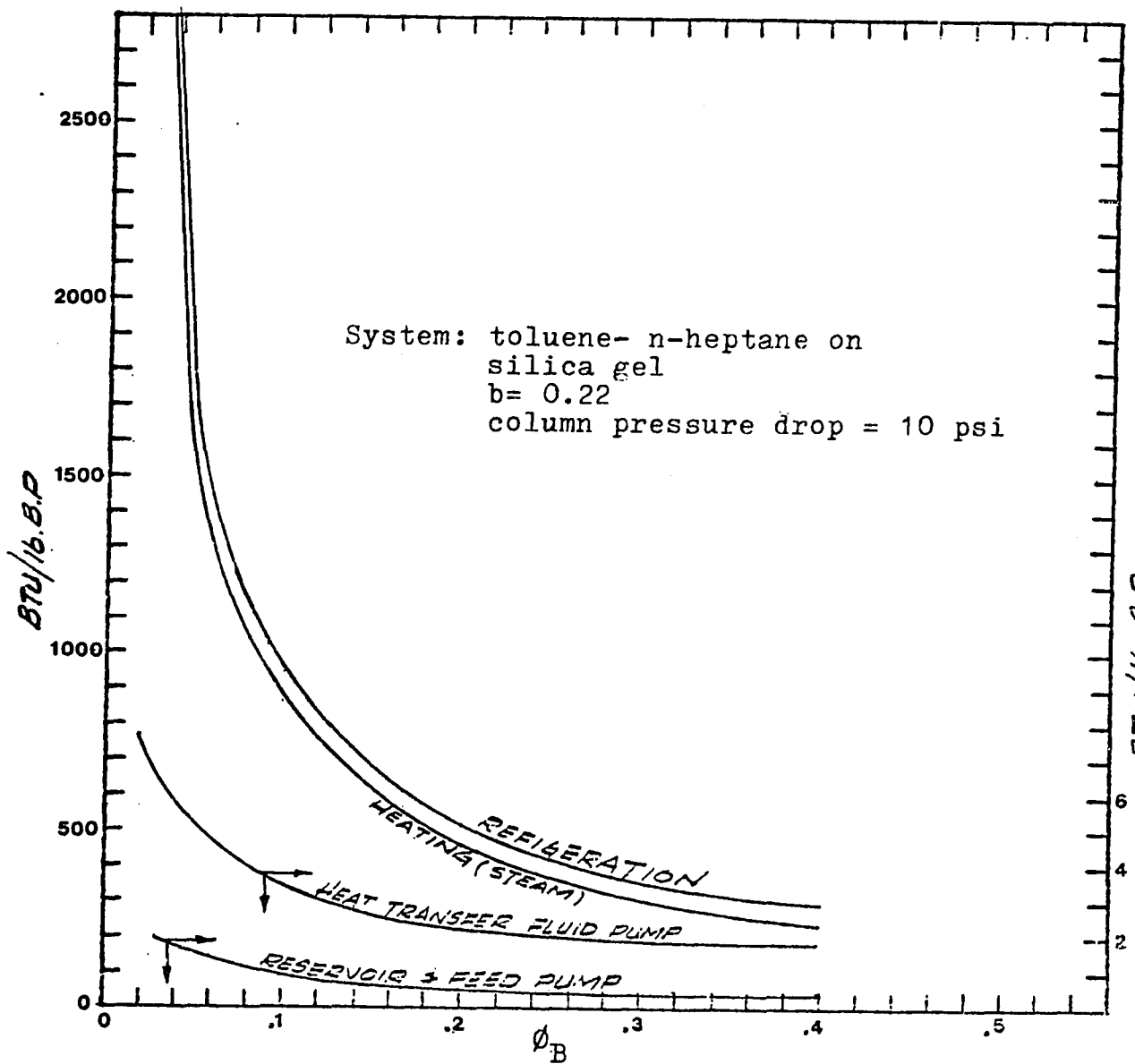
FIGURE (28)

Parametric Pumping Energies vs Bottom
Product/ Reservoir Ratio
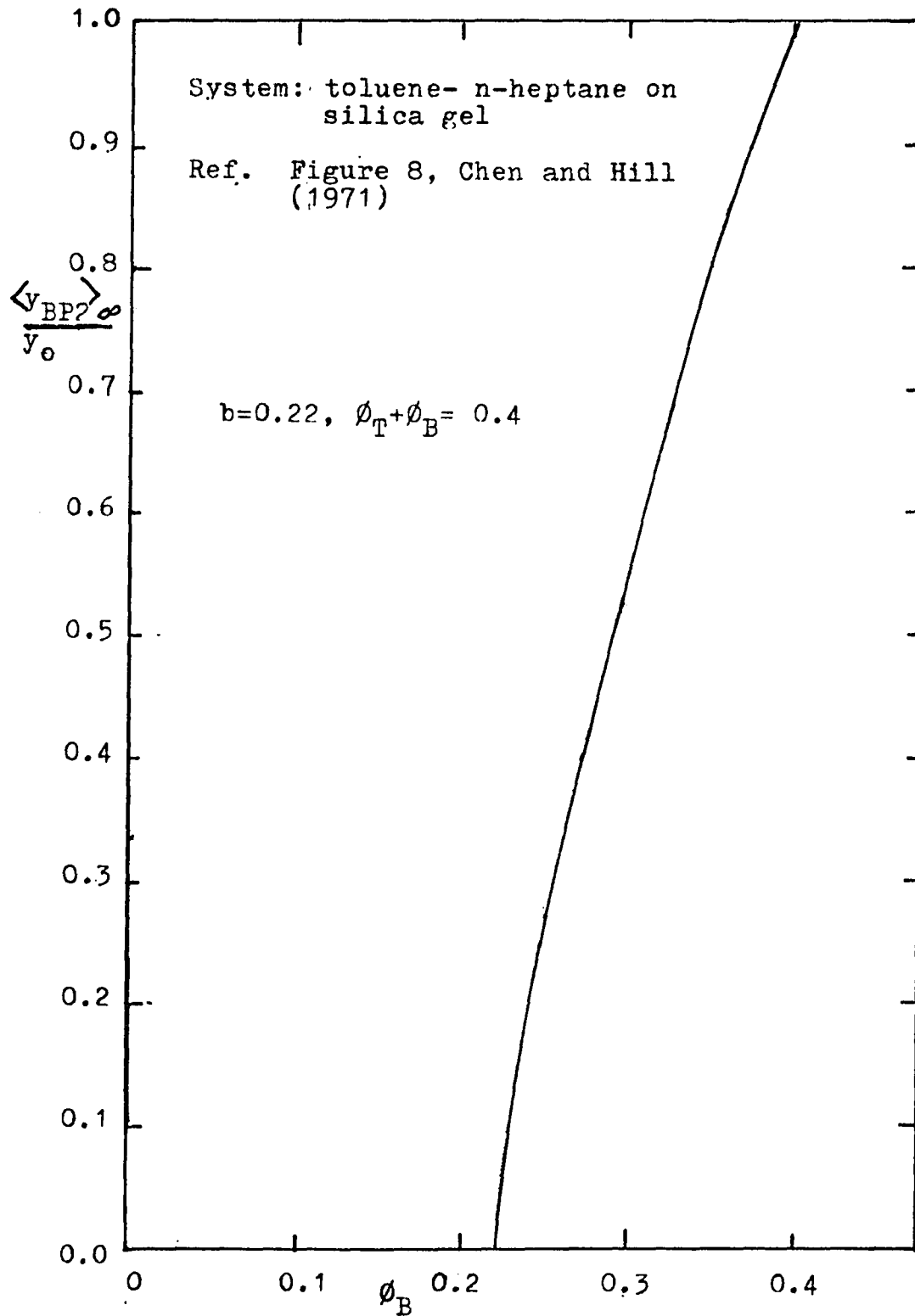
FIGURE (29)

Bottom Product Concentration vs ϕ_B

Comparison of Energies with Distillation Energies.

The energy consumption for parametric pumping is the same order of magnitude as other means of separation, such as distillation. If, for simplicity, the sensible heat requirements for distillation are neglected, the total heat requirements for the condenser and reboiler are easily shown to be $2\lambda_V$ (where λ_V is the latent heat of vaporization) BTU/lb of product for a simple stripping column (comparable to a Region 2 type of separation) and $2\lambda_V(R+1)$ for a fractionating column (comparable to a Region 1 separation). Now for parametric pumping, the total heating and cooling requirements are given by summing Equations (100, 103) to give

$$\frac{q}{2P_B\pi/\omega} = \frac{170.8}{\emptyset_B} + 107.6$$

If toluene is the compound being separated in both cases, then we have in Table 6,

TABLE 6

ENERGIES: PARAMETRIC PUMPING VS. DISTILLATION

Distillation Type	Moderate Separation Stripping Column	Good Separation Fractionator
Condenser, Reboiler, q	$2\lambda v$	$2\lambda_v (R+1)$
Reflux Ratio, R	0	3
Duties, BTU/lb product	311	1246
Parametric Pumping Operation	**Region 2**	**Region 1**
Heating and Cooling, q	$170.8/\emptyset_B + 107.6$	$170.8/\emptyset_B + 107.6$
Bottom Product Ratio, $\emptyset_B$	0.35	0.22
Duties, BTU/lb product	596	900

Commercial Scale Parametric Pumping System

The heart of the system is the parapump column
assembly described in the first two parts of this chapter.
But of course this unit must be augmented by auxiliary
tanks, pumps, and other equipment, and the entire system
must be instrumented. The design of this auxiliary equip-
ment is standard and not pertinent to this work. Never-
theless, it is useful to briefly describe the operation
of this equipment and thus point out what is required for
a complete parametric pumping system.

The parametric pumping system may be conveniently
divided into four sections: the parapump column assembly;
the process reservoir tanks, pumps, and controls; the
process feed and product tanks, pumps, and controls; and
the heat transfer reservoir tanks, pumps, and controls.
The supporting systems for (refrigeration) cooling and
(steam) heating are also required but are not described
because these systems are usually present as utilities in
most large chemical plants.

The equipment is all listed in Table (7) and is shown
in the diagram in Figure (30).

TABLE 7

PARAPUMP SYSTEM EQUIPMENT LIST

	Pos. No.	Description
Tanks	T1	Bottom Reservoir
	T2	Top Reservoir
	T3	Hot Heat Transfer Fluid Reservoir
	T4	Cold Heat Transfer Fluid Reservoir
	T5	Feed Tank
	T6	Bottom Product Receiver
	T7	Top Product Receiver
Pumps	P1	Feed Pump
	P2	Bottom Reservoir Pump
	P3	Top Reservoir Pump
	P4	Heat Transfer Fluid Pump
Exchanger	E1	Parapump Column Assembly
Agitators	M1	Bottom Reservoir Mixing Tee
	M2	Top Reservoir Mixing Tee
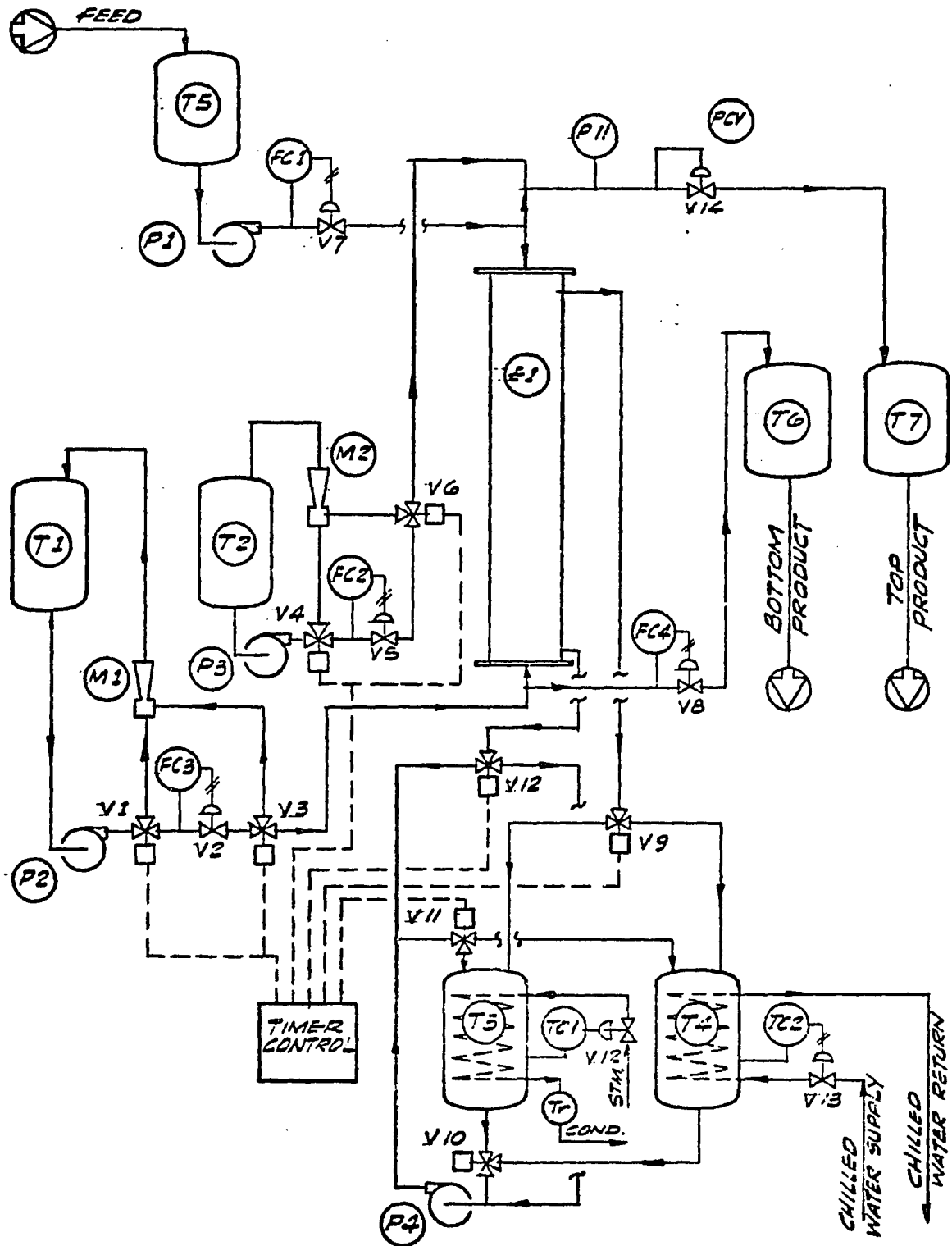
FIGURE (30): Parapump System Diagram

Process description. At the start of the hot upflow
half cycle, the timer control switches valves (V1,V3,V4,
V6) and the bottom reservoir process fluid is pumped (P2)
under flow control (FC3,V2) through the parapump column
(E1) and into the top process reservoir (T2) via the
mixing tee (M2) where it is thoroughly mixed with top
reservoir process fluid pumped (P3) around the recycle
loop.

At the same time, valves (V9,V10,V11,V12) are set
so the hot water is pumped (P4) from the hot fluid reser-
voir (T3) into the bottom inlet shellside nozzle of the
parapump column (E1). The hot heat transfer fluid leaving
the top shellside nozzle (E1) flows through valve (V9) and
back into the hot fluid reservoir (T3). Since the water
reentering the reservoir has been cooled, the reservoir
temperature starts to drop and the temperature controller
admits steam to the coil to maintain the hot fluid tem-
perature.

Just prior to the end of the hot half cycle, valves
(V10,V11,V12) are switched to divert the flow to the suc-
tion side of pump (P4) from the hot fluid reservoir (T3)
to the inlet shellside nozzle (E1). Also, the discharge
side of pump (P4) is diverted from the inlet shellside

nozzle (E1) to the top of the hot fluid reservoir (T3).
Then the hot heat transfer fluid is pumped out of the
parapump (E1) shell and back into the reservoir so that
it will not mix with the cold heat transfer fluid at the
start of the cold downflow half cycle.

Continuously, throughout the hot upflow and cold
downflow half cycles, process feed is pumped (P1) from
the feed tank (T5) to the top of the parapump column (E1)
under flow control (FC1,V7). The top product process
fluid leaving the parapump (E1) flows through a back
pressure valve (PCV) and into the top product tank (T7).
The bottom product flows from the bottom of the parapump
column (E1) under flow control (FC4,V8) and into the
bottom product tank (T6). By means of this instrumentation
scheme, the flow rates of all streams are regulated, the
column is kept under a constant back pressure, and air
or gas which could affect the adsorption is kept out of
the parapump column.

At the start of the cold downflow half cycle, valves
(V1,V3,V4,V6) in the process reservoir system are switched.
Fluid from the top reservoir (T2) is now pumped (P3) into
the top of the parapump column (E1). The effluent from
the bottom enters the bottom process reservoir (T2),

being thoroughly mixed with the reservoir contents via the mixing tee (M1) and recycling pump (P2).

At the same time, valves (V9,V10,V11,V12) are switched so the cold water is pumped (P4) from the cold fluid reservoir (T4) into the bottom inlet shellside nozzle of the parapump column (E1). The cold heat transfer fluid leaving the top shellside nozzle (E1) flows through valve (V9) and back to the cold fluid reservoir (T4). Since the water reentering the reservoir has been heated, the reservoir temperature starts to rise and the temperature controller admits chilled water to the coil to maintain the cold fluid temperature.

Just prior to the end of the cold half cycle, valves (V10,V11,V12) are switched and the residual cold water in the shell is pumped back into the cold fluid reservoir in the same manner as previously described for the end of the hot half cycle. At this point, the entire procedure is repeated as described above.

Details of the column assembly. The parapump column assembly is basically a heat exchanger, each tube being a packed column. The columns (or tubes) are 0.5 inch o.d. 18 BWG mounted in an 11/16 inch triangular pitch. The tube size was selected as the equivalent of the

laboratory columns used for parametric pumping in which
the 0.402 inch inside diameter equals the approximate
1 centimeter diameter of the laboratory columns.

The number of tubes and their length are related to
the fluid velocity or flow rate in the tubes, the rela-
tionship having been shown in the design example.

The distribution of the fluid to the tubes is impor-
tant. The fluid flows into a special flat cylindrical
head, through a distributor and into the tubes. The key
to good distribution is that the lateral pressure drop
between the tubes must be less than one tenth that of
the perpendicular pressure drop (in the direction of the
tube axis) through the distributor. One way to achieve
this is with an orfice plate, the hole diameters being
calculated by the usual orfice formulas. Another way
would be the use of a sintered filter plate, the pressure
drop across the plate being a function of the porosity.

The tubes are held together in a bundle by the
shellside baffles and the bundle assemble is contained
in a cylindrical shell, usually a pipe of standard nominal
size. The relationship between the shell diameter and the
number of tubes is shown in Table (3). Since the pres-
sure drop is related to the shell diameter, it is also

related to the number of tubes of a given diameter and
spacing (pitch). And since the shellside fluid flows
in a particular pattern, the pressure drop is predictable,
being a function of the flow rate and number of tubes.

The details of the parapump assembly as described
above are illustrated in Figure (31).
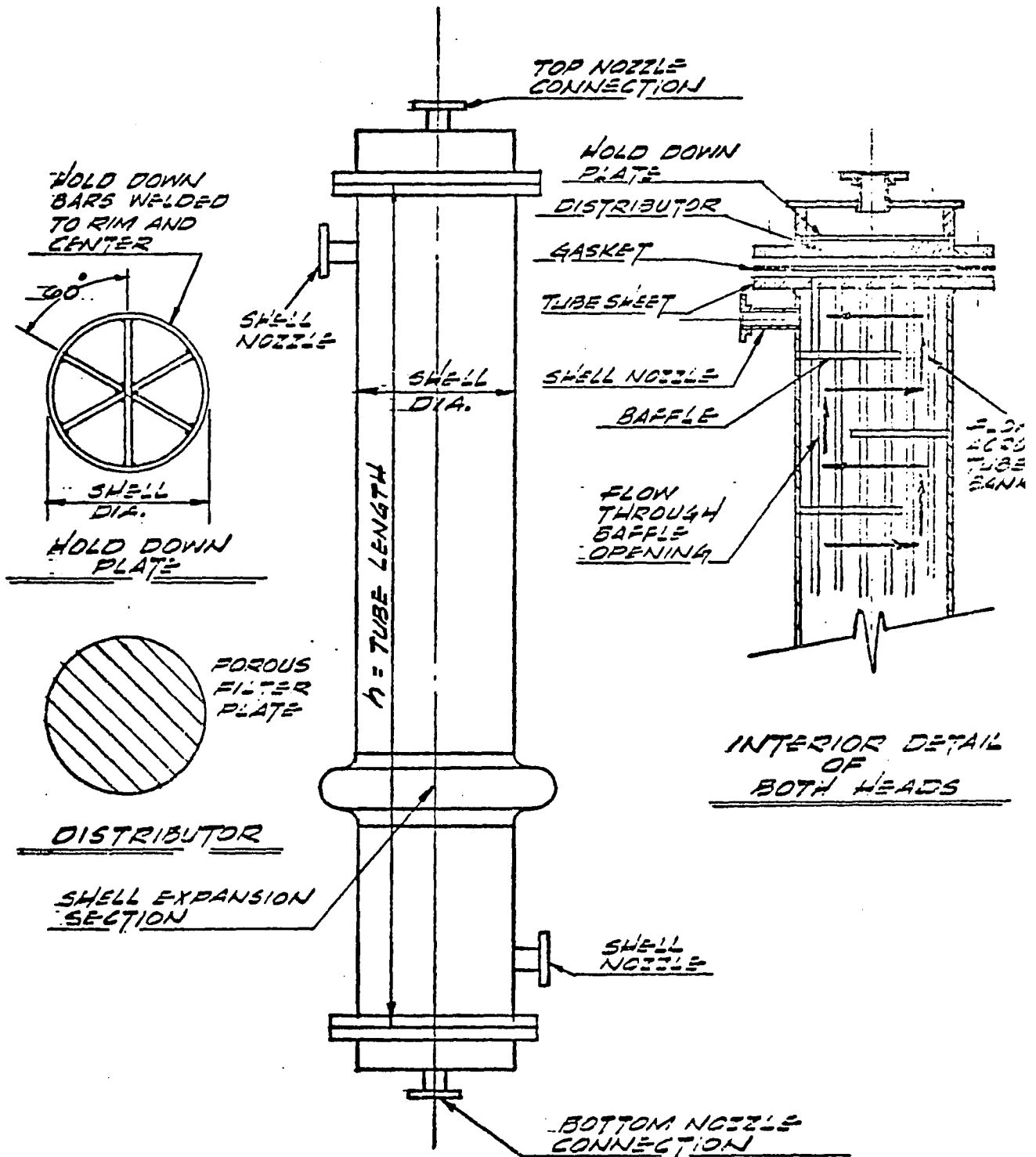
FIGURE (31)

Parapump Column Assembly

Operational and Design Changes

Design criteria review. At the beginning of the
chapter it was stated that the basis for designing para-
metric pumps is the same for multicomponent and binary
systems. This design basis can be more easily understood
if the key equations (Eq. 74,75) are combined and rearranged
to give a dimensionless packed bed volume.

$$\frac{Nha_t\varepsilon}{Q\pi/\omega} \geqq \frac{(1+\emptyset_B)}{(1+b_i)(1+m_{oi})} \tag{120}$$

which incorporates the principal design parameters. The
numerator of the dimensionless volume is equal to the
total packed bed void volume and the denominator is equal
to the reservoir displacement.

The inequality stems from the criteria (Eq. 23)
necessary for complete removal of solute from the bottom
product stream. Due to the usual values of $\emptyset_B (<1)$, b_i
(<1), and $m_{oi} (>1)$, the dimensionless void volume is less
than unity and this means that the reservoir volume
will be larger than the void volume of the packed bed.
Another criteria requires that $\emptyset_B \leq bi$, and for the multi-
component system (Eq. 34) this means that

$$b_1 > b_2 > \text{-----} > b_k \geq \emptyset_B > b_{k+1} \text{-----} > b_s$$

All solute with values of b_i greater than ϕ_B will
theoretically be removed from the bottom product stream.
In the extreme case where k = s, the bottom stream would
consist only of pure solvent. This is the case with the
binary system used for the design example except that
$b_k = b_s = 0.22$ for toluene and toluene was the only solute.
Thus the normal design range of ϕ_B for the multicomponent
system would be similar to that of the binary system
except that the upper limit would be b_k and the lower
limit would not be zero but rather b_{k+1}. For example,
if a solute with $b_{k+1} = 0.1$ were added to the toluene-
heptane binary, the design criteria for the new system
would be identical to the binary--the only difference
being that, in actual operation, the bottom product would
now contain the new solute as well as the heptane solvent.

Operational changes on an existing system. The
equipment designed for a solute split in a multicomponent
system could be used for another split in the same general
system provided the values of b_k and m_{ok} were both known.
The value of ϕ_B would be adjusted so as to keep the
dimensionless void volume (Eq. 120) constant. The effect
of adjusting ϕ_B on the energies can best be determined by
examining the energy equations in Appendix III (Eq. III-
45,47,52,53,58,62,63,66,67,70,71). But, simply stated,

if $\emptyset_B$ is reduced (smaller bottom product stream), the
following energy changes occur. All energies as BTU/lb
bottom product increase because of the smaller amount
of bottom product withdrawn from the system. However
the rate (BTU/hr) of heat supplied for hot upflow and
the pumping requirement for hot upflow both increase
as a result of the increased volume of flow in the
packed bed. Also, the rate of cooling (BTU/hr) and
also the reservoir pumping and feed pumping requirements
for cold downflow decrease because less fluid is pumped
down the packed columns during the cold downflow half
cycle.

Now if $\emptyset_B$ is increased (instead of reduced) the
energy changes are in reverse of those described above
to account for the decrease in column flow during hot
upflow and the increase during cold downflow.

To summarize, the normal design for a multicomponent
system is the same as for the binary--the design value
of $\emptyset_B$ is equal to or slightly less than the value of b_i
immediately above it. If the widest possible range of
operation is desired, the lowest values of b_i and m_{oi}
should be used for design. Then the pump could be used
for the lowest solute split (solute with the lowest
value of b_i). Then, with the same equipment, higher

splits could be made by increasing $\emptyset_B$ to allow for the
higher values of b_i. This would be done at the expense
of decreasing $\emptyset_T$ (smaller top product stream) until $\emptyset_T$
was reduced to zero. Up to this point, the energies
would have to be modified to allow for increasing $\emptyset_B$.
If $\emptyset_T$ were to become zero as a result of increasing $\emptyset_B$,
the parapump assembly itself $(Nha_t\varepsilon)$ would have to be
made larger to allow for the larger $Q\pi/\omega$ due to the need
for a larger feed stream.

CHAPTER 6

DISCUSSION AND CONCLUSIONS

In this dissertation, the emphasis has been on the separation of solutes from multicomponent mixtures in both dilute and concentrated solutions, and on the design and scale-up of a multi-tube parametric pump assembly for operation in the direct thermal mode.

Separation of solutes from dilute multicomponent solutions was shown to be predictable from binary information. It was demonstrated that dilute multicomponent solutions could be treated as pairs of pseudo binary systems, each system comprising one solute as one component and the common solvent as the other component. The mathematical model used for predicting separations was obtained by adapting the binary model to multicomponent use. This model consisted of the analytical solutions to the basic mass balance, equilibrium, and rate expressions commonly used for parametric pumping and was based on the equilibrium theory. The calculated product concentration profiles with time were in reasonable agreement with the experimental results for the toluene-aniline-n-heptane-silica gel system.

The separation of solutes from concentrated multi-component solutions could not be predicted by simple

analytical solutions to the basic mass balance, equilibrium, and rate expressions. It was necessary to resort to computer calculations and numerical solutions via the method of characteristics. The computed concentration profiles agreed reasonably well with the experimental results. The basic parameters affecting the separations were the bottom product rate, the cycle time, and, of course, the solute concentrations in the feed. The separation of solute(s) from the bottom product stream was significantly increased by decreasing the bottom product rate and increasing the cycle time. The column became saturated and the separation capability dropped off sharply as the total solute concentrations reached 40 volume percent.

Significantly, the mathematical model for the separation from concentrated solutions dealt with the mass transfer and equilibria of individual solutes. Equilibrium expressions dealing with the interplay of all the solutes were not successfully incorporated into the model. Apparently, in the case of the toluene-acetophenone-n-heptane-silica gel system used for the work with concentrated solutions, the effect of the concentration of the individual solutes was more significant then the interplay between solutes.

Separation of solutes from multicomponent systems on
a commercial scale has often been mentioned in connection
with parametric pumping. To this end, design equations
based on the analytical equations of the dilute solution
theory were developed and presented. The pilot plant and
commercial systems described take the form of multi-tube
units in a heat exchanger configuration to permit opera-
tion via direct thermal mode where rapid temperature
changes between the hot and cold half-cycles are essential.
Construction of these units is probably feasible as
described, and the energies (steam, refrigeration,
electrical) required were shown to be of the same order
of magnitude as other separation techniques such as
distillation. Energy consumption was also shown to vary
with separation efficiency. The practical operating range
of solute separations from 50-100% required 590-900 BTU
per lb. of product for the system studied as compared to
310 to 1,250 for distillation.

In addition to the design of the parametric pumping
assembly itself, a description of a complete system in-
cluding auxilliary equipment (tanks, pumps) and instrumenta-
tion is shown along with a process description of the
operation.

APPENDIX I

PARAMETRIC PUMPING RUNS FOR SOLUTE CONCENTRATION EFFECT

EXPERIMENTAL DATA

Run No. 1

Run No. 1 was a short test run to test the parametric pumping equipment. The duration was four 40-minute cycles, each hot upflow and cold downflow half cycle (π/ω) lasting 20 minutes. The feed concentration (y_o) was 2.5 volume % toluene in n-heptane. The ratio of bottom product to reservoir displacement ($\emptyset_B$) was 0.15. The ratio of feed to reservoir displacement ($\emptyset_T + \emptyset_B$) was 0.40. The reservoir displacement ($Q\pi/\omega$) was 20 cc. The hot half cycle temperature (T_1) was $70^\circ C$. and the cold half cycle temperature (T_2) was $25^\circ C$.

Run No. 2

Conditions: Binary system- dilute.

π/ω = 20 min.; $Q\pi/\omega$ = 35 cc.

y_O = 2.5 vol. % acetophenone in n-heptane

ϕ_B = 0.1; $\phi_T + \phi_B$ = 0.40

T_1 = 70°C.; T_2 = 25°C.

Run No. 2 was generally successful and lasted for 16 cycles. The sample containers, however, were not solvent tight and the analyses were unacceptable. The sample containers (snap-on type) were replaced with screw-cap type vials and the run was repeated (see Run No. 4).

Run No. 3

Conditions: Binary system- dilute n-heptane solution

y_{o1} (toluene) = 2.5 vol. %; y_{o2} (acetophenone) = 0

π/ω = 20 min.; $Q\pi/\omega$ = 35 cc

$\varnothing_B$ = 0.035; $\varnothing_B + \varnothing_T$ = 0.400

T_1 = 70°C; T_2 = 25°C

Cycle No.	Temp. °C	Feed cc	Top Product cc	y_1/y_{o1}	y_2/y_{o2}	Bottom Product cc	y_1/y_{o1}	y_2/y_{o2}
1	71	14	6.8	–	–	1.5	–	–
1	23	14	6.4	0.663	0	1.1	0.949	0
2	70.5	14	7.2	–	–	1.6	–	–
2	24	14	6.8	0.989	0	1.2	0.731	0
3	70.5	14	7.4	–	–	1.4	–	–
3	25	14	6.8	1.214	0	1.0	0.436	0
4	71	14	10.0	–	–	1.4	–	–
4	25	14	6.2	1.241	0	1.3	0.381	0
5	71	14	10.8	–	–	1.3	–	–
5	25	14	8.0	1.171	0	1.0	0.215	0
6	71	14	8.8	–	–	1.0	–	–
6	24	14	9.0	1.581	0	1.2	0.144	0
7	71	14	10.5	–	–	1.2	–	–
7	25	14	10.8	1.519	0	1.6	0.0967	0
8	70.5	14	12.2	–	–	1.1	–	–
8	24.5	14	8.0	1.567	0	1.5	0.0711	0
9	71	14	14.5	–	–	1.2	–	–
9	25	14	12.0	1.696	0	1.3	0.0515	0
10	70.5	14	7.5	–	–	1.0	–	–
10	24.5	14	9.1	1.291	0	1.0	–	0

Run No. 4

Conditions: Binary system- dilute n-heptane solution

y_{o1} (toluene) = 0; y_{o2} (acetophenone) = 2.5 vol. %

π/ω = 20 min.; $Q\pi/\omega$ = 35 cc

$\emptyset_B$ = 0.035; $\emptyset_T + \emptyset_B$ = 0.400

T_1 = 70°C; T_2 = 25°C

Cycle No.	Temp. ^{o}C	Feed cc	Top Product cc	y_1/y_{o1}	y_2/y_{o2}	Bottom Product cc	y_1/y_{o1}	y_2/y_{o2}
1	70	14	5.4	–	–	1.1	–	–
1	25	14	6.2	0	0.337	1.2	0	0.893
2	71	14	9.3	–	–	1.2	–	–
2	25	14	9.6	0	0.468	1.2	0	0.420
3	70	14	10.8	–	–	1.2	–	–
3	25	14	6.8	0	0.707	1.1	0	0.128
4	70	14	13.7	–	–	1.3	–	–
4	25	14	9.0	0	0.823	1.1	0	0.108
5	70	14	12.8	–	–	1.4	–	–
5	25	14	10.8	0	0.822	1.2	0	0.037
6	71	14	9.2	–	–	1.0	–	–
6	25	14	8.6	0	0.991	2.0	0	0.028
7	71	14	12.2	–	–	1.2	–	–
7	25	14	9.2	0	0.853	1.2	0	0.038
8	71	14	11.0	–	–	2.4	–	–
8	25	14	11.2	0	0.872	0.6	0	0.009
9	71	14	10.0	–	–	1.0	–	–
9	25	14	8.6	0	1.060	1.0	0	0.008
10	71	14	13.7	–	–	1.2	–	–
10	25	14	9.6	0	0.885	1.1	0	0.004
11	71	14	16.0	–	–	1.1	–	–
11	25	14	10.8	0	0.800	1.2	0	0.002
12	70	14	12.0	–	–	1.2	–	–
12	25	14	11.2	0	0.983	1.0	0	0.001
13	70	14	14.8	–	–	1.3	–	–
13	25	14	11.0	0	1.040	1.2	0	0.0007
14	70	14	11.8	–	–	1.4	–	–
14	25.5	14	7.0	0	0.980	1.3	0	0
15	71	14	16.0	–	–	1.3	–	–
15	25	14	12.2	0	1.040	1.1	0	0
16	71.2	14	12.8	–	–	1.2	–	–
16	26	14	10.4	0	0.880	1.1	0	0

Run No. 5

Conditions: Ternary system- conc. n-heptane solution

y_{o1} (toluene) = 10; y_{o2} (acetophenone) = 10 vol. %

π/ω = 20 min.; $Q\pi/\omega$ = 25 cc

$\emptyset_B$ = 0.25; $\emptyset_T + \emptyset_B$ = 0.40

T_1 = 70°C; T_2 = 25°C

Cycle No.	Temp. °C	Feed cc	Top Product			Bottom Product		
			cc	y_1/y_{o1}	y_2/y_{o2}	cc	y_1/y_{o1}	y_2/y_{o2}
1	71	10	1.6	–	–	1.5	–	–
1	25	10	1.4	1.03	0.790	3.0	1.01	0.514
2	71	10	3.4	–	–	6.25	–	–
2	25	10	2.0	1.18	0.839	5.7	0.594	0.219
3	71	10	3.65	–	–	6.1	–	–
3	25	10	1.3	1.17	0.911	6.0	0.487	0.117
4	71	10	4.9	–	–	6.5	–	–
4	25	10	0.7	1.49	0.875	5.9	0.647	0.0443
5	71.2	10	3.6	–	–	6.1	–	–
5	25	10	1.3	1.19	1.140	5.8	1.02	0.0400
6	71	10	4.1	–	–	6.3	–	–
6	25.5	10	2.0	1.14	1.27	6.2	1.22	0.0265
7	71.1	10	4.0	–	–	6.2	–	–
7	25.5	10	2.1	1.03	1.31	6.2	1.35	0.0167
8	71	10	2.8	–	–	6.2	–	–
8	25	10	1.6	0.896	1.19	6.1	1.36	0.0129
9	71.1	10	3.7	–	–	6.2	–	–
9	24.5	10	1.3	0.893	1.39	6.2	1.30	0.0449
10	71	10	4.1	–	–	6.2	–	–
10	24.5	10	1.8	0.957	1.45	6.2	1.22	0.240
11	71	10	4.8	–	–	6.3	–	–
11	25	10	1.2	0.957	1.49	6.4	1.18	0.383
12	71	10	4.5	–	–	6.3	–	–
12	25	10	2.3	0.958	1.46	5.9	1.12	0.477
13	71.2	10	5.2	–	–	6.2	–	–
13	25.1	10	1.6	0.957	1.51	6.0	1.10	0.719
14	71	10	4.2	–	–	6.25	–	–
14	25	10	1.3	0.950	1.52	6.25	1.08	0.615
15	71	10	3.8	–	–	6.2	–	–
15	25	10	1.7	0.978	1.44	5.95	1.05	0.684
16	71	10	3.7	–	–	6.2	–	–
16	25.3	10	1.1	0.956	1.56	6.1	1.03	0.777

Run No. 6

Conditions: Ternary system- dilute n-heptane solution

y_{o1} (toluene) - 2.5; y_{o2} (acetophenone) - 2.5 vol. %

π/ω = 20 min.; $Q\pi/\omega$ = 25 cc

$\emptyset_B$ = 0.25; $\emptyset_T + \emptyset_B$ = 0.40

T_1 = 70°C; T_2 = 25°C

Cycle	Temp.	Feed	Top Product			Bottom Product		
No.	°C	cc	cc	y_1/y_{o1}	y_2/y_{o2}	cc	y_1/y_{o1}	y_2/y_{o2}
1	71	10	2.4	–	–	4.2	–	–
1	25	10	1.0	0.997	0.881	5.2	0.746	0.416
2	71	10	5.0	–	–	6.25	–	–
2	26	10	1.0	1.23	0.696	6.1	0.478	0.126
3	71	10	3.7	–	–	6.2	–	–
3	24	10	1.4	1.34	0.953	5.8	0.377	0.100
4	71.1	10	3.6	–	–	6.2	–	–
4	25	10	1.5	1.36	1.27	6.2	0.288	0.040
5	71	10	3.6	–	–	6.2	–	–
5	25	10	1.0	1.25	1.69	6.0	0.246	0.035
6	71	10	2.0	–	–	6.3	–	–
6	25.1	10	2.1	1.48	1.46	5.8	0.219	0.024
7	71	10	5.0	–	–	6.3	–	–
7	25	10	2.0	1.29	1.52	6.1	0.124	0.010
8	71	10	1.0	–	–	5.8	–	–
8	25.1	10	0.8	1.65	1.43	6.2	0.133	0.007
9	71	10	3.7	–	–	6.2	–	–
9	25	10	1.0	1.47	1.90	7.2	0.189	0.007
10	71	10	3.8	–	–	5.6	–	–
10	24.9	10	2.3	1.30	1.63	5.8	0.253	0.005
11	71.5	10	3.1	–	–	6.4	–	–
11	25	10	1.4	1.30	2.11	6.2	0.349	0.005
12	71	10	5.2	–	–	6.2	–	–
12	25	10	1.6	1.56	1.77	6.1	0.435	0.005
13	71	10	4.7	–	–	6.25	–	–
13	25	10	1.7	1.54	1.84	6.0	0.481	0.002
14	71.2	10	4.2	–	–	6.4	–	–
14	24.9	10	3.5	1.43	1.90	6.2	0.587	0.001
15	71	10	3.5	–	–	6.2	–	–
15	25	10	2.1	1.35	1.97	6.2	0.709	0.001
16	71.2	10	3.8	–	–	7.0	–	–
16	24.9	10	1.3	1.35	1.94	5.7	0.739	0

Run No. 7

Conditions: Ternary system- conc. n-heptane solution

y_{o1} (toluene) = 10; y_{o2} (acetophenone) = 10 vol. %

π/ω = 20 min.; $\Omega\pi/\omega$ = 25 cc

ϕ_B = 0.035; $\phi_T + \phi_B$ = 0.400

$T_1 = 70°C$; $T_2 = 25°C$

Cycle No.	Temp. °C	Feed cc	Top Product			Bottom Product		
			cc	y_1/y_{o1}	y_2/y_{o2}	cc	y_1/y_{o1}	y_2/y_{o1}
1	71.1	10	7.8	-	-	1.0	-	-
1	24.1	10	4.0	0.959	0.567	0.8	1.00	0.542
2	71	10	11.0	-	-	0.8	-	-
2	24	10	7.5	1.00	0.636	0.8	0.804	0.286
3	71.2	10	11.0	-	-	1.0	-	-
3	23	10	7.0	1.04	0.775	0.9	0.685	0.178
4	71	10	9.5	-	-	0.8	-	-
4	25	10	6.9	1.14	0.825	0.9	0.673	0.098
5	71	10	11.0	-	-	0.9	-	-
5	24	10	6.5	1.26	0.888	0.9	0.611	0.0617
6	71.1	10	11.0	-	-	0.85	-	-
6	25	10	7.6	1.10	0.682	0.8	0.505	0.0382
7	71	10	10.7	-	-	0.9	-	-
7	24.8	10	7.5	1.12	0.924	0.9	0.527	0.0493
8	71	10	11.0	-	-	0.9	-	-
8	25	10	6.8	1.10	0.885	0.8	0.425	0.0221
9	71	10	11.0	-	-	0.8	-	-
9	25	10	6.4	1.18	0.956	0.95	0.435	0.0227
10	71.1	10	9.8	-	-	0.8	-	-
10	25	10	6.7	1.04	0.997	1.0	0.415	0.0162
11	71	10	9.6	-	-	1.0	-	-
11	25	10	7.4	1.06	1.55	1.1	0.459	0.0292
12	71	10	11.4	-	-	0.85	-	-
12	24.9	10	6.4	1.03	1.05	1.0	0.452	0.0126
13	71.1	10	9.6	-	-	0.8	-	-
13	25	10	6.4	1.12	1.06	0.9	0.428	0.0164
14	70	10	9.8	-	-	1.1	-	-
14	24.9	10	6.0	1.03	1.11	0.85	0.412	0.0111
15	71	10	9.9	-	-	0.85	-	-
15	25	10	6.2	1.03	1.07	0.9	0.396	0.0078
16	71.1	10	11.0	-	-	0.9	-	-
16	25	10	6.1	1.03	1.13	0.9	0.376	0.0064

Run No. 7 (continued)

Cycle No.	Temp. °C	Feed cc	Top Product cc	y_1/y_{o1}	y_2/y_{o2}	Bottom Product cc	y_1/y_{o1}	y_2/y_{o2}
17	71	10	8.5	–	–	0.9	–	–
17	25	10	6.0	1.03	1.15	0.8	0.440	0.0281
18	71	10	11.0	–	–	1.0	–	–
18	25	10	5.9	1.08	1.16	1.0	0.439	0.0169
19	70.9	10	11.1	–	–	0.8	–	–
19	24.9	10	7.0	1.08	1.14	0.85	0.455	0.0090
20	71	10	9.8	–	–	0.95	–	–
20	24	10	6.9	1.03	1.15	0.9	0.362	0.0030
21	71	10	11.7	–	–	0.9	–	–
21	25	10	7.6	1.05	1.09	0.85	0.383	0.0023
22	71.1	10	11.3	–	–	0.95	–	–
22	24.9	10	7.1	1.08	1.08	0.95	0.413	0.0015
23	71	10	9.7	–	–	1.0	–	–
23	25	10	6.1	1.21	1.08	0.95	0.446	0.0011
24	70.9	10	11.2	–	–	1.0	–	–
24	25.2	10	6.7	1.10	1.05	0.8	0.434	–
25	71.1	10	11.7	–	–	0.8	–	–
25	25	10	7.7	1.12	1.07	0.8	0.324	0.0006
26	71	10	11.0	–	–	0.8	–	–
26	25	10	7.0	1.10	1.11	0.8	0.324	0.0003
27	71	10	11.3	–	–	0.8	–	–
27	25.1	10	6.8	1.08	1.16	0.9	0.311	0
28	71	10	11.4	–	–	0.95	–	–
28	25	10	7.5	1.16	1.10	0.8	0.301	0.0003
29	71.1	10	10.8	–	–	0.9	–	–
29	24.9	10	6.2	1.06	1.05	0.9	0.267	0.0003
30	71	10	11.3	–	–	1.0	–	–
30	25	10	7.3	1.12	1.04	0.9	0.330	0
31	71	10	11.2	–	–	0.95	–	–
31	25	10	6.2	1.11	0.961	0.8	0.213	0
32	71	10	9.7	–	–	0.9	–	–
32	25	10	6.3	1.14	1.05	0.8	0.201	0

Run No. 8

Conditions: Ternary system- conc. n-heptane solution

Y_{o1} (toluene) = 10; Y_{o2} (acetophenone) = 10 vol. %

π/ω = 10 min.; $Q\pi/\omega$ = 25 cc

$\emptyset_B$ = 0.035; $\emptyset_T + \emptyset_B$ = 0.400

T_1 = 70°C; T_2 = 25°C

Cycle	Temp.	Feed	Top Product			Bottom Product		
No.	°C	cc	cc	y_1/y_{o1}	y_2/y_{o2}	cc	y_1/y_{o1}	y_2/y_{o2}
1	71	10	5.8	–	–	0.8	–	–
1	25	10	6.2	1.01	0.635	0.8	0.710	0.325
2	71.1	10	9.9	–	–	0.9	–	–
2	24.9	10	4.5	1.05	0.570	0.8	0.662	0.185
3	71.2	10	10.2	–	–	0.9	–	–
3	25	10	7.1	1.09	0.811	0.8	0.620	0.111
4	71.1	10	10.2	–	–	0.9	–	–
4	25.1	10	6.6	1.64	0.886	0.8	0.548	0.056
5	71	10	11.3	–	–	0.9	–	–
5	24.9	10	7.2	1.12	0.958	0.8	0.674	0.0315
6	70.9	10	11.4	–	–	0.9	–	–
6	25	10	7.7	1.08	1.02	0.9	0.502	0.0187
7	71	10	10.4	–	–	1.0	–	–
7	25	10	7.0	1.12	0.979	0.8	0.548	0.0199
8	71	10	10.9	–	–	0.8	–	–
8	25	10	6.8	1.25	1.03	0.85	0.530	0.0139
9	70.8	10	11.0	–	–	0.9	–	–
9	26.1	10	7.0	1.07	1.06	0.85	0.517	0.0088
10	71	10	10.0	–	–	0.8	–	–
10	26	10	6.5	1.12	1.02	0.95	0.477	0.0091
11	71	10	11.6	–	–	0.8	–	–
11	25	10	6.2	1.08	1.04	0.8	0.499	0.0070
12	71	10	11.4	–	–	0.85	–	–
12	25	10	7.5	1.05	1.01	1.1	0.497	0.0051
13	71	10	11.2	–	–	0.9	–	–
13	26	10	7.2	1.03	1.02	0.9	1.008	0.0041
14	71	10	11.1	–	–	1.0	–	–
14	25	10	6.7	1.04	1.06	0.9	0.465	0.0040
15	71	10	11.3	–	–	1.0	–	–
15	25	10	6.6	1.04	1.11	1.0	0.448	0.0032
16	71	10	10.8	–	–	0.8	–	–
16	25	10	6.9	1.03	1.04	0.9	0.507	0.0026

Run No. 8 (continued)

Cycle No.	Temp. °C	Feed cc	Top Product cc	Y_1/Y_{o1}	Y_2/Y_{o2}	Bottom Product cc	Y_1/Y_{o1}	Y_2/Y_{o2}
17	71	10	11.4	–	–	1.0	–	–
17	25	10	6.6	1.00	1.07	0.9	0.479	0.0026
18	71	10	11.7	–	–	0.8	–	–
18	25	10	6.9	1.05	1.08	0.8	0.435	0.00306
19	71.2	10	10.6	–	–	0.85	–	–
19	25	10	6.8	1.04	1.11	0.85	0.436	0.00181
20	71	10	11.4	–	–	0.9	–	–
20	25	10	6.7	1.03	1.02	0.8	0.794	0.00181
21	71	10	4.2	–	–	0.8	–	–
21	25	10	5.6	0.818	1.14	0.8	0.964	0.00411
22	71	10	10.1	–	–	0.85	–	–
22	25	10	7.3	0.847	1.13	0.8	0.964	0.00257
23	71.1	10	10.0	–	–	0.8	–	–
23	25	10	7.3	1.31	1.19	0.8	0.891	0.459
24	71	10	11.1	–	–	0.9	–	–
24	26	10	7.0	1.07	1.14	0.9	0.729	0.00154
25	71	10	11.0	–	–	0.9	–	–
25	26	10	6.7	0.808	1.20	0.85	0.795	0.00103
26	71	10	11.6	–	–	1.0	–	–
26	25.5	10	7.9	0.653	1.17	0.8	0.787	0.00154
27	71.1	10	10.7	–	–	0.9	–	–
27	25	10	7.5	0.890	1.19	0.8	0.886	0.00103
28	71	10	10.4	–	–	1.05	–	–
28	24.9	10	7.8	0.907	1.23	1.0	0.591	0.00041

Run No. 9

Conditions: Ternary system- Conc. n-heptane solution

Y_{o1} (toluene) = 10; Y_{o2} (acetophenone) = 10 vol. %

π/ω = 5 min.; $Q\pi/\omega$ = 25 cc

$\emptyset_B$ = 0.035; $\emptyset_T + \emptyset_B$ = 0.400

T_1 = 70°C; T_2 = 25°C

Cycle No.	Temp. $^\circ$C	Feed cc	Top Product			Bottom Product		
			cc	Y_1/Y_{o1}	Y_2/Y_{o2}	cc	Y_1/Y_{o1}	Y_2/Y_{o2}
1	71	10	2.0	–	–	0.4	–	–
1	25	10	5.1	0.896	0.744	1.0	0.778	0.398
2	71	10	11.1	–	–	0.8	–	–
2	25	10	7.5	0.741	0.708	0.9	0.957	0.293
3	71	10	10.6	–	–	0.95	–	–
3	25	10	7.5	0.932	0.744	0.9	0.690	0.267
4	71	10	11.5	–	–	0.8	–	–
4	27	10	7.4	0.848	0.849	1.1	0.782	0.172
5	71	10	11.0	–	–	0.8	–	–
5	26	10	6.9	0.906	0.891	0.9	0.980	0.989
6	71	10	11.2	–	–	0.8	–	–
6	26	10	6.8	0.726	0.943	0.8	0.850	0.0716
7	71	10	11.5	–	–	0.8	–	–
7	26	10	6.7	1.04	1.01	1.0	0.692	0.508
8	71	10	11.2	–	–	0.8	–	–
8	26.2	10	6.9	0.916	1.06	0.8	0.712	0.0423
9	71	10	10.9	–	–	0.8	–	–
9	25	10	6.5	0.972	0.998	0.8	1.08	0.0378
10	71	10	12.0	–	–	0.8	–	–
10	25	10	7.1	0.927	0.958	0.8	0.720	0.0289
11	71.1	10	11.2	–	–	0.8	–	–
11	25	10	6.9	1.04	1.09	1.0	1.03	0.0208
12	71	10	10.3	–	–	0.8	–	–
12	25	10	8.7	0.929	1.11	1.0	0.691	0.0212
13	71	10	10.4	–	–	0.8	–	–
13	26	10	7.7	0.909	1.09	1.0	0.678	0.0189
14	71	10	10.7	–	–	0.8	–	–
14	25	10	6.5	1.21	1.12	0.8	0.884	0.0131
15	71	10	11.5	–	–	0.8	–	–
15	25	10	7.5	0.879	1.17	0.8	0.604	0.0090
16	71	10	11.1	–	–	0.8	–	–
16	25	10	6.8	0.976	1.09	0.8	1.18	0.0148

Run No. 9 (continued)

Cycle No.	Temp. $^{\circ}C$	Feed cc	Top Product cc	y_1/y_{o1}	y_2/y_{o2}	Bottom Product cc	y_1/y_{o1}	y_2/y_{o2}
17	71	10	9.0	–	–	0.8	–	–
17	23	10	6.0	1.24	1.14	0.9	1.06	0.0667
18	71	10	11.7	–	–	0.8	–	–
18	25	10	6.7	1.27	1.21	0.8	1.00	0.0145
19	69	10	11.7	–	–	1.2	–	–
19	26	10	6.9	1.26	1.18	0.8	0.996	0.0111
20	71	10	11.8	–	–	0.8	–	–
20	25	10	6.8	1.25	1.18	0.8	1.015	0.0074
21	71	10	11.5	–	–	0.9	–	–
21	25	10	7.6	1.26	1.19	0.8	1.018	0.0045
22	71	10	11.3	–	–	0.8	–	–
22	26	10	7.0	1.25	1.20	0.8	1.032	0.0037

Run No. 10

Conditions: Ternary system- conc. n-heptane solution

Y_{o1} (toluene) = 20; Y_{o2} (acetophenone) = 20 vol. %

π/ω = 10 min.; $Q\pi/\omega$ = 25 cc

ϕ_B = 0.035; $\phi_T + \phi_B$ = 0.400

T_1 = 70°C; T_2 = 25°C

Cycle No.	Temp. °C	Feed cc	Top Product cc	Y_1/Y_{o1}	Y_2/Y_{o2}	Bottom Product cc	Y_1/Y_{o1}	Y_2/Y_{o2}
1	71	10	1.3	–	–	0.4	–	–
1	25	10	2.0	1.02	0.637	0.8	1.01	1.03
2	71	10	9.0	–	–	0.8	–	–
2	25	10	6.0	1.06	0.833	0.8	0.997	0.430
3	71	10	10.5	–	–	0.8	–	–
3	25	10	6.5	1.03	0.946	0.8	1.05	0.382
4	71	10	11.4	–	–	0.8	–	–
4	25	10	6.2	1.03	1.04	0.8	1.08	0.308
5	71	10	11.3	–	–	0.8	–	–
5	25	10	6.3	1.12	1.06	1.0	1.09	0.273
6	70.9	10	11.1	–	–	0.9	–	–
6	24.9	10	7.9	1.01	1.01	0.8	1.10	0.252
7	71	10	10.5	–	–	0.9	–	–
7	25	10	6.6	0.986	1.09	1.0	1.12	0.212
8	71	10	11.2	–	–	0.8	–	–
8	24.9	10	6.8	0.986	1.10	0.8	1.11	0.243
9	70.9	10	10.6	–	–	0.9	–	–
9	25	10	7.0	1.00	1.09	0.8	1.33	0.207
10	71.1	10	11.2	–	–	0.9	–	–
10	24.9	10	7.0	1.00	1.11	0.9	1.11	0.209
11	71	10	11.3	–	–	0.85	–	–
11	25	10	7.7	0.997	1.10	0.9	1.12	0.174
12	71	10	10.2	–	–	1.2	–	–
12	25	10	7.3	0.999	1.10	0.7	1.12	0.193
13	69.9	10	10.7	–	–	0.8	–	–
13	24.9	10	7.6	0.986	1.08	0.8	1.13	0.163
14	71	10	11.2	–	–	0.8	–	–
14	25	10	7.0	0.985	1.10	0.8	1.12	0.150
15	71	10	11.3	–	–	0.8	–	–
15	24.9	10	7.0	0.917	1.11	1.0	1.15	0.152
16	71	10	11.7	–	–	0.8	–	–
16	25	10	6.9	0.991	1.10	0.9	1.12	0.146

Run No. 10 (continued)

Cycle No.	Temp. °C	Feed cc	Top Product cc	y_1/y_{o1}	y_2/y_{o2}	Bottom Product cc	y_1/y_{o1}	y_2/y_{o2}
17	71	10	12.1	–	–	1.0	–	–
17	25	10	6.6	0.979	1.081	0.8	1.13	0.128
18	71	10	11.2	–	–	0.8	–	–
18	25	10	7.1	0.982	1.10	0.8	1.15	0.230
19	71	10	11.4	–	–	1.2	–	–
19	25	10	7.1	0.996	1.08	0.8	1.20	0.105
20	71.1	10	11.4	–	–	0.9	–	–
20	25.5	10	6.7	0.994	1.10	0.8	1.12	0.107

Run No. 11

Conditions: Ternary system- conc. n-heptane solution

y_{oi} (toluene) = 20 vol. %; y_{o2} (acetophenone) = 10 vol.

π/ω = 10 min.; $Q\pi/\omega$ = 25 cc

$\emptyset_B$ = 0.035; $\emptyset_T + \emptyset_B$ = 0.400

T_1 = 70°C; T_2 = 25°C

Cycle No.	Temp. °C	Feed cc	Top Product			Bottom Product		
			cc	y_1/y_{ol}	y_2/y_{o2}	cc	y_1/y_{ol}	y_2/y_{o2}
1	71	10	8.7	-	-	0.9	-	-
1	25	10	1.8	1.03	0.755	0.8	0.918	0.656
2	71	10	11.4	-	-	0.85	-	-
2	24.9	10	6.9	1.05	0.854	0.8	1.23	0.296
3	71.1	10	10.9	-	-	0.9	-	-
3	24	10	6.3	1.02	0.918	0.8	0.915	0.187
4	71	10	12.0	-	-	0.8	-	-
4	25	10	6.7	1.02	1.00	0.8	0.951	0.110
5	71	10	11.0	-	-	0.9	-	-
5	25	10	6.9	1.00	1.05	0.8	0.925	0.0654
6	71	10	11.5	-	-	0.8	-	-
6	25	10	7.1	1.01	1.13	0.8	0.905	0.0389
7	71	10	11.2	-	-	0.8	-	-
7	25	10	7.1	1.01	1.10	0.9	0.924	0.0321
8	71	10	11.0	-	-	0.8	-	-
8	25	10	7.7	0.996	1.10	0.8	0.901	0.0218
9	71.1	10	11.1	-	-	0.9	-	-
9	25.5	10	8.1	0.992	1.11	1.2	0.893	0.0200
10	70.9	10	11.6	-	-	0.8	-	-
10	24.9	10	6.8	1.01	1.13	0.8	0.885	0.0148
11	71	10	11.5	-	-	0.8	-	-
11	25	10	11.7	1.22	1.08	0.9	0.906	0.0148
12	71	10	11.3	-	-	1.0	-	-
12	25	10	7.6	1.00	1.15	0.8	0.876	0.0121
13	71	10	11.3	-	-	0.8	-	-
13	24.9	10	7.5	1.00	1.15	0.8	0.900	0.0082
14	71	10	11.4	-	-	0.9	-	-
14	25	10	7.0	1.00	1.17	0.9	0.892	0.0090
15	71	10	10.9	-	-	0.9	-	-
15	25	10	8.2	1.01	1.16	0.8	0.909	0.0087
16	71	10	11.0	-	-	0.8	-	-
16	25	10	7.7	0.995	1.08	0.8	0.871	0.0109

Run No. 11 (continued)

Cycle No.	Temp. $^{\circ}C$	Feed cc	Top Product			Bottom Product		
			cc	y_1/y_{o1}	y_2/y_{o2}	cc	y_1/y_{o1}	y_2/y_{o2}
17	71	10	10.8	–	–	0.9	–	–
17	25	10	6.8	0.999	1.120	0.8	0.877	0.0070
18	69.8	10	11.3	–	–	0.8	–	–
18	25	10	6.5	1.01	1.13	0.9	0.865	0.0104
19	71	10	11.6	–	–	0.8	–	–
19	25	10	4.0	1.02	1.10	0.8	0.868	0.0092
20	71	10	10.0	–	–	0.8	–	–
20	25	10	8.0	1.02	1.10	0.8	0.890	0.0047

Run No. 12

Conditions: Binary system- conc. n-heptane solution

y_{o1}(toluene) - 0; y_{o2}(acetophenone) = 10 vol. %

π/ω = 20 min. $Q\pi/\omega$ = 35 cc

$\emptyset_B$ = 0.035; $\emptyset_T + \emptyset_B$ = 0.400

T_1 - 70°C; T_2 = 25°C

Cycle No.	Temp °C	Feed cc	Top Product			Bottom Product		
			cc	y_1/y_{o1}	y_2/y_{o2}	cc	y_1/y_{o1}	y_2/y_{o2}
1	71	14	11.0	–	–	1.2	–	–
1	24.5	14	10.0	0	0.268	1.2	0	0.912
2	70	14	15.2	–	–	1.2	–	–
2	23	14	10.7	0	0.715	1.2	0	0.662
3	70.5	14	15.6	–	–	1.2	–	–
3	24.9	14	11.2	0	0.938	1.2	0	0.362
4	70.5	14	14.8	–	–	1.2	–	–
4	24.5	14	11.1	–	0.895	1.2	0	0.221
5	71	14	15.7	–	–	1.2	–	–
5	24.5	14	8.7	0	1.114	1.2	0	0.180
6	71	14	15.5	–	–	1.2	–	–
6	25	14	9.4	0	1.097	1.4	–	0.148
7	71.1	14	14.3	–	–	1.4	–	–
7	25.2	14	10.8	–	1.194	1.2	–	0.074
8	71	14	16.2	–	–	1.2	–	–
8	25.1	14	9.7	0	1.227	1.2	0	0.040
9	70.9	14	14.8	–	–	1.2	–	–
9	25.1	14	10.5	0	1.073	1.2	0	0.031
10	71.1	14	15.5	–	–	1.3	–	–
10	25.0	14	10.6	0	1.061	1.2	0	0.016
11	71.1	14	16.1	–	–	1.2	–	–
11	25.0	14	9.8	–	1.141	1.2	0	0.013
12	71.1	14	14.4	–	–	1.2	–	–
12	25.1	14	10.1	–	1.361	1.2	0	0.008
13	71	14	13.8	–	–	1.2	–	–
13	25.0	14	10.5	0	1.253	1.2	0	0.012
14	71	14	15.9	–	–	1.2	–	–
14	25.1	14	10.2	0	0.946	1.3	0	0.008

APPENDIX II

COMPUTER PROGRAM

NOMENCLATURE

```
 1         PROGRAM KIM
 2   C     PARAMETRIC PUMPING CALCULATION      CHONG YONG KIM
 3   C     SYMBOL                 DISCRIPTION                    DIMENSIO
 4   C     VISA1=VISCOSITY OF HEPTANE IN HOT TEMPERATURE         G/CM MIN
 5   C     VISA2=VISCOSITY OF HEPTANE IN COLD TEMPERATURE        G/CM MIN
 6   C     VISB1=VISCOSITY OF TOLUENE IN HOT TEMPERATURE         G/CM MIN
 7   C     VISB2=VISCOSITY OF TOLUENE IN COLD TEMPERATURE        G/CM MIN
 8   C     VISC1=VISCOSITY OF ACETOPHENONE IN HOT TEMPERATURE    G/CM MIN
 9   C     VISC2=VISCOSITY OF ACETOPHENONE IN COLD TEMPERATURE   G/CM MIN
10   C     H=HEIGHT OF COLUMN                                    CM
11   C     TIME=HALF CYCLE TIME                                  MIN
12   C     YA=INITIAL CONCENTRATION OF HEPTANE                   G MOLE/CC
13   C     YBO=INITIAL CONCENTRATION OF TOLUENE                  G-MOLE/CC
14   C     YCO=INITIAL CONCENTRATION OF ACETOPHENONE             G-MOLE/CC
15   C     O=DISPLACEMENT                                        CC
16   C     VT=DEAD VOLUME OF TOP RESERVOIR                       CC
17   C     VB=DEAD VOLUME OF BOTTOM RESERVOIR .                  CC
18   C     VOID=VOID VOLUME
19   C     DENS=DENSITY OF SOLID                                 G-SOLID/CC
20   C     ERR=ERROR
21   C     A=CROSSSECTIONAL AREA                                 SQ. CM
22   C     AP=SURFACE AREA OF SOLID PER GRAM OF SOLID            CU. CM/G-SOLI
23   C     DENB=DENSITY OF TOLUENE                               G-MOLE/CC
24   C     DENC=DENSITY OF ACETOPHENONE                          G-MOLE/CC
25   C     DB,DC=CONSTANTS IN MODIFIED LANGMUIR ISOTHERM         CC PORE/G
26   C     DP=SOLID PARTICLE DIAMETER                            CM
27   C     TEM1=TEMPERATURE OF HOT CYCLE                         DEGREE K
28   C     TEM2=TEMPERATURE OF COLD CYCLE                        DEGREE K
29   C     VMB=MOLAR VOLUME OF TOLUENE                           DE
30   C     VMB=MOLAR VOLUME OF TOLUENE                           CC/MOLE
31   C     VMC=MOLAR VOLUME OF ACETOPHENONE                      CC/MOLE
32   C     AMW=MOLECULAR WEIGHT OF HEPTANE                       G/G-MOLE
33   C     BMW=MOLECULAR WEIGHT OF TOLUENE                       G/G-MOLE
34   C     CMW=MOLECULAR WEIGHT OF ACETOPHENONE                  G/G-MOLE
35   C     NOMENCLATURES OF SYMBOLS THAT ARE USED IN THIS PROGRAM
36   C     N=NUMBER OF CYCLES
37   C     NNZ=NUMBER OF INTERVALS
38   C     NCASE=NUMBER OF CASES OF PHOB(I)
39   C     NITER=NUMBER OF ITERATIONS
40   C     PB1,QB1=EQUILIBRIUM CONSTANTS OF TOLUENE IN HOT TEMPERATURE
41   C     PB2,QB2=EQUILIBRIUM CONSTANTS OF TOLUENE IN COLD TEMPERATURE
42   C     PC1,QC1=EQUILIBRIUM CONSTANTS OF ACETOPHENONE IN HOT TEMPERATURE
43   C     PC2,QC2=EQUILIBRIUM CONSTANTS OF ACETOPHENONE IN COLD TEMPERATURE
44         DIMENSION PHOT(10),PFOB(10),XB2(500),XC2(500),YBTP2(500)
45   1    ,YCTP2(500),YB2(500),YC2(500),YBBP2(500),YCBP2(500),XXB2(500),
46   2    XXC(500),YYB(500),YYC(500),XBT(500),XCT(500),XXBS(500),XXCS(500),
47   3    YYBS(500),YYCS(500),NTR(500),XXC2(500),YYB2(500),XXB(500),
48   4    YYC2(500),YYB2ES(500),YYC2ES(500),YYB2ES(500),YYC2ES(500),
49   5    RATB(500),RATC(500),RABB(500),RABC(500)
50         READ 10,N,NNZ,NCASE,NITER
```

PROGRAM

```
   1              PROGRAM KIM
   2  C           PARAMETRIC PUMPING CALCULATION      CHONG YONG KIM
   3              DIMENSION PHOT(10),PHOB(10),XB2(500),XC2(500),YBTP2(500)
   4          1  ,YCTP2(500),YB2(500),YC2(500),YBBP2(500),YCBP2(500),XXB2(500),
   5          2  XXC(500),YYB(500),YYC(500),XBT(500),XCT(500),XXBS(500),XXCS(500),
   6          3  YYBS(500),YYCS(500),NTR(500),XXC2(500),YYB2(500),XXB(500),
   7          4  YYC2(500),YYB2EO(500),YYC2EO(500),YYB2ES(500),YYC2ES(500),
   8          5  RATB(500),RATC(500),RABB(500),RABC(500)
   9              READ 10,N,NNZ,NCASE,NITER
  10  10        FORMAT(4I10)
  11              READ 12,PB1,PB2,PC1,PC2
  12  12        FORMAT(4F20.2)
  13              READ 13,QB1,QB2,QC1,QC2
  14  13        FORMAT(4F20.2)
  15              READ 14,VISA1,VISA2,VISB1,VISB2,VISC1,VISC2
  16  14        FORMAT(6F12.6)
  17              READ 15,H,TIME,YA,YEO,YCO,Q,VT,VB,VOID,DENS,ERR,A
  18  15        FORMAT(8F10.5)
  19              READ 16,AP,DENB,DENC,LB,DC,DP
  20  16        FORMAT(6F12.6)
  21              READ 17,TEM1,TEM2,VKB,VKC
  22  17        FORMAT(4F10.2)
  23              READ 18,AMW,BMW,CMW
  24  18        FORMAT(3F10.4)
  25              READ 20,(PHOT(I),PHOB(I), I=1,NCASE)
  26  20        FORMAT(2F10.4)
  27              DO 600 I=1,NCASE
  28  2020      FORMAT( '1' )
  29  11        FORMAT(///)
  30              PRINT 2020
  31              PRINT3030
  32  3030      FORMAT(9X,'N',8X,'NNZ',5X,'NCASE',5X,'NITER'//)
  33              PRINT 10,N,NNZ,NCASE,NITER
  34              PRINT 11
  35              PRINT 3040
  36  3040      FORMAT(10X,'PB1',10X,'PB2',10X,'PC1',10X,'PC2'//)
  37              PRINT 12,PB1,PB2,PC1,PC2
  38              PRINT 11
  39              PRINT 3050
  40  3050      FORMAT(10X,'QB1',10X,'QB2',10X,'QC1',10X,'QC2'//)
  41              PRINT 13,QB1,QB2,QC1,QC2
  42              PRINT 11
  43              PRINT 3060
  44  3060      FORMAT(7X,'VISA1',7X,'VISA2',7X'VISB1',7X,'VISB2',7X,'VISC1',7X,
  45          1  'VISC2')
  46              PRINT 14,VISA1,VISA2,VISB1,VISB2,VISC1,VISC2
  47              PRINT 11
  48              PRINT 3070
  49  3070      FORMAT(5X,'H',5X,'TIME',5X,'YA',5X,'YBO',5X,'YCO',5X,'Q',5X,
  50          1  'VT',5X,'VB')
```

```
FORTRAN IV (VER 45 ) SOURCE LISTING: KIM     PROGRAM

  51            PRINT 15,H,TIME,YA,YBC,YCO,Q,VT,VB
  52            PRINT 11
  53            PRINT 3080
  54 3080       FORMAT(7X,'VOID',7X,'DENS',7X,'ERR',7X,'A'///)
  55            PRINT 15,VOID,DENS,ERR,A
  56            PRINT 11
  57            PRINT3090
  58 3090       FORMAT(10X,'AP',10X,'DENB',10X,'DENC',10X,'DB',10X,'DC',10X,'DP')
  59            PRINT 16,AP,DENB,DENC,DB,DC,DP
  60            PRINT 11
  61            PRINT 4010
  62 4010       FORMAT(10X,'TEM1',10X,'TEM2',10X,'VMB',10X,'VMC'//)
  63            PRINT 17,TEM1,TEM2,VMB,VMC
  64            PRINT 11
  65            PRINT 4020
  66 4020       FORMAT(10X,'AMW',10X,'BMW',10X,'CMW'///)
  67            PRINT 18,AMW,BMW,CMW
  68            PRINT 11
  69            PRINT 7070
  70 7070       FORMAT(6X,'PHOT',6X,'PHOB'//)
  71            PRINT 20,PHOT(I),PHOB(I)
  72            PRINT 2020
  73            V1=(1.-PHOB(I))*Q/(A*VOID*TIME)
  74            V2=(1.+PHOB(I))*Q/(A*VOID*TIME)
  75            DT1= H/(NNZ*V1)
  76            DT2= H/(NNZ*V2)
  77            PRINT 111,V1,V2,DT1,DT2
  78 111        FORMAT(15X,'V1',19X,'V2',15X,'DT1',15X,'DT2'//4(10X,F10.5))
  79            NZ= NNZ+1
  80            YBT1= YB0
  81            YCT1= YC0
  82            DO 30     J=1,NZ
  83            YB2(J)= YB0
  84            YC2(J)= YC0
  85 30         CALL EQYTOX(PB1,PC1,QE1,QC1,DB,DC,YB2(J),YC2(J),DENB,DENC,XB2(J),
  86          1 XC2(J))
  87            M= 1
  88            IF(M-1) 31,31,32
  89 31         YBTP22=YB0
  90            YCTP22=YC0
  91            GO TO 33
  92 32         YBTP22=YBTP2(M-1)
  93            YCTP22=YCTP2(M-1)
  94 33         YBTP1=((PHOT(I)+PHOB(I))*YB0+(1.-PHOB(I))*YBT1)/(1.+PHOT(I))
  95            YCTP1=((PHOT(I)+PHOB(I))*YC0+(1.-PHOB(I))*YCT1)/(1.+PHOT(I))
  96            IND=2
  97            YBTP2(M)=(Q*YBTP1+VT*YBTP22)/(VT+Q)
  98            YCTP2(M)=(Q*YCTP1+VT*YCTP22)/(VT+Q)
  99            YBT2=((PHOT(I)+PHCB(I))*YB0+(1.-PHOT(I))*YBTP2(M))/(1.+PHOB(I))
 100            YCT2=((PHOT(I)+PHCB(I))*YC0+(1.-PHOT(I))*YCTP2(M))/(1.+PHOB(I))
```

FORTRAN IV (VER 45) SOURCE LISTING: KIM   PROGRAM

```
    101         YBIN=YBT2
    102         YCIN=YCT2
    103 C
    104         PRINT 222,YBTP1,YCTP1,YBT2,YCT2
    105 222     FORMAT('-',5X,'YBTP1',E20.5,5X,'YCTP1',E20.5,5X,'YBT2',E20.5,5X,
    106       1 'YCT2',E20.5//)
    107         CALL XYCAL(VOID,DENS,VISA1,VISA2,VISB1,VISB2,VISC1,VISC2,
    108       1 TEM1,PB1,PB2,QB1,QB2,FC1,PC2,QC1,QC2,V1,V2,IND,DT1,DT2,NITER,XB2,
    109       2 XC2,YB2,YC2,YBIN,YCIN,TIME,NZ,XXB,XXC,YYB,YYC,YBB,YCB,M,ERR,DENB,
    110       3 DENC,TEM2,VMB ,VMC ,DB,DC,AMW,BMW,CMW,DP,AP,YA)
    111         YBBP2(M)=YBB
    112         YCBP2(M)=YCB
    113         PRINT 800,M,YBTP2(M),YCTP2(M),YBBP2(M),YCBP2(M)
    114 800     FORMAT(3X,'M',I10, 5X,'YBTP2',E15.5, 5X,'YCTP2',E15.5, 5X,
    115       1 'YBBP2',E15.5, 5X,'YCBP2',E15.5//)
    116         RATB(M)=YBTP2(M)/YBC
    117         RATC(M)=YCTP2(M)/YCC
    118         RABB(M)=YBBP2(M)/YBC
    119         RABC(M)=YCBP2(M)/YCC
    120         PRINT 900,RATB(M),RATC(M),RABB(M),RABC(M)
    121 900     FORMAT(5X,'RATB',E15.5,5X,'RATC',E15.5,5X,'RABB',E15.5,5X,
    122       1 'RABC',E15.5//)
    123         IF(M-N) 50,500,500
    124 50      IF(M-1) 51,51,52
    125 51      YBBP22=YBC
    126         YCBP22=YCC
    127         GO TO 53
    128 52      YBBP22=YBBP1
    129         YCBP22=YCBP1
    130 53      YBBP1=(Q*YBBP2(M)+VB*YBBP22)/(Q+VB)
    131         YCBP1=(Q*YCBP2(M)+VB*YCBP22)/(Q+VB)
    132         PRINT 333,YBBP1,YCBP1
    133 333     FORMAT(5X,'YBBP1',E20.5,5X,'YCBP1',E20.5//)
    134         M=M+1
    135         YBIN=YBBP1
    136         YCIN=YCBP1
    137         DO 60  L=1,NZ
    138         LL=L-1
    139         XB2(L)=XXB(NZ-LL)
    140         XC2(L)=XXC(NZ-LL)
    141         YB2(L)=YYB(NZ-LL)
    142 60      YC2(L)=YYC(NZ-LL)
    143         IND=1
    144 C
    145         CALL XYCAL(VOID,DENS,VISA1,VISA2,VISB1,VISB2,VISC1,VISC2,
    146       1 TEM1,PB1,PB2,QB1,QB2,FC1,PC2,QC1,QC2,V1,V2,IND,DT1,DT2,NITER,XB2,
    147       2 XC2,YB2,YC2,YBIN,YCIN,TIME,NZ,XXB,XXC,YYB,YYC,YBT1,YCT1,M,ERR,
    148       3 DENB,DENC,TEM2,VMB ,VMC ,DB,DC,AMW,BMW,CMW,DP,AP,YA)
    149         DO 70  L=1,NZ
    150         LL=L-1
```

```
FORTRAN IV (VER 45 ) SOURCE LISTING: KIM     PROGRAM

    151          XP2(L)=XXB(NZ-LL)
    152          XC2(L)=XXC(NZ-LL)
    153          YB2(L)=YYB(NZ-LL)
    154 70       YC2(L)=YYC(NZ-LL)
    155          GO TO 32
    156 500      PRINT 510,(M,YBTP2(M),YCTP2(M),YBRP2(M),YCBP2(M),M=1,N)
    157 510      FORMAT('-',3X,'M',5X,'YBTP2',5X,'YCTP2',5X,'YBRP2',5X,'YCBP2'//
    158        1 (5X,I5,4E15.5))
    159          PRINT 520,(M,RATB(M),RATC(M),RABB(M),RABC(M), M=1,N)
    160 520      FORMAT('-',3X,'M',5X,'RATB',5X,'RATC',5X,'RABB',5X,'RABC'//
    161        1 (5X,I5,4E15.5))
    162 600      CONTINUE
    163          STOP
    164          END
```

```
FORTRAN IV (VER 45 ) SOURCE LISTING: XYCAL    SUBROUTINE

     1           SUBROUTINE XYCAL(VOID,DENS,VISA1,VISA2,VISB1,VISB2,VISC1,VISC2,
     2         1 TEM1,PB1,PB2,QB1,QB2,PC1,PC2,QC1,QC2,V1,V2,IND,DT1,DT2,NITER,XB2,
     3         2 XC2,YB2,YC2,YBIN,YCIN,TIME,NZ,XXB,XXC,YYB,YYC,YYBAV,YYCAV,M,ERR,
     4         3 DENB,DENC,TEM2,VHB ,VHC ,DB,DC,AMW,BMW,CMW,DP,AP,YA)
     5           DIMENSION XB2(500),XC2(500),YB2(500),YC2(500),XXB2(500),
     6         1 XXC(500),YYB(500),YYC(500),XBT(500),XCT(500),YXBS(500),XXCS(500),
     7         2 YYBS(500),YYCS(500),NIR(500),XXC2(500),YYB2(500),XXB(500),
     8         3 YYC2(500),YYB2ES(500),YYC2ES(500),YYB2ES(500),YYC2ES(500)
     9           SUMB=YB2(NZ)
    10           SUMC=YC2(NZ)
    11           IF((-1)**IND) 20,10,10
    12   10      VISA=VISA2
    13           VISB=VISB2
    14           VISC=VISC2
    15           V=V2
    16           PB=PB2
    17           PC=PC2
    18           QB=QB2
    19           QC=QC2
    20           DT=DT2
    21           TEM=TEM2
    22           GO TO 30
    23   20      VISA=VISA1
    24           VISB=VISB1
    25           VISC=VISC1
    26           V=V1
    27           PB=PB1
    28           PC=PC1
    29           QB=QB1
    30           QC=QC1
    31           DT=DT1
    32           TEM=TEM1
    33   30      CNSTB=-(1.-VOID)*DENS/VOID
    34           CNSTC=-(1.-VOID)*DENS/VOID
    35           XBT(1)=XB2(1)
    36           XCT(1)=XC2(1)
    37           DO 22  L=1,NZ
    38           XXB2(L)=XB2(L)
    39           XXC2(L)=XC2(L)
    40           YYB2(L)=YB2(L)
    41   22      YYC2(L)=YC2(L)
    42           K=1
    43  155      CNK=K
    44           TT=DT*CNK
    45           YYB(1)=YBIN
    46           YYC(1)=YCIN
    47           CALL EQXTOY (PB,PC,QB,QC,DB,DC,YBEQI,YCEQI,DENB,DENC,XXB2(1),
    48         1 XXC2(1))
    49           CALL RK(YYB2(1),YYC2(1),YBEQI,YCEQI,XXB2(1),XXC2(1),PB,PC,QB,QC,
    50         1 DB,DC,DENB,DENC,XB,XC,DT,YA,AMW,BMW,CMW,VISA,VISB,VISC,DP,VOID,
```

FORTRAN IV (VER 45) SOURCE LISTING: XYCAL   SUBROUTINE

```
  51       2 VMB,VMC,V,AP,TEM)
  52         XBT(K+1)=XB
  53         XCT(K+1)=XC
  54         XXB(1)=XBT(K+1)
  55         XXC(1)=XCT(K+1)
  56         I=2
  57 C
  58 85      ITER=1
  59         NTR(1)=1
  60         YYB2EQ(1)=YBEQI
  61         YYC2EQ(1)=YCEQI
  62         CALL CMSS(YA,YYB2(I-1),YYC2(I-1),AMW,BMW,CMW,VISA,VISB,VISC,DP,
  63       1 VOID,AP,VMB,VMC,CLB,CLC,V,TEM)
  64         YYBS(I)=YYB2(I-1)+CNSTB*CLB*DT*(YYB2(I-1)-YYB2EQ(I-1))
  65         YYCS(I)=YYC2(I-1)+CNSTC*CLC*DT*(YYC2(I-1)-YYC2EQ(I-1))
  66         CALL EQXIDY(PB,PC,QB,CC,DB,DC,YYB2EQ(I),YYC2EQ(I),DENB,DENC,
  67       1 XXB2(1),XXC2(1))
  68         XXBS(I)=XXB2(I)+CLB*DT*(YYB2(I)-YYB2EQ(I))
  69         XXCS(I)=XXC2(I)+CLC*DT*(YYC2(I)-YYC2EQ(I))
  70 101     CALL EQXIDY(PB,PC,QB,CC,DB,DC,YYB2ES(I),YYC2ES(I),DENB,DENC,
  71       1 XXBS(I),XXCS(I))
  72         YYB(I)=YYB2(I-1)+(DT/2.)*CNSTB*CLB*(YYBS(I)+YYB2(I-1)-YYB2ES(I)-
  73       1 YYB2EQ(I-1))
  74         YYC(I)=YYC2(I-1)+(DT/2.)*CNSTC*CLC*(YYCS(I)+YYC2(I-1)-YYC2ES(I)-
  75       1 YYC2EQ(I-1))
  76         XXB(I)=XXB2(I)+(CLB*DT/2.)*(YYBS(I)+YYB2(I)-YYB2ES(I)-YYB2EQ(I))
  77         XXC(I)=XXC2(I)+(CLC*DT/2.)*(YYCS(I)+YYC2(I)-YYC2ES(I)-YYC2EQ(I))
  78         DEVYB=(YYB(I)-YYBS(I))/YYBS(I)
  79         DEVYC=(YYC(I)-YYCS(I))/YYCS(I)
  80         IF(ABS(DEVYB)-ERR) 50,50,60
  81 50      IF(ABS(DEVYC)-ERR) 70,70,60
  82 70      DEVXB=(XXB(I)-XXBS(I))/XXBS(I)
  83         DEVXC=(XXC(I)-XXCS(I))/XXCS(I)
  84         IF(ABS(DEVXB)-ERR) 80,80,60
  85 80      IF(ABS(DEVXC)-ERR) 71,71,60
  86 60      IF(ITER-NITER) 81,71,71
  87 81      YYBS(I)=YYB(I)
  88         YYCS(I)=YYC(I)
  89         XXBS(I)=XXB(I)
  90         XXCS(I)=XXC(I)
  91         ITER=ITER+1
  92         GO TO 101
  93 71      NTR(I)=ITER
  94         IF(I-NZ) 82,90,90
  95 82      I=I+1
  96         GO TO 85
  97 90      SUMB=SUMB+YYB(NZ)
  98         SUMC=SUMC+YYC(NZ)
  99         IF(TT-TIME) 150,200,200
 100 150     DO 151 L=1,NZ
```

FORTRAN IV (VER 45) SOURCE LISTING: YYCAL   SUBROUTINE

```
    101          YYB2(L)=YYB(L)
    102          YYC2(L)=YYC(L)
    103          XXB2(L)=XXB(L)
    104 151      XXC2(L)=XXC(L)
    105          K=K+1
    106          GO TO 155
    107 200      TOTK=K+1
    108          YYBAV=SUMB/TOTK
    109          YYCAV=SUMC/TOTK
    110          RETURN
    111          END
```

FORTRAN IV (VER 45) SOURCE LISTING: RK   SUBROUTINE

```
    1          SUBROUTINE RK(YBI,YCI,YBEQI,YCEQI,XBI,XCI,PB,PC,QB,QC,
    2        1 DC,TC,DENB,DENC,XB,XC,TT,YA,AMW,BMW,CMW,VISA,VISB,VISC,DP,VOID,
    3        2 VMB,VMC,V,AP,TEM)
    4          CALL CMSS(YA,YBI,YCI,AMW,BMW,CMW,VISA,VISB,VISC,DP,VOID,AP,VMB,
    5        1 VMC,CLB,CLC,V,TEM)
    6          AKB1=CLB*(YBI-YBEQI)*TT
    7          AKC1=CLC*(YCI-YCEQI)*TT
    8          X2B=XCI+(AKB1/2.)
    9          X2C=XCI+(AKC1/2.)
   10          CALL EQXTJY(PB,PC,QB,QC,DB,DC,YBEQ,YCEQ,DENB,DENC,X2B,X2C)
   11          AKB2=CLB*(YBI-YBEG)*TT
   12          AKC2=CLC*(YCI-YCEG)*TT
   13          X3B=XBI+(AKB2/2.)
   14          X3C=XCI+(AKC2/2.)
   15          CALL EQXTJY(PB,PC,QB,QC,DB,DC,YBEQ,YCEQ,DENB,DENC,X3B,X3C)
   16          AKB3=CLB*(YBI-YBEG)*TT
   17          AKC3=CLC*(YCI-YCEG)*TT
   18          X4B=XBI+AKB3
   19          X4C=XCI+AKC3
   20          CALL EQXTJY(PB,PC,QB,QC,DB,DC,YBEQ,YCEQ,DENB,DENC,X4B,X4C)
   21          AKB4=CLB*(YBI-YBEG)*TT
   22          AKC4=CLC*(YCI-YCEG)*TT
   23          DXB=(AKB1+2.*AKB2+2.*AKB3+AKB4)/6.
   24          DXC=(AKC1+2.*AKC2+2.*AKC3+AKC4)/6.
   25          XB=XBI+DXB
   26          XC=XCI+DXC
   27          RETURN
   28          END
```

```
FORTRAN IV (VER 45 ) SOURCE LISTING: CMSS    SUBROUTINE

     1          SUBROUTINE CMSS(YA,YB,YC,AMW,BMW,CMW,VISA,VISB,VISC,DP,VOID,AP,
     2        1 VMB,VMC,CLB,CLC,V,TEM)
     3          ALPHB=0.0L5*EXP(-YB/0.00045)
     4          ZC=YC/0.0005
     5          ALPHC=0.005-0.00282*ZC+0.000925*ZC**2-0.000103*ZC**3
     6          DEN=YA*AMW+YB*BMW+YC*CMW
     7          VIS=(VISA*YA+VISB*YB+VISC*YC)/(YA+YB+YC)
     8          FACT=(DP**2*VOID*DEN)/(VIS*(1.-VOID))
     9          FJB=ALPHB*(FACT**(-0./6))
    10          FJC=ALPHC*(FACT**(-0./8))
    11          DCONST=(7.4*10.**(-8.0))*60.*(AMW**(0.5))
    12          DBA=DCONST*TEM/(VIS*VMB**(0.6))
    13          DCA=DCONST*TEM/(VIS*VMC**(0.6))
    14          CLB=AP*FJB*V*VOID*((DEN*DBA/VIS)**(2./3.))
    15          CLC=AP*FJC*V*VOID*((DEN*DCA/VIS)**(2./3.))
    16          RETURN
    17          END
```

FORTRAN IV (VER 45) SOURCE LISTING: EQYTCX SUBROUTINE

```
    1          SUBROUTINE EQYTCX(PB,PC,QB,QC,DB,DC,YB,YC,DENB,DENC,XB,XC)
    2          XB=PB*YB/(1.+QB*YC/DENB)+DB*YB
    3          XC=PC*YC/(1.+QC*YC/DENC)+DC*YC
    4          RETURN
    5          END
```

```
FORTRAN IV (VER 45 ) SOURCE LISTING: FOXTOY  SUBROUTINE

    1          SUBROUTINE FOXTOY(PB,PC,QB,QC,DB,DC,YB,YC,DENB,DENC,XB,XC)
    2          CONSRB=(PB+DB)*DENB-QB*XB
    3          YB=(-CONSRB+SQRT(CONSRB**2+4.*QB*DB*XB*DENB))/(2.*QB*DB)
    4          CONSRC=(PC+DC)*DENC-QC*XC
    5          YC=(-CONSRC+SQRT(CONSRC**2+4.*QC*DC*XC*DENC))/(2.*QC*DC)
    6          RETURN
    7          END
```

APPENDIX III

DEVELOPMENT OF SCALE-UP AND DESIGN EQUATIONS

Capacity and Column Diameter

In most ion exchange and adsorption applications, column diameters of three feet or more are not uncommon, and, at first, it would appear that the same would be true with parametric pumping columns. In the latter case however, heat transfer is an important consideration-- especially if the system obeys the equilibrium theory of Pigford et al (1969) where instantaneous temperature change between the hot upflow and cold downflow half- cycles is a prime requisite. The longer the switchover time (downtime), the longer the overall cycle time, and the lower the capacity for a given installation.

The duration of the switchover time depends on the speed of heat penetration into the column which, in turn, depends on the tube diameter. Sweed (1969) used an equation derived from Carslaw and Jaeger (1959) and applied it to laboratory scale parametric pumping.

$$t_{90} = 0.5 \; r^2/k \qquad\qquad (III-1)$$

The time t_{90} for the axis temperature to reach 90% of its ultimate value is directly proportional to the

square of the column radius r, and inversely proportional to the thermal diffusivity k. This equation taken from Carslaw and Jaeger (1959) is basically the same one developed by other workers and shown in the textbook by Bird, Stewart, and Lightfoot (1960). The equation is one solution of the general equation for unsteady state heat conduction,

$$\frac{\partial T}{\partial t} = \alpha \nabla^2 T$$

where α is the thermal diffusivity of the solid. In applying this equation to a packed column an "effective" thermal diffusivity may be used.

This general equation has been solved for practically all conceivable sizes and shapes and the results plotted as constant dimensionless times where, in the case of a cylinder,

$$Y = \frac{T-T_0}{T_1-T_0} ,$$ dimensionless temperature or ordinant

and

$$X = \frac{r}{R} ,$$ dimensionless radius or abscissa, against which are plotted the dimensionless time curves, $\alpha t/R^2$. In these equations, T is the temperature at the point in question, T_0 is the initial cylinder temperature, T_1

is the surface temperature for all t > O, r is the distance from the center of the cylinder, and R is the radius of the cylinder.

Since the point of interest is only the axis (r=O), the relationship is simplified to one of dimensionless temperature and dimensionless time--the equivalent of reading the ordinant at the intersections of the dimensionless time curves. At the point on the ordinant where the dimensionless temperature is 0.9, the column axis temperature is 90% of the ultimate temperature and $\alpha t/R^2 = 0.5$. This is the equation used by Sweed (1969) and is shown here as Equation (III-1).

Using the thermal diffusivity value of 0.001 cm^2/sec. for the hydrocarbon system toluene-heptane, Sweed calculated two minutes switchover time for the laboratory column. The actual measured time was only 0.75 minutes (which corresponded to a diffusivity of 0.003). In any case, the time was short enough so that the switchover time could be considered "instantaneous" as compared to the half-cycle time of 20 minutes.

Now consider the case where several small tubes are used with the same total cross section area as one large tube. Then, applying Equation (III-1) to both the large

tube (subscript 1) and the small tubes (subscript 2),

$$t_1/t_2 = r_1^2/r_2^2 = d_1^2/d_2^2 \qquad\qquad (III-2)$$

because, after dividing the two equations, the 0.5 factor and the k (thermal diffusivity) cancel out. Moreover if N is equal to the number of tubes and N (area of one small tube) equals the area of one large tube of $Na_2 = a_1$ where a_1 and a_2 are the cross section areas of the large and the small tubes respectively, then $1/N = (d_2/d_1)^2$ and

$$t_1/t_2 = N \qquad\qquad (III-3)$$

Therefore the time required for the temperature switchover in the case of the single tube is N times that for N small tubes. For example, the time required for a normal 45 second switchover for one large tube compared to only 26 small tubes would be 20 minutes--the entire time for a typical half cycle. And, since a production scale unit could require as many as 2226 tubes in a single 3 foot diameter shell heat exchanger configuration, we are talking about a switchover time for a single tube equivalent unit of nearly 28 hours idle time between 20 minute half cycles.

Clearly, if the direct thermal mode (heating and cooling through the walls of the tubes) is to be used

in commercial units, the only way to scale up is by means of multitube parametric pumps in a shell and tube "heat exchanger" configuration.

Capacity and Column Length

In addition to increasing capacity by increasing the number of columns, it is also possible to increase capacity by increasing the fluid velocity through each column. The latter procedure will involve both an increase in pressure drop which will be discussed later, and an effect on the axial adsorption penetration distance which will be discussed in this section.

Chen and Hill (1971) clearly defined one of the fundamental principles of parametric pumping systems obeying the equilibrium theory, the relationship of column length versus capacity. Three distinct regions of operation were described, the boundaries of which were outlined by the relationship of column length and the wave front penetration distances on the hot upflow and cold downflow half-cycles.

Of particular interest in design was their region I and the corresponding equations which defined the limitations of pump operation necessary to insure high separation capabilities. The basic requirement was that

the penetration distance on cold downflow must be less than

or equal to the penetration distance on hot upflow or the

height of the column. That is

$$L_2/L_1 \leq 1 \text{ and } L_2 \leq h \qquad \text{(III-4)}$$

where L_1 and L_2 are the wave front penetration distances

on hot upflow and cold downflow respectively and h is the

height or length of the column.

Chen et al (1972) conveniently defined L_1 and L_2

for the continuous parametric pump as

$$L_2 = \frac{v_o(1+\emptyset_B)}{(1+b)(1+m_o)} \frac{\pi}{\omega} \qquad \text{(III-5)}$$

and

$$L_2/L_1 = \frac{1+\emptyset_B}{1-\emptyset_B} \frac{1+b}{1-b} \qquad \text{(III-6)}$$

And, as shown by Chen at al (1974) these equations are

converted to a multicomponent system by simply adding

the subscript i to L_1, L_2, m_o, and b. L_1 and L_2 were

previously defined while m_o and b are dimensionless

equilibrium constant parameters. $\emptyset_B$, v_o, and π/ω are

general terms, and represent the bottom product/reservoir

rate, interstitial velocity and the half-cycle time

respectively. It should be pointed out that b (or b_i) and the other parameters that bear the subscript i refer to a particular component in relation to the common solvent whether the system is a binary or multicomponent. For the present design purposes, once the key component has been selected and the values assigned, the subscript i may be dropped. This will be done in the equations that follow.

As pointed out by Chen et al (1972)(1974), $\emptyset_B$ must be set at a value less than b, a condition for the operation of the column such that the component i, at steady state, does not appear in the bottom product stream. Also, as a condition for design, L_2 = h, which means that as a design limit for maximum separation

$$h \geqslant L_2 = \frac{(1+\emptyset_B) \frac{\pi}{\omega}}{(1+b)(1+m_o)} \cdot v_o \qquad \text{(III-7)}$$

so that if the operating conditions of the bottom product rate ratio, $\emptyset_B$, the half-cycle time, π/ω, are set for a given system (fixed b and m_o), then as a limit

$$h \geqslant (\text{constant}) \, v_o \qquad \text{(III-8)}$$

or, in terms of the superficial velocity, v,

$$h \geqslant K \, v/\varepsilon = K'v \qquad \text{(III-9)}$$

where $K' = (1+\phi_B)(\pi/\omega)/[(1+b)(1+m_o)\varepsilon]$ (III-10)

h, the column length, may be related to column capacity since

$$v = Q/a_t N$$ (III-11)

where Q is the reservoir displacement rate, a_t is the cross section area of one tube, and N is the number of tubes.

Therefore

$$h \geq K'Q/a_t N = K''Q/N$$ (III-12)

where

$$K'' = \frac{(1+\phi_B)(\pi/\omega)}{(1+b)(1+m_o)\varepsilon a_t}$$ (III-13)

so that, for a given system, product rate, and tube size, there is a direct relationship between tube length and capacity.

Heat and Material Balances Around the Top of the Column

The heat and material balances around the top of the column are required to calculate the true temperature of the fluid re-entering the column on cold downflow. This temperature value is required for an accurate esti-mate of the cooling requirements for the cold downflow

half-cycle. Heat and material balances for both the
hot upflow and cold downflow half-cycles must be con-
sidered. In all cases, the reference temperature will
be $0^{\circ}K$.

Hot Upflow Balance

Heat Input from the Feed $= (\emptyset_T + \emptyset_B) Q \rho_F c_F (T_F - 0)$

Heat Input from the Column $= (1 - \emptyset_B) Q \rho_{T1} c_{T1} (T_1 - 0)$

Heat Output to Top Product $= \emptyset_T Q \rho_{TP1} c_{TP1} (T_{TP1} - 0)$

Heat Output to Reservoir $= Q \rho_{TP1} c_{TP1} (T_{TP1} - 0)$

$$(\emptyset_T + \emptyset_B) Q \rho_F c_F T_F + (1 - \emptyset_B) Q \rho_{T1} c_{T1} T_1 = Q (1 + \emptyset_T) \rho_{TP1} c_{TP1} T_{TP1}$$

Cold Downflow Balance

Heat Input from the Feed $= (\emptyset_T + 0_B) Q \rho_F c_F (T_F - 0)$

Heat Input from Reservoir $= Q \rho_{TP1} c_{TP1} (T_{TP1} - 0)$

Heat Output to Top Product $= \emptyset_T Q \rho_{TP2} c_{TP2} (T_{TP2} - 0)$

Heat Output to the Column $= Q (1 + \emptyset_B) \rho_{T2H} (T_{2H} - 0) c_{2H}$

$$(\emptyset_T + \emptyset_B) Q \rho_F c_F T_F + Q \rho_{TP1} c_{TP1} T_{TP1} = Q \emptyset_T \rho_{TP2} c_{TP2} T_{TP2}$$

$$+ Q (1 + \emptyset_B) \rho_{T2H} c_{T2H} T_{2H}$$

Combining the two heat balances:

$$2 (\emptyset_T + \emptyset_B) \rho_F c_F T_F + (1 - \emptyset_B) \rho_{T1} c_{T1} T_1 - \emptyset_T \rho_{TP1} c_{TP1} T_{TP1} - \emptyset_T \rho_{TP2} c_{TP2} T_{TP2}$$

$$- (1 + \emptyset_B) \rho_{T2H} c_{T2H} T_{2H} = 0 \qquad .$$

and

$$T_{2H} = \frac{2 (\emptyset_T + \emptyset_B) \rho_F c_F T_F + (1 - \emptyset_B) \rho_{T1} c_{T1} T_1 - \emptyset_T \rho_{TP1} T_{TP1} - \emptyset_{TP2} c_{TP2} T_{TP2}}{(1 + \emptyset_B) \rho_{T2H} c_{T2H}}$$

$$\tag{III-14}$$

The overall effect is to lower the temperature of
the stream (T_{2H}) re-entering the column. It is twice
lowered by the feed stream and lowered by heat removed
in the top product stream during both the hot upflow and
cold downflow half cycles.

The effect of the heat removed can be neglected if
it is assumed that the feed enters the top of the column
at the same temperature as the fluid leaving the column
during the hot half cycle. In this case the operation
would be isothermal in both the hot upflow and cold down-
flow half cycles and the temperature in all cases would
be T_1, the hot upflow temperature of the fluid leaving
the column.

This assumption of a relatively hot feed temperature
is not unreasonable because, in many real cases, the
feed could come from an exothermic reaction and any excess
enthalpy could be usefully "siphoned" off via a heat
exchanger external to the parametric pumping process.

Also in those cases where the feed temperature is
normally lower than T_1, it could be increased by heat
exchange with the slightly warmer product stream. In
any actual case, the temperature differences of the streams
around the top of the column would be small, and, for
purposes of this usage, could be considered isothermal.

Heating and Cooling Requirements

Heat is provided by a recirculating liquid system heated indirectly by steam. The total duty is the sum of the duty for heating the tubes and tube contents from the cold to the hot temperature plus the duty for heating the fresh fluid as it is pumped into the column during the hot half cycle. Duty required to heat the exchanger shell, tubesheets, and external piping can be neglected for rough estimates if it is assumed that these equipment sections are insulated. The duty for heating or cooling the residual heat transfer fluid left in the shell is not included because this fluid is dumped to the appropriate reservoir prior to starting the next half cycle. The heat that is saved by this procedure is estimated by Equation (III-50).

The duty for heating the tubes and tube contents is:

$$q_t = (w_t c_t + w_s c_s + w_f c_f)(T_1 - T_2)(N)(h) \qquad \text{(III-15)}$$

where w and c are the mass per unit length and heat capacity at constant pressure of the tubes, the solid adsorbent, and the fluid phase surrounding the adsorbent. T_1 and T_2 are the hot upflow and cold downflow column temperatures respectively, N is the number of tubes in the exchanger, and h is the height (length) of the exchanger tubes.

The duty for heating the process fluid being pumped through the tubes during the hot half cycle is:

$$q_1' = Q(1-\phi_B)(\rho_1)(T_1-T_2)(\pi/\omega)(c_1) \qquad \text{(III-16)}$$

where $Q(1-\phi_B)$ is the volumetric flow rate in the column, ρ_1 is the fluid density at T_1, π/ω is the half cycle time duration, and c_1 is the specific heat of the incoming fluid.

Now if n is the number of half cycles (or cycles) for any time period under consideration, the total heating duty for that time period is:

$$q_1 = \left[(w_t c_t + w_s c_s + w_f c_f)(N)(h) + Q(1-\phi_B)(\rho_1)(c_1)(\pi/\omega)\right]$$
$$(T_1-T_2)(n)$$

$$\text{(III-17)}$$

The cooling duty estimation is slightly complicated by the fact that the effluent leaving the top of the column is contacted by the feed and is heated (or cooled) by the incoming feed. Also, some heat is removed by the effluent top product stream. The same is true during the cold downflow half cycle when the top reservoir effluent is again heated or cooled by contact with the feed, and more heat is removed by the top product stream. In this situation, the temperature of the fluid (T_{2H}) would be

different for each design and its value can be estimated
from the equation derived previously.

$$T_{2H} = \frac{2(\phi_B + \phi_T)(\rho cT)_F + (1-\phi_B)(\rho cT)_1 - \phi_T(\rho cT)_{TP1} - \phi_T(\rho cT)_{TP2}}{(1+\phi_B)(\rho c)_{T2H}}$$

(III-14)

In this equation, the reservoir volumetric term Q,
being common to all the streams in the heat balance can-
cels out, leaving the terms ϕ_T and ϕ_B, the ratios of the
top and bottom product stream flow rates to the reservoir
flow rate. Similarly, the terms $(\phi_T + \phi_B)$, $(1-\phi_B)$, and
$(1+\phi_B)$ refer to the feed, the column upflow, and column
downflow rates, respectively. The subscripts F, 1, TP1,
and T2H refer to the feed, hot upflow column effluent,
top product during column up and downflow half cycles,
and to the stream re-entering the column during cold
downflow.

The overall cooling duty is therefore:

$$q_2 = (w_t c_t + w_s c_s + w_f c_f)(N)(h)(T_1 - T_2)(n)$$

$$+ (1+\phi_B)(\rho_2)(c_2)(\pi/\omega)(T_{2H} - T_2)(n)$$

(III-18)

This equation is quite similar to the equation for
the heating half cycle except for the T_{2H} and $(1+\phi_B)$
terms. For rough estimations, it would not be unreasonable
to assume that the feed enters at the same temperature

as the hot upflow column effluent. This could easily
be the case if the feed were the product of an exothermic
reaction. If adiabatic operation around the top of the
column were also assumed, then the common temperature T_1
would apply to all the streams and $T_{2H} = T_1$.

Column Pressure Drop

The total pressure drop includes, in addition to the
drop through the column, the pressure drop in the lines,
static drop, expansion and contraction losses, etc.
With careful design and attention to layout, these in-
cidential losses can be considered negligable compared
to the drop through the columns. Also, the amount of
dead volume (volume of the reservoir, pump, and lines
in excess of the column displacement) can be accounted
for by the theory, and only the drop through the column
itself need be considered.

The pressure drop in the packed bed may be expressed
by the dimensionless Blake-Kozeny equation for laminar
flow:

$$\frac{\Delta p g_c \rho}{G^2} \frac{D_p}{h} \frac{\varepsilon^3}{1-\varepsilon} = \frac{150 \ (1-\varepsilon)}{D_p G/\mu} \qquad \text{(III-19)}$$

where Δp is the pressure drop in lb_f/ft^2

G is the rate in lb/hr/ft^2 = $v\rho$

μ is the viscosity in lb$_m$/hr/ft

Rearranging and substituting,

$$\Delta p = \frac{150\ (1-\epsilon)^2}{D_p^2\ g_c \epsilon^3}\ (\mu)(h)(v) \qquad\qquad \text{(III-20)}$$

where v = velocity = $Q/A(1-\emptyset_B)$ for hot upflow and

$Q/A(1+\emptyset_B)$ for cold downflow in ft/hr

g_c = conversion factor = 4.17×10^8 = (lb$_m$/hr^2/ft)(ft^2/lb$_f$)

Q = reservoir flow rate in ft^3/hr

A = total crossflow area = flow area/tube x no. of tubes

$\quad$ = $a_t N$

Now if the static head, $(h\rho)$ is to be handled

separately as a part of the overall pumping system layout,

$$\Delta p = \frac{150(1-\epsilon)^2}{D_p^2\ g_c \epsilon^3}\ \frac{\mu h}{a_t N}\ Q(1 \mp \emptyset_B) \qquad\qquad \text{(III-20)}$$

for hot upflow and cold downflow respectively.

Now the rate of flow is $Q(1-\emptyset_B)$ for hot upflow and

$Q(1+\emptyset_B)$ for cold downflow.

The hydraulic horsepower for the pump is easily

calculated as follows:

$$(\Delta p) \ (lb_f/ft^2) \ (Q(1\overline{+}\phi_B) \ (ft^3/hr) \ (Hp\text{-}hr/1.98x10^6ft\text{-}lb_f)$$

$$Hp_1 = \frac{150(1\text{-}\varepsilon)^2}{D_p^2 \ g_c \varepsilon^3} \ \frac{h}{a_t N} \ Q^2 \ \mu_1 (1\text{-}\phi_B)^2 \ (1.98x10^6)^{-1}$$

$$(III\text{-}21)$$

$$Hp_2 = \Delta p_2 (Q) \ (1+\phi_B) (1.98x10^6)^{-1} \qquad (III\text{-}22)$$

It should be noted that the viscosity could be roughly estimated from the equation from Bird, Stewart and Lightfoot (1960)

$$\mu = 9.65x10^{-3}\rho/M \ exp \ (3.8T_B/T) \ lb_m ft^{-1}hr^{-1}$$

Substitution of this equation would eliminate the viscosity variable. However, the accuracy would be poor and would not allow for the concentration effect.

Heat Transfer Fluid Pressure Drop

The equations used in this derivation are based on those presented by Donohue (1955). The pressure drop through the shellside of a heat exchanger may be divided into two main parts, the drop through the baffle openings and the drop across the rows of tubes between the baffles.

The pressure drop through each baffle opening is:

$$\Delta p_b' = 3.76 \ G_b^2/(s.g.x10^6) \qquad \text{Donohue (1955)}$$

where G_b = w/A_b = mass flow rate/area = lb/sec/ft^2

and A_b = 3.14/4 (d^2-ND^2) B_c

in which A_b = area through the baffle opening

      d = i.d. shell, ft.

      D = o.d. tubes, ft.

      B_c = baffle cutout fraction

      N = no. tubes in the shell

      s.g. = specific gravity of the fluid

Now the number of baffle openings in h/B_s-1

      where h = tube length, ft.

      and B_s = baffle spacing, ft.

Therefore the total pressure drop through all the baffle openings is:

$$\Delta P_b = 6.10 \times 10^{-6} w^2 B_c^{-2} (d^2-ND^2)^{-2} (h/B_s-1) \quad \text{(III-23)}$$

The pressure drop across each tube bank for turbulent flow is: $\Delta p_c' = 1.98 \times 10^{-6} (G_c)^{1.8} (\mu \cdot^2/s.g.)(N')(P-D)^{-0.2}$

<div align="right">Donohue (1955)</div>

where G_c = w/A_c = mass flow rate/area = lb/sec/ft^2

and A_c = $(d-N_c D)(B_s)$

where N_c = number of crossflow tubes = 1 + (outer diameter tube bundle-tube diameter)/(space between tubes). The outer tube bundle diameter (for the case of a tri-angular pitch (equal to 1.375D and the flow perpendicular to the apex) was calculated for 5,6,8,10,12, and 36 inch

shells and was found to range from 92-96% of the shell i.d. so that OTL = 0.94d ± 2%. Furthermore, for this configuration, the space between the tubes is equal to the pitch so that:

$$N_c = 1 + (0.94d - D)/1.375D = (0.94d + 0.375D)/1.375D$$

$$N_c D = (0.94d + .375D)/1.375 \qquad \text{(III-24)}$$

$$\text{and } A_c = \left[(0.435d - 0.375D)/1.375\right](B_s) \qquad \text{(III-25)}$$

$$\text{Therefore } G_c = 1.375w/(0.435d - 0.375D)/ \ B_s$$

$$\text{(III-26)}$$

Now N' = number of tube rows in the direction of flow which are covered by one baffle

$$N' = (1-B_c)(OTL-D)/0.866P = (1-B_c)(0.94d-D)/1.191D$$

$$P-D = 1.375D - D = 0.375D = 4.5D \text{ where D is in ft.}$$

$$\text{and } \Delta p'_c = \frac{2.183 \times 10^{-6}(w)^{1.8}(\mu)^{0.2}(1-B_c)(0.94d-D)}{(0.435d-0.375D)^{1.8}(B_s)^{1.8}(s.g.)(D)^{1.2}}$$

$$\text{(III-27)}$$

Now the number of tube rows crossed is h/B_s.

Therefore, for turbulent flow:

$$\Delta p_c = \frac{2.183 \times 10^{-6}(w)^{1.8}(u)^{0.2}(1-B_c)(0.94d-D)(h)}{(0.435d-0.375D)^{1.8}(B_s)^{2.8}(s.g.)(D)^{1.2}}$$

$$\text{(III-28)}$$

In the case of laminar flow:

$$\Delta p'_c = 8.37 \times 10^{-7} \, N \cdot s.g.^{-1} (G'_c)(\mu) / \dot{P} - D) \quad \text{Donohue (1955)}$$

$$\Delta p_c = \frac{2.147 \times 10^{-7} (1 - B_c)(0.94d - D)(w)(\mu)(h)}{(s.g.)(0.435d - 0.375D)(B_s)^2 (D)^2} \quad \text{(III-29)}$$

The total pressure drop through the exchanger shell is:

$\Delta p = \Delta p_b + \Delta p_c$ and the drop can be calculated accurately from the equations derived. However, if some simplifying assumptions are made, e.g.:

$B_c = 0.2$ A 25% cutout for baffles is a common design

$Bs = 0.5$ ft.   A 6 inch baffle spacing may be assumed

$D = 0.5/12$ ft.   1/2 inch tubes approximate lab columns

s.g. $\overset{\sim}{=} 1$ Assume the fluid is water

$\mu^{.2} \overset{\sim}{=} 1$ This is reasonable even for water at high temp.

For turbulent flow, the simplified total pressure drop is:

$$\Delta p = \frac{1.525 \times 10^{-4} (w)^2 (2h-1)}{(d^2 - 0.001736N)^2} + \frac{2.756 \times 10^{-4} (w)^{1.8} (.94d - .0417) 2h}{(0.435d - 0.01563)^{1.8}}$$

$$\text{(III-30)}$$

For laminar flow, the simplified total pressure drop is:

$$\Delta p = \frac{1.525 \times 10^{-4} (w)^2 (2h-1)}{(d^2 - 0.001736N)^2} + \frac{1.979 \times 10^{-4} (.94d - .0417) 2w\mu h}{(0.435d - .01563)}$$

(III-31)

As shown in Figure (32) for the configuration described,

$$d = 0.07571N^{0.4734} \text{ and } d^2 = 0.005732^{0.9474}$$

(III-32)

Therefore, for turbulent flow:

$$\Delta p = \frac{1.525 \times 10^{-4} (w)^2 (2h-1)}{(0.005732N^{.9474} - 0.001736N)^2} +$$

$$\frac{2.756 \times 10^{-4} (w)^{1.8} (.07117N^{.4737} - .0417) 2h}{(.03293N^{.4737} - .01563)^{1.8}}$$

(III-33)

And for laminar flow:

$$\Delta p = \frac{1.525 \times 10^{-4} (w)^2 (2h-1)}{(0.005732N^{.9474} - 0.001736N)^2} +$$

$$\frac{1.979 \times 10^{-4} (.07117N^{.4737} - .0417) 2w\mu h}{(.03293N^{.4737} - .01563)}$$

(III-34)

$$d = 0.9085 \ N^{0.4737}$$

d= shell i.d., inches

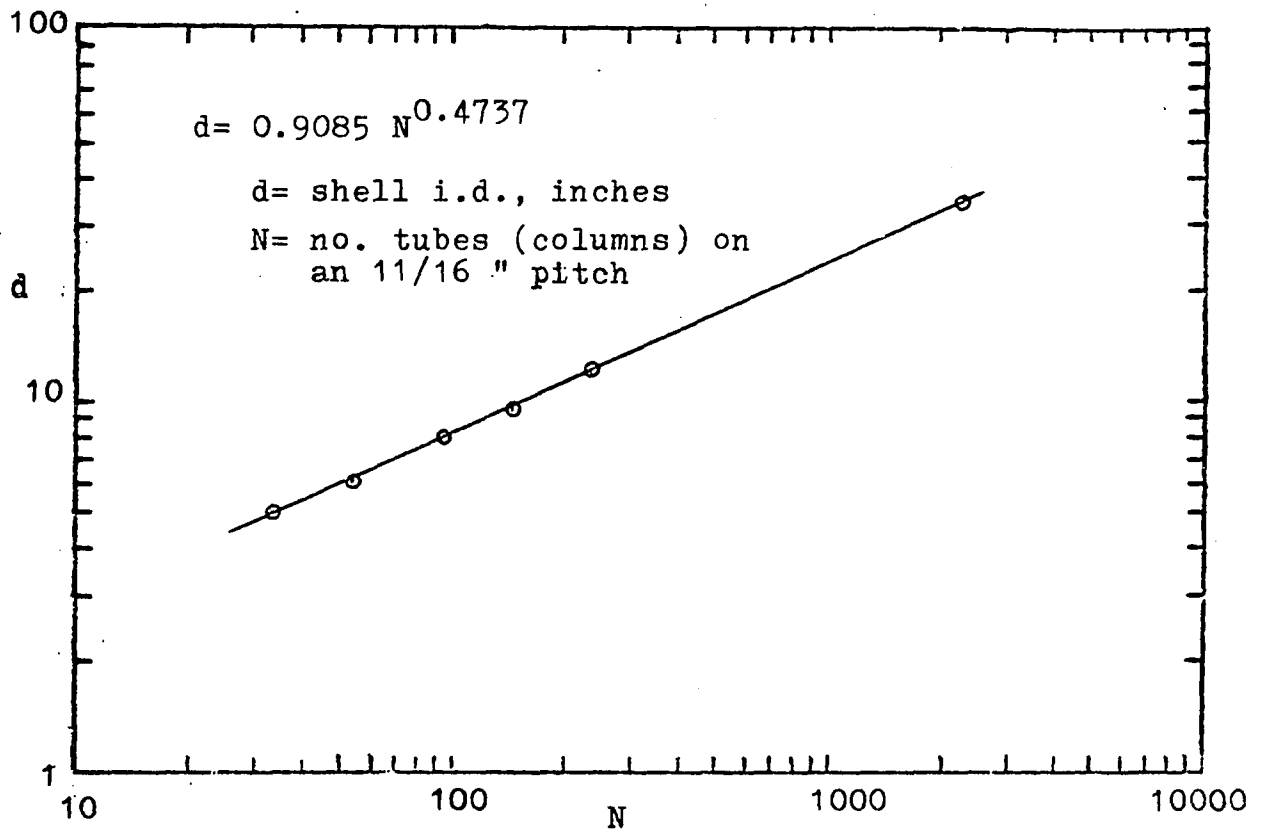N= no. tubes (columns) on an 11/16 " pitch

FIGURE (32)

Heat Exchanger: No. Tubes vs Shell Diameter

where w = fluid (water) rate in lbs/second

h = length of the exchanger tubes, ft.

Δp= pressure drop in psi

N = number of tubes in the exchanger. This must be the full number of tubes that will fill a given shell diameter. Otherwise, "dummy" tubes must be used or the pressure drop calculated will not apply. Also, the tubes must be arranged in a triangular pitch with the flow directed perpendicular to the apex, and the pitch must be 1.375x tube diameter. Finally, it was also assumed that the baffle cutout was 20% (25% area) and that the baffle spacing was 0.5 ft. Most of these assumptions are typical for design, and even the baffle spacing is quite reasonable for the present purpose. However, if it is required, the complete equation with only the first four assumptions, including the 1.375 D pitch, is available in the Appendix.

Also, for the case of laminar flow, the viscosity, μ, is included in the equation. In the case of turbulent flow, the viscosity term was raised to the 0.2 power and, as such could be neglected.

The hydraulic horsepower for the pump is easily calculated from the pressure drop as follows:

$$Hp = \Delta p, \; lb_f/in^2 (144 \; in^2/ft^2)(w \; lb_m/sec)(3600 \; sec/hr)$$

$$(ft^3/62.3 \; lb_m)(Hp\text{-}hr/1.98\times10^6 ft\text{-}lb_f)$$

$$Hp = 0.00420\Delta p(w) \hspace{3cm} (III\text{-}35)$$

Feed and Product Pressure Drop

The feed pump must overcome the line resistance to
the column, the pressure developed in the column due to
the action of the hot upflow and cold downflow reservoir
pumps, and the resistance in the lines to the top and
bottom product receivers. During the hot upflow half
cycle, the column back pressure is almost nil because
the pressure exerted by the hot upflow reservoir pump
is spent as the effluent leaves the column. However,
the back pressure during the cold downflow half cycle
is, for all practical purposes, equal to the full pres-
sure developed by the cold downflow reservoir pump.
Therefore, if a positive displacement pump is used for
feeding the column, the pressure and the power required
is much less during the hot upflow half cycle than during
the cold downflow half cycle.

However, if a centrifugal pump is used, the feed
rate must be kept at a constant value by means of a flow
rate controller and valve. In this case, the feed pump
develops full pressure during both hot upflow and cold

downflow half cycles. During the cold downflow half
cycle, the back pressure is high and the control valve
compensates by assuming a wide open position. During
the hot upflow half cycle, the pressure is low and the
control valve must exert the missing back pressure in
order to maintain a constant flow rate to the column.
Therefore, during both the hot upflow and cold downflow
half cycles, a centrifugal type feed pump would deliver
a constant pressure and would consume a constant amount
of power.

The pressure required to overcome the resistance
in the top and bottom product lines must be developed
by all three pumps (feed, hot upflow reservoir, and cold
downflow reservoir pumps) because these lines eminate
from the two common high pressure points at the top and
bottom of the column. One way of assuring constant flow
rates and sufficient pressure to overcome the resistance
in the lines would be to install a back-pressure valve
in the top product line and a flow controller and control
valve in the bottom product line. Exact control of the
bottom product rate is desirable because this value is
critical to the process. Flow control of the top product
stream is thus obtained indirectly because the feed stream
is also controlled.

As previously discussed, the pressure drop during the hot upflow half cycle is, essentially, the line pressure drop. Since the flow rates are very low, the equations for laminar flow would apply:

$$\Delta p = \frac{4fl}{D_i} \frac{v^2 \rho}{2g_c}$$

$$f = \frac{16}{Re} = \frac{16\mu}{D_i v \rho}$$

$$\Delta p = \frac{64\mu l}{D_i^2 v \rho} \frac{v^2 \rho}{2g_c} = \frac{32\mu l v}{D_i^2 g_c}$$

where μ = viscosity $lb_m/hr/ft$

l = line length, ft.

v = velocity, ft/hr

ρ = fluid density lb_m/ft^3

g_c = conversion factor = $4.17 \times 10^8 = (lb_m/hr^2/ft)(ft^2/lb_f)$

D_i = inside diameter conduit, ft.

$\Delta p = lb_f/ft^2$

now if $v_F = (\emptyset_T + \emptyset_B)Q/.785\ D_i^2$ for the feed   (III-36)

$\qquad v_{TP} = \emptyset_T Q/\ .785D_i^2$ for the top product(III-37)

$\qquad v_{BP} = \emptyset_B Q/\ .785D_i^2$ for the bottom product

(III-38)

then the total pressure drop for the hot upflow half cycle is:

$$\Delta p = \frac{32Q}{.785D_i^4 g_c} \left[\mu_F l_F (\emptyset_T + \emptyset_B) + \mu_{TP} l_{TP} \emptyset_T + \mu_{BP} l_{BP} \emptyset_B \right] + \Delta p_V$$

$$(III-39)$$

where Δp_V = pressure drop for the control valve.

For the case where a positive displacement pump is used,

$$\Delta p_V = 0$$

For the case where a centrifugal pump is used, Δp_V is the full pressure drop developed by the reservoir pump. This was previously derived and the equation is:

$$\Delta p_V = \frac{150(1-\varepsilon)^2}{D_p^2 \, g_c \varepsilon^3} \frac{\mu h}{a_t N} \, Q(1+\emptyset_B) \qquad (III-20)$$

It should be pointed out that this pressure drop was that derived for the cold downflow. The equation derived for hot upflow would not be applicable because it represents the pressure developed at the discharge of the hot upflow reservoir pump at the bottom of the column whereas the feed input is at the top of the column.

The overall equation for the feed pump pressure drop for the cold downflow half cycle for both the centrifugal and positive displacement pumps is:

$$\Delta p_F = \frac{32Q}{.785 D_i^4 g_c} \left[\mu_F l_F (\varnothing_T + \varnothing_B) + \mu_{TP} l_{TP} \varnothing_T + \mu_{BP} l_{BP} \varnothing_B \right]$$

$$+ \frac{150(1-\varepsilon)^2}{D_p^2 g_c \varepsilon^3} \frac{\mu h}{a_t N} Q(1+\varnothing_B) \qquad (III-40)$$

This is also the pressure drop equation for the centrifugal pump for the hot upflow half cycle. As previously discussed, due to the action of the control valve, the pressure drops for both the hot upflow and cold downflow half cycles are the same.

The hydraulic horsepower is easily calculated for the cold downflow half cycle for both the centrifugal and P.D. pumps:

$$Hp_F = \Delta p \ lb_f/ft^2 (rate, \ ft^3/hr) (Hp-hr/1.98 \times 10^6 ft-lb_f)$$

$$Hp_{F2} = \frac{2.059 \times 10^{-5} \ Q^2}{D_i^4 g_c} \left[\mu_F l_F (\varnothing_T + \varnothing_B)^2 + \mu_{TP} l_{TP} \varnothing_T^2 + \mu_{BP} l_{BP} \varnothing_B^2 \right]$$

$$+ \frac{7.576 \times 10^{-5} (1-\varepsilon)^2}{D_p^2 g_c \varepsilon^3} \frac{\mu h}{a_t N} Q^2 (1+\varnothing_B)^2 \qquad (III-41)$$

For the hot upflow half cycle, the equations are:

For the centrifugal pump:

$$Hp_{F1} = \frac{2.059 \times 10^{-5} Q^2}{D_i^4 g_c} \left[\mu_F l_F (\phi_T + \phi_B)^2 + \mu_{TP} l_{TP} \phi_T^2 + \mu_{BP} l_{BP} \phi_B^2 \right]$$

$$+ \frac{7.576 \times 10^{-5} (1-\epsilon)^2}{D_p^2 g_c \epsilon^3} \frac{\mu h}{a_t N} Q^2 (1 + \phi_B)(1 - \phi_B)$$

$$(III-42)$$

For the positive displacement (P.D.) pump:

$$Hp_{F1} = \frac{2.059 \times 10^{-5} Q^2}{D_i^4 g_c} \left[\mu_F l_F (\phi_T + \phi_B)^2 + \mu_{TP} l_{TP} \phi_T^2 + \mu_{BP} l_{BP} \phi_B^2 \right]$$

$$(III-43)$$

Utility Cost Equations

The cost of operating the parametric pumping system is a useful criteria on which to base the choice of a feed material. Certainly, the value of the products from separation would have to equal, as a bare minimum, the cost of the utilities. In any real design, the costs of depreciation, labor, and overhead would also have to be met. But these costs can vary widely depending on the materials of construction, the use of new or existing equipment, the labor costs in particular area, the degree of automatic control adopted, and other factors. For the present case, the purpose is mainly to provide a basic yardstick against which to measure the feasibility of

attempting the separation at all. The other factors
can be readily taken into account once the actual
basic cost of operating the equipment has been es-
tablished.

The utility operating costs can best be esti-
mated on a yearly basis. In the case of pumping,
the design equations were developed for the hydraulic
horsepower for the hot up and cold downflow half
cycles. To obtain the yearly costs, it is necessary
to multiply the hydraulic horsepower by the duration
of the half cycles, (π/ω), the number of half cycles
per year (n), the reciprocal of the pump efficiency
(1/E), the conversion factor (0.746 kw-hr./Hp-hr.),
and the cost of electricity in \$/kw-hr (C_{EL}).

For the heating and cooling requirements, the
duties were developed as equations for the duration
of the hot upflow and cold downflow half cycles. The
cost of heating may be taken as the cost of the steam
used during all the hot upflow half cycles during the
year and the cost of cooling may be taken as the cost
of brine refrigeration consumed during the cold down-
flow half cycles. Therefore, if (n) is taken as the
number of cycles (or half cycles) per year, the cost

of heating may be estimated by multiplying the appropriate equation by the reciprocal of the heating value of a pound of steam (roughly 1/1000) and by the cost of a pound of steam (C_{ST}).

The cost of cooling (refrigeration) would be estimated by multiplying the appropriate equation by the conversion factor (ton-hr/12000 BTU) and by the cost of the brine in dollars per ton-hr (C_{BR}).

The overall cost of the utilities for operating the plant would be as follows:

$$C_0 = \left[(w_t c_t + w_s c_s + w_f c_f)(N)(h) + Q(1-\emptyset_B)(\rho_1)(c_1)(\pi/\omega) \right]$$

$$(T_1 - T_2)(n)(C_{ST}/1000)$$

$$+ \left[(w_t c_t + w_s c_s + w_f c_f (N)(h) + Q(1+\emptyset_B)(\rho_2)(c_2)(\pi/\omega) \right]$$

$$(T_2 - T_{2H})(n)(C_{BR}/12000)$$

$$+ 0.00420(n)(2\pi/\omega)(0.746/E)(C_{EL})$$

$$\left[\frac{1.525 \times 10^{-4}(w)^3(2h-1)}{(0.005732N^{0.9474}-0.001736N)^2} \right.$$

$$\left. + \frac{2.756 \times 10^{-4}(w)^{2.8}(0.07117N^{0.4737}-0.04117)(2h)}{(0.03293N^{0.4737}-0.01563)^{1.8}} \right]$$

$$+(1.98 \times 10^6)^{-1}(\pi/\omega)(n)(0.746/E)(C_{EL})$$

$$\left[\frac{150(1-\varepsilon)^2}{D_p^2 g_c \varepsilon^3} \quad \frac{\mu h}{a_t N} \quad (Q^2) \right] \left[\mu_1(1-\emptyset_B)^2 + \mu_2(1+\emptyset_B)^2 \right]$$

$$+ (1.98 \times 10^6)^{-1}(\pi/\omega)(n)(0.746/E)C_{EL}$$

$$\left\{ \frac{2 \times 32 \, Q^2}{0.785 D_i^4 \, g_c} \left[\mu_F l_F(\emptyset_B+\emptyset_T)^2 + \mu_{TP} l_{TP} \emptyset_T^2 + \mu_{BP} l_{BP} \emptyset_B^2 \right] \right.$$

$$\left. + \frac{150 \, (1-\varepsilon)^2}{D_p^2 \, g_c \varepsilon^3} \quad \frac{\mu_2 h Q^2}{a_t N} \left[(1+\emptyset_B)^2 + (1+\emptyset_B)(1-\emptyset_B) \right] \right\}$$

$$(III-44)$$

These equations apply to the conditions of turbulent
flow in the parapump assembly shell, laminar flow in the
feed and product lines, and the use of a centrifugal type
feed pump. Equations have been derived for alternate
conditions and are presented in the design equation sec-
tions and in the Appendix. However, the equations used
in the cost equation represent the most likely conditions
to be met in any actual design.

Energy Equations

In this section the energy equations for steam, refrigeration, and electrical pumping power are developed as functions of the key parameters of reservoir displacement $(Q\pi/\omega)$, the bottom product/reservoir ratio $(\emptyset_B)$, the reservoir displacement rate (Q), the cycle time (π/ω), and the number of tubes (n) in the multicolumn parapump assembly.

To put the energy equations on a common basis, the electrical energies will be converted to their equivalents in BTU/cycle. Then all energy equations will also be presented as BTU/lb of bottom product.

Steam heating. The duty in BTU/cycle is obtained by combining Equations (III-12, 13) with Equation (III-17)

$$q_1 = \left[\frac{(w_t c_t + w_s c_s + w_f c_f)(T_1 - T_2)}{(1+m_o)(1+b)(\varepsilon)(a_t)}\right] (Q\pi/\omega)(1+\emptyset_B)$$

$$+ \ \rho_f c_f (T_1 - T_2)(Q\pi/\omega)(1-\emptyset_B) \tag{III-45}$$

Now since the pounds of bottom product per cycle is

$$P_B(2\pi/\omega) = Q\emptyset_B \rho_f (2\pi/\omega) = 2\rho_f(Q\pi/\omega)\emptyset_B \tag{III-46}$$

the duty per pound of bottom product is

$$\frac{q_1}{P_B(2\pi/\omega)} = \left[\frac{(w_t c_t + w_s c_s + w_f c_f)(T_1 - T_2)}{(1+m_o)(1+b)(\varepsilon)(a_t)(2\rho_f)}\right] \frac{(1+\emptyset_B)}{\emptyset_B}$$

$$+ \ \left[\frac{c_f(T_1 - T_2)}{2}\right] \frac{(1-\emptyset_B)}{\emptyset_B} \tag{III-47}$$

Heat transfer fluid. If the parapump system design is correct, heat transfer fluid left in the shell at the end of a hot or cold half cycle should normally be displaced to the reservoir servicing the column during that half cycle. The heat saved by this procedure can be a substantial portion of the total. This heat content is

$$q_s = V_s \rho_{HTF} c_{HTF} (T_1 - T_2)$$

where V_s is the volume of the shellside fluid, and

$$V_s = .785h(d^2 - D^2 N) \qquad \text{(III-48)}$$

Now, from Equations (III-12,13),

$$h \geq \left[\frac{1}{(1+b)(1+m_o)\varepsilon(a_t)} \right] \left(Q\frac{\pi}{\omega} \right) \left(\frac{1+\phi_B}{N} \right) = K_h \left(Q\frac{\pi}{\omega} \right) \frac{1+\phi_B}{N}$$

$$\text{(III-48a)}$$

and

$$d = 0.07571 \ N^{0.4737} \qquad \text{(III-32)}$$

Then

$$V_s = \frac{(1+\phi_B)(Q\pi/\omega)}{(1+b)(1+m_o)\varepsilon(a_t)} \ (0.0045 N^{-0.0526} - 0.785 D^2) \qquad \text{(III-49)}$$

and

$$q_s = \frac{(1+\phi_B)(Q\pi/\omega)(\rho c)_{HTF}(T_1 - T_2)}{(1+b)(1+m_o)(\varepsilon)(a_t)} \left[\frac{0.0045}{N^{0.0526}} - .785 D^2 \right] \qquad \text{(III-50)}$$

Now Equation (III-50) represents the heat content of the heat transfer fluid surrounding the tubes at the end of each half cycle and is ordinarily ignored in bench scale operations. However, even in this case, there is occasionally some difficulty in restoring the hot and cold operating temperatures of the baths during the recuperation periods when there is no direct process heat or cooling load.

If the design or the operation is poor and the shellside heat transfer fluid is, at the end of the cold half cycle, dumped into the hot fluid reservoir, then the temperature of the reservoir must be raised above the normal operating level to provide the sensible heat needed to cope with the instantaneous load represented by Equation (III-50) in addition to the instantaneous load due to the temperature switchover of the tubes (Equation III-15). The same duties apply to the cold fluid reservoir and the refrigeration load.

Therefore, Equation (III-50) is a potential maximum additional duty for both steam and refrigeration in units of BTU/cycle. In BTU per pound of bottom product,

$$\frac{q_s}{P_B(2\pi/\omega)} = \frac{(\rho_{HTF})(c_{HTF})(T_1-T_2)}{(1+b)(1+m_o)(\epsilon)(a_t)(2\rho_f)} \left[\frac{0.0045}{N^{0.0526}} - .785D^2\right] \frac{1+\emptyset_I}{\emptyset_B}$$

(III-51)

Refrigeration cooling. The equations for cooling are almost identical to those for heating. Combining Equations (III-12, 13 and III-18), the BTU/cycle

$$q_2 = \left[\left[\frac{(w_t c_t + w_s c_s + w_f c_f)}{(1+m_o)(1+b)(\epsilon)(a_t)} + \rho_f c_f\right] (T_1-T_2)\right] Q\pi/\omega)(1+\emptyset_B)$$

(III-52)

and the duty per pound of bottom product is

$$\frac{q_2}{P_B(2\pi/\omega)} = \left[\left[\frac{(w_t c_t + w_s c_s + w_f c_f)}{(1+m_o)(1+b)(\epsilon)(a_t)(2\rho_f)} + \frac{c_f}{2}\right] (T_1-T_2)\right] \frac{(1+\emptyset_B)}{\emptyset_B}$$

(III-53)

Heat transfer fluid pump. The power for heat transfer fluid pumping depends first on the heat transfer during the switchover period, which, by combining Equations (III-15) and (III-12, 13) is, in BTU/switchover,

$$q_t = \left[\frac{(w_t c_t + w_s c_s + w_f c_f)(T_1 - T_2)}{(1+m_o)(1+b)(\varepsilon)(a_t)} \right] (Q\pi/\omega)(1+\emptyset_B)$$

$$(III-54)$$

The time for the switchover, as discussed in Chapter 5 and Appendix III in general, and specifically in the assumptions for the Chapter 5 process design example, is short (τ = 120 seconds). The switchover heat transfer rate (q_t/τ) is then, as shown in Figure (23) typically 18 to 20 times the overall rate for either the heating or cooling half cycle. The pumping rate for the heat transfer fluid (water) is then obtained from a heat balance (Eq. 93) combined with Eq. (III-54) to give

$$w = \left[\frac{(w_t c_t + w_s c_s + w_f c_f)(T_1 - T_2)}{(1+m_o)(1+b)(\varepsilon)(a_t)(\tau)(c_{HTF})(\Delta T_w)} \right] Q\frac{\pi}{\omega}(1+\emptyset_B)$$

$$= (K_w)(Q\pi/\omega)(1+\emptyset_B) \qquad (III-54a)$$

The temperature rise (ΔT_w), as discussed under the general assumptions for the Chapter 5 process design example, may be taken as $15.2^{\circ}R$, and c_{HTF} is 1 BTU/lb/$^{\circ}R$.

The pressure drop for the heat transfer fluid was given by Equation (III-33) which, in a simpler form, is

$$\Delta p_{HTF} = F_{N1} w^2 (2h-1) + F_{N2}(2h)w^{1.8} \qquad (96)$$

where F_{N1} and F_{N2} are functions of the number of columns or tubes in the parapump assembly and are listed in Table (3) for different values of N. The water rate (w) in pounds per second was given above and the tube length (h) may be taken from Equation (III-48a). Combining (III-48a, 54a, and 96) gives

$$
\Delta P_{HTF} = (2F_{N1}K_w^2K_h)(Q\pi/\omega)^3(1+\emptyset_B)^3/N
$$

$$
- (F_{N1}K_w^2)(Q\pi/\omega)^2(1+\emptyset_B)^2
$$

$$
+ (2F_{N2}K_w^{1.8}K_h)(Q\pi/\omega)^{2.8}(1+\emptyset_B)^{2.8}/N \qquad \text{(III-54b)}
$$

The hydraulic horsepower for the heat transfer fluid is obtained by combining Equations (III-35), (93), and (III-54) to give

$$
Hp_{HTF} = 0.0042 \left[\frac{w_tc_t+w_sc_s+w_fc_f)(T_1-T_2)(\Delta p_{HTF})}{(1+m_o)(1+b)(\varepsilon)(a_t)(\tau)(c_{HTF})(\Delta T_w)} \right] Q\frac{\pi}{\omega}(1+\emptyset_B)
$$

$$
\text{(III-55)}
$$

The BTU/cycle equivalent of the horsepower is

$$
q_{HTF} = Hp_{HTF}(2\pi/\omega \text{ hr/cycle})(2546 \text{ BTU/Hp-hr}) \qquad \text{(III-56)}
$$

or

$$
q_{HTF} = \left[\frac{21.4(w_tc_t+w_sc_s+w_fc_f)(T_1-T_2)(\Delta p_{HTF})}{(1+m_o)(1+b)(\varepsilon)(a_t)(\tau)(c_{HTF})(\Delta T_w)} \right] Q\frac{\pi}{\omega}(1+\emptyset_B)(\frac{\pi}{\omega})
$$

$$
\text{(III-57)}
$$

And the equation for the BTU/lb of bottom product
is a combination of Equations (III-57) and (III-50).

$$\frac{q_{HTF}}{P_B(2\pi/\omega)} = \left[\frac{10.7(w_t c_t + w_s c_s + w_f c_f)(T_1 - T_2)(\Delta p_{HTF})}{(1+m_o)(1+b)(\varepsilon)(a_t)(\tau)(c_{HTF}\Delta T_w)(\rho_f)}\right]\left[\frac{1+\phi_B}{\phi_B}\right]\frac{\pi}{\omega}$$

(III-58)

Bottom reservoir pump. The pressure drop for the
bottom reservoir pump is given by combining Equations
(III-20) and (III-12, 13) to give

$$\Delta p_{BRP} = \left[\frac{150(1-\varepsilon)^2(\mu_1)}{D_p^2(g_c)(\varepsilon)^4(a_t)^2(1+m_o)(1+b)}\right]\left(\frac{Q}{N}\right)^2 (1-\phi_B^2)\frac{\pi}{\omega}$$

(III-59)

The horsepower for the bottom reservoir pump is

$$HP_{BRP} = \Delta p_{BRP}(Q)(1-\phi_B)(Hp-hr/1.98 \times 10^6 ft-lb_f)$$

(III-60)

where the pressure drop is in lb_f/ft^2 and the rate term
is in ft^3/hr. In more exact terms,

$$Hp_{BRP} = \left[\frac{150(1-\varepsilon)^2(\mu_1)(1.98\times10^6)^{-1}}{D_p^2(g_c)(\varepsilon)^4(a_t)^2(1+m_o)(1+b)}\right]\left(\frac{Q}{N}\right)^2 (1-\phi_B)^2(1+\phi_B) Q\frac{\pi}{\omega}$$

(III-61)

The BTU/cycle equivalent to Equation (III-61) is
obtained by multiplying by the factor 2546 BTU/Hp-hr and
the hours per cycle of operation (π/ω). The result is

$$q_{BRP} = \left[\frac{0.193(1-\varepsilon)^2(\mu_1)}{D_p^2(g_c)(\varepsilon)^4(a_t)^2(1+m_o)(1+b)}\right]\left(\frac{Q}{N}\right)^2 (1-\emptyset_B)^2(1+\emptyset_B) Q\left(\frac{\pi}{\omega}\right)^2$$

$$(III-62)$$

The heat transfer in BTU/lb of bottom product is

$$\frac{q_{BRP}}{P_B(2\pi/\omega)} = \left[\frac{0.193(1-\varepsilon)^2(\mu_1)(2\rho_f)^{-1}}{D_p^2(g_c)(\varepsilon)^4(a_t)^2(1+m_o)(1+b)}\right]\left(\frac{Q}{N}\right)^2 (1-\emptyset_B)^2(1+\emptyset_B) \frac{\left(\frac{\pi}{\omega}\right)}{\emptyset_B}$$

$$(III-63)$$

Top reservoir pump. The pressure drop for the top reservoir pump is obtained by combining Equations (III-20) and (III-12, 13) to give

$$\Delta p_{TRP} = \left[\frac{150 \ (1-\varepsilon)^2(\mu_2)}{D_p^2(g_c)(\varepsilon)^4(a_t)^2(1+m_o)(1+b)}\right]\left(\frac{Q}{N}\right)^2 (1+\emptyset_B)^2\left(\frac{\pi}{\omega}\right)$$

$$(III-64)$$

The horsepower for the top reservoir pump is obtained, as before, by multiplying the pressure drop by the flow rate $Q(1+\emptyset_B)$ and by the factor (Hp-hr/1.98x10^6 ft-lb$_f$).

$$Hp_{TRP} = \left[\frac{150 \ (1-\varepsilon)^2(\mu_2)(1.98x10^6)^{-1}}{D_p^2(g_c)(\varepsilon)^4(a_t)^2(1+m_o)(1+b)}\right]\left(\frac{Q}{N}\right)^2(1+\emptyset_B)^3 (Q\pi/\omega)$$

$$(III-65)$$

The BTU/cycle equivalent to Equation (III-65) is obtained by multiplying by the factor 2546 BTU/Hp-hr and the hours per cycle (π/ω) of operation. The result is

$$q_{TRP} = \left[\frac{0.193(1-\varepsilon)^2(\mu_2)}{D_p^2(g_c)(\varepsilon)^4(a_t)^2(1+m_o)(1+b)} \right] \left(\frac{Q}{N} \right)^2 (1+\emptyset_B)^3 (Q\pi/\omega) \frac{\pi}{\omega}$$

$$(III-66)$$

The heat transfer in BTU/lb of bottom product is

$$\frac{q_{TRP}}{P_B(2\pi/\omega)} = \left[\frac{0.193(1-\varepsilon)^2(\mu_2)(2\rho_f)^{-1}}{D_p^2(g_c)(\varepsilon)^4(a_t)^2(1+m_o)(1+b)} \right] \left(\frac{Q}{N} \right)^2 \frac{(1+\emptyset_B)^3}{\emptyset_B} \left(\frac{\pi}{\omega} \right)$$

$$(III-67)$$

<u>Feed pump</u>. The pressure drop for the feed pump is in two parts, the resistance of the lines and the resistance due to the column. This was discussed at length (see pages 198 to 203). The equation for the pressure drop is obtained by combining Equations (III-40) and (III-12, 13).

$$\Delta P_{FP} = \frac{32Q}{.785_i^4 \ g_c} \left[\mu_F l_F (\emptyset_T + \emptyset_B) + \mu_{TP} l_{TP} \emptyset_T + \mu_{BP} l_{BP} \emptyset_B \right]$$

$$+ \frac{150(1-\varepsilon)^2(\mu_2)}{D_p^2(g_c)(\varepsilon)^4(a_t)^2(1+m_o)(1+b)} \left(\frac{Q}{N} \right)^2 (1+\emptyset_B)^2 \left(\frac{\pi}{\omega} \right)$$

$$(III-68)$$

It will be noticed that the second half of the equation is identical to Equation (III-64) for the top reservoir pump. This, as was discussed previously, is due to the fact that the feed pump must exceed the maximum pressure imposed on the column which is at the point of entry during cold downflow.

The hydraulic horsepower for the feed pump is obtained by multiplying each half of Equation (III-68) by the respective flow rates and by the factor $(Hp\text{-}hr/1.98\text{x}10^6)$.

$$Hp_{FP} = \frac{20.6\text{x}10^{-6}Q^2}{D_i^4 \, g_c} \left[\mu_F l_F (\emptyset_T + \emptyset_B)^2 + \mu_{TP} l_{TP} \emptyset_T^2 + \mu_{BP} l_{BP} \emptyset_B^2\right]$$

$$+ \left[\frac{150(1-\epsilon)^2 (\mu_2)(1.98\text{x}10^6)^{-1}}{D_p^2 (g_c)(\epsilon)^4 (a_t)^2 (1+m_o)(1+b)}\right] \left(\frac{Q}{N}\right)^2 \quad (1+\emptyset_B)^3 (Q\pi/\omega)$$

$$(\text{III-69})$$

The BTU/cycle equivalent to Equation (III-69) is obtained by multiplying by the factor 2546BTU/Hp-hr and the hours of operation per cycle $(2\pi/\omega)$. The result is

$$q_{FP} = \frac{0.105Q^2\pi/\omega}{D_i^4 \, g_c} \left[\mu_F l_F (\emptyset_T + \emptyset_B)^2 + \mu_{TP} l_{TP} \emptyset_T^2 + \mu_{BP} l_{BP} \emptyset_B^2\right]$$

$$+ \frac{0.385(1-\epsilon)^2 (\mu_2)}{D_p^2 (g_c)(\epsilon)^4 (a_t)^2 (1+m_o)(1+b)} \left(\frac{Q}{N}\right)^2 (1+\emptyset_B)^3 (Q\pi/\omega)\frac{\pi}{\omega}$$

$$(\text{III-70})$$

The heat transfer in BTU/lb of bottom product is

$$\frac{q_{FP}}{P_B(2\pi/\omega)} = \frac{0.0525}{\rho_f D_i^4 g_c} \left(\frac{Q}{\emptyset_B}\right)\left[\mu_F l_F (\emptyset_T + \emptyset_B)^2 + \mu_{TP} l_{TP} \emptyset_T^2 + \mu_{BP} l_{BP} \emptyset_B^2\right]$$

$$+ \frac{0.385(1-\epsilon)^2 (\mu_2)(2\rho_f)^{-1}}{D_p^2 (g_c)(\epsilon)^4 (a_t)^2 (1+m_o)(1+b)} \left(\frac{Q}{N}\right)^2 \frac{(1+\emptyset_B)^3}{\emptyset_B} \frac{\pi}{\omega}$$

$$(\text{III-71})$$

APPENDIX IV

PHYSICAL AND THERMODYNAMIC DATA

The data presented in this section are used in the
process design example for the toluene-heptane-silica
gel system in Chapter 5 and also for the salt-water-resin
system in Appendix V. The two systems, insofar as engi-
neering and physical properties are concerned, are repre-
sentative of two general types--an aqueous system with an
ion-exchange resin, and an organic anhydrous system with
a solid adsorbent. The data appear in the following
tables and graphs:

Properties of Adsorbents and Column Materials   Table 8

Viscosities of Toluene-n-Heptane Mixtures   Table 9

Properties of Dilute $NaNO_3$ Solutions   Table 10

Viscosities of Toluene and n-Heptane   Figure 33

Specific Heats of Toluene and n-Heptane   Figure 34

Specific Gravity of Aqueous $NaNO_3$ Solutions   Figure 35

Specific Heat of Aqueous $NaNO_3$ Solutions   Figure 36

Viscosity of Aqueous $NaNO_3$ Solutions   Figure 37

TABLE 8

Properties of Adsorbents and Column Materials

Silica Gel (Fisher Scientific Co.)

Specific heat, calories/gram/$^{\circ}$C	0.316
Void fraction, ϵ	0.38
Specific gravity	2.2
Packing density, grams/cm^3	0.722
Pore volume, cm^3/gm dry adsorbent	0.43
Moisture, weight %	0
Particle size--range, microns	250-550
average, feet	13.2 x 10^{-4}

Ion Exchange Resin (Bio Rad AG 11 A8)

Specific heat, calories/gram/$^{\circ}$C	0.65
Void fraction, ϵ	0.38
Density, gm dry resin/cm^3 wet resin	0.766
Packing density, gm dry resin per cm^3 of bed volume	0.475
Pore volume, cm^3/gm dry resin	0.522
Moisture, weight %	36.8-40.3
Particle size, microns	149
feet	4.89 x 10^{-4}

Column Materials

Specific heat, calories/gm/$^{\circ}$C	
borosilicate glass	0.20
stainless steel	0.12
Specific gravity, grams/cm^3	
borosilicate glass	2.24
stainless steel	8.02

TABLE 9

Viscosities of Toluene-n-Heptane Mixtures, Centipoise

Temp., $^\circ$C	n-Heptane	Toluene	20% Toluene	10% Toluene
80	.25	.33	.26	.26
70	.27	.36	.28	.28
60	.29	.40	.31	.30
50	.33	.45	.35	.34
40	.37	.49	.39	.38
30	.40	.54	.42	.41
20	.44	.60	.46	.45
10	.48	.67	.51	.49
5	.50	.70	.53	.51
0	.54	.75	.57	.56

Source: Perry's Chemical Engineers' Handbook, 4th ed.,
         Figure 3-43

Mixture viscosities calculated from the Kern equation

$$1/\mu_{Lm} = w_1/\mu_1 + w_2/\mu_2 \quad \text{where } w = \text{wt. fract.}$$

TABLE 10

Properties of Dilute NaNO$_3$ Solutions

	Temp., $^{\circ}C$	Sp. Gr.	Visc., cp	Sp. Heat
Water				
	0	0.99987	1.7938	1.0087
	25	0.99707	0.8954	0.9977
	50	0.98807	0.5492	0.9983
	75	0.97489	0.3807	1.0016
	100	0.95838	0.2839	1.0065
5% NaNO$_3$				
	0	1.0322*	1.9** 20°	0.9706***
	25	1.0293*	1.0713 20°	0.9608***
	50	1.0200*	0.65**	0.9619***
	75	1.0064*	0.48**	0.9656***
	100	0.9894*	0.32**	0.9708***
10% NaNO$_3$				
	0	1.0673*	2.05** 20°	0.9325***
	25	1.0643*	1.1279 20°	0.9239***
	50	1.0547*	0.75**	0.9255***
	75	1.0406*	0.50**	0.9295***
	100	1.0230	0.38**	0.9352***

Notes:

* Calculated from the specific gravity at 20/4°C for 5% NaNO$_3$ (1.0323) and 10% NaNO$_3$ (1.0674).

** Estimated from the viscosity data at 20°C and the generalized chart, Fig. 3-61, Perry, 4th ed.

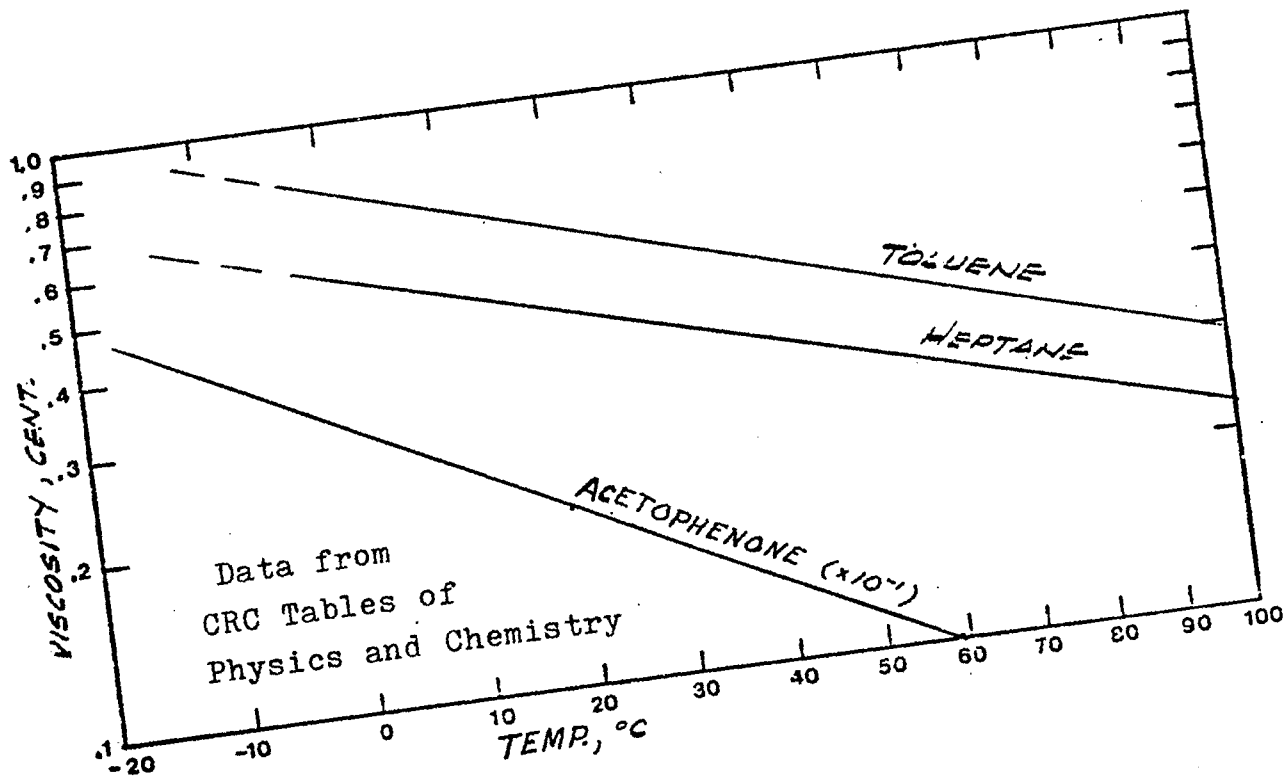*** Calculated from the values for water and for solid NaNO$_3$ (0.247 at 0° and 0.270 at 50°C).

Data from
CRC Tables of
Physics and Chemistry

FIGURE (33)

Viscosities of Toluene, n-Heptane, and
Acetophenone

Data from Perry's Chemical Engineers' Handbook,

Fourth Edition (1963)

C_p, calories/gram/ $^{\circ}$C.

T, $^{\circ}$C
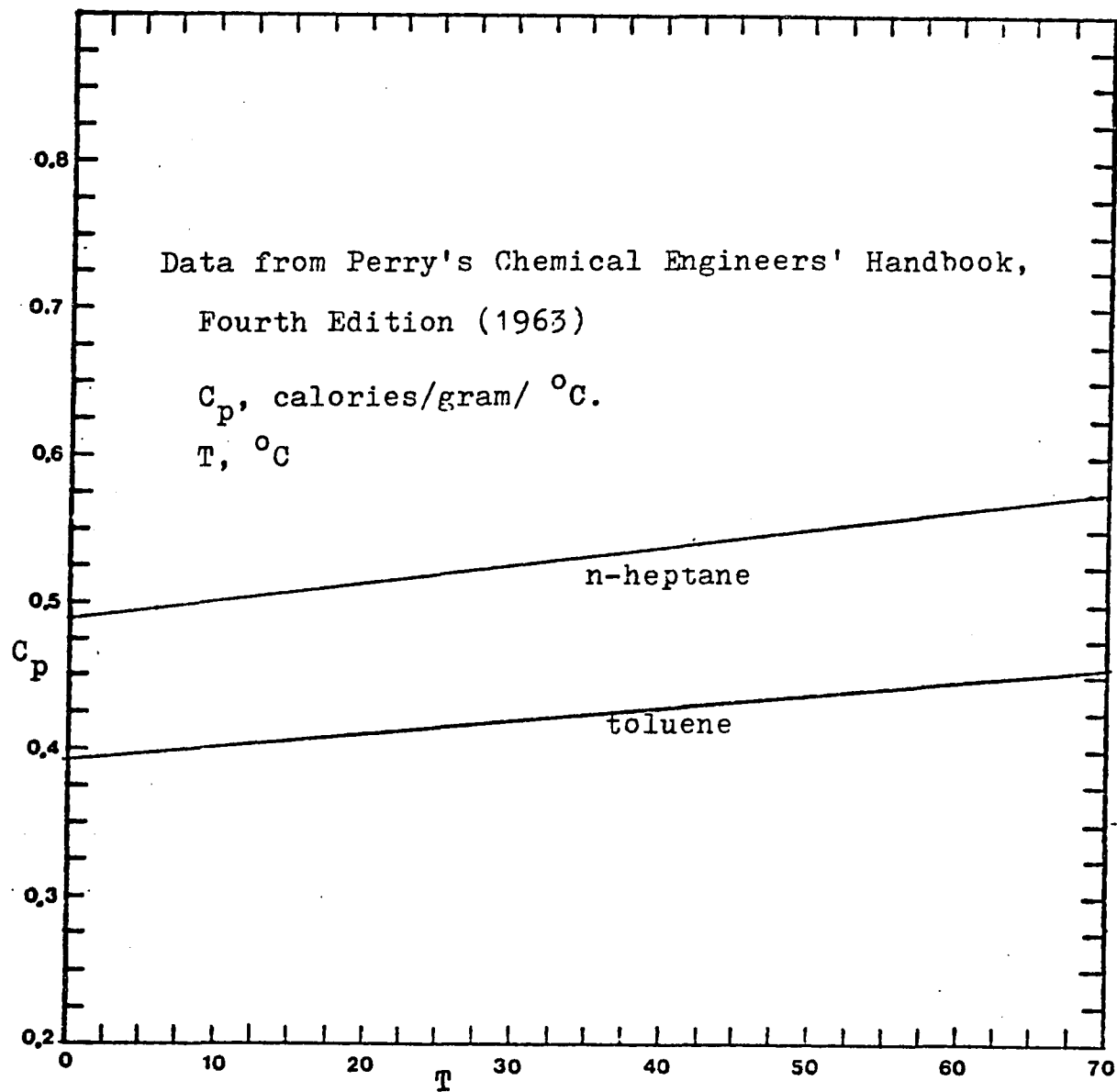
n-heptane

toluene

FIGURE (34)

Specific Heats of Toluene, n-Heptane
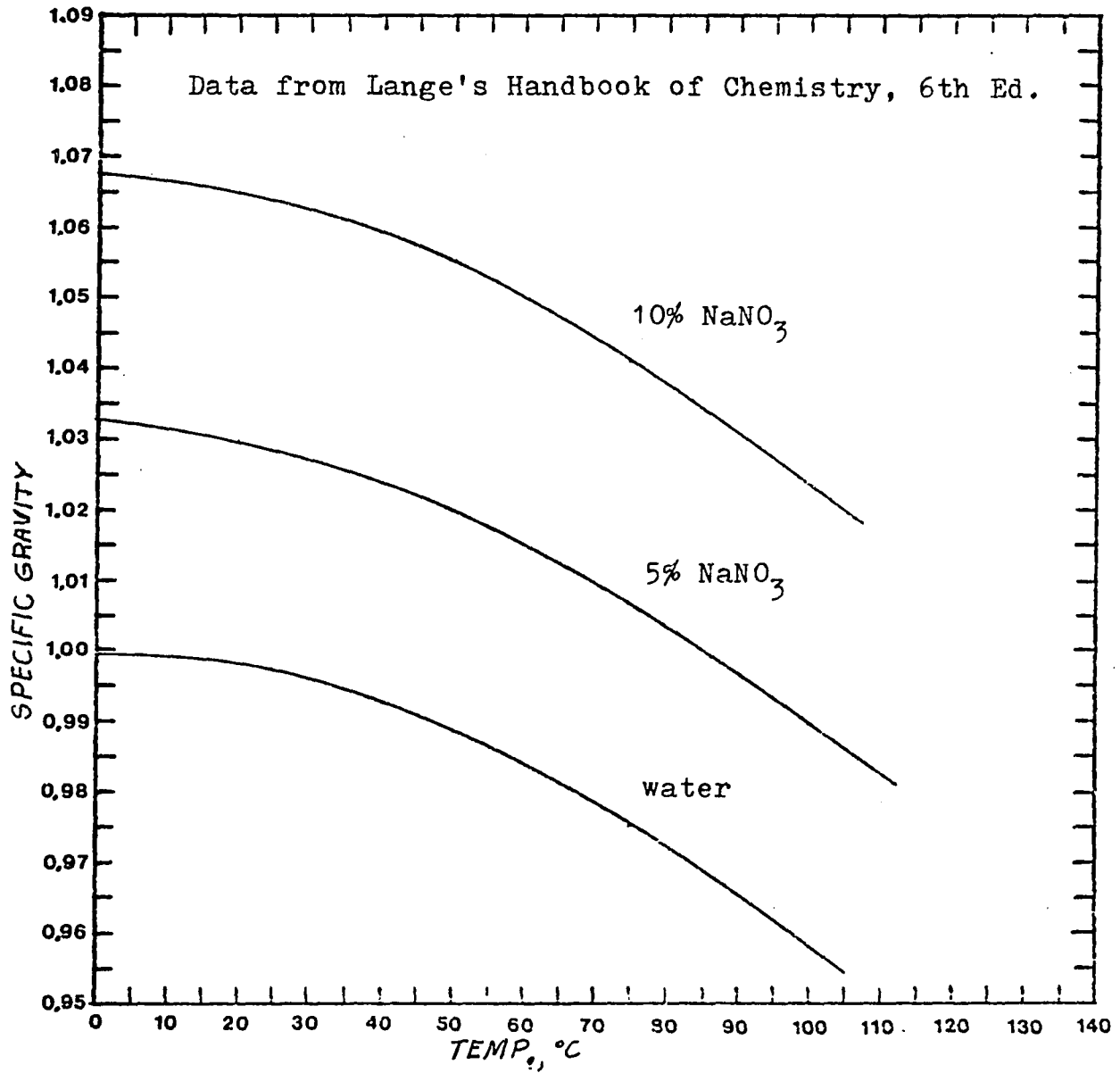
FIGURE (35)

Specific Gravities of Aqueous NaNO₃ Solutions

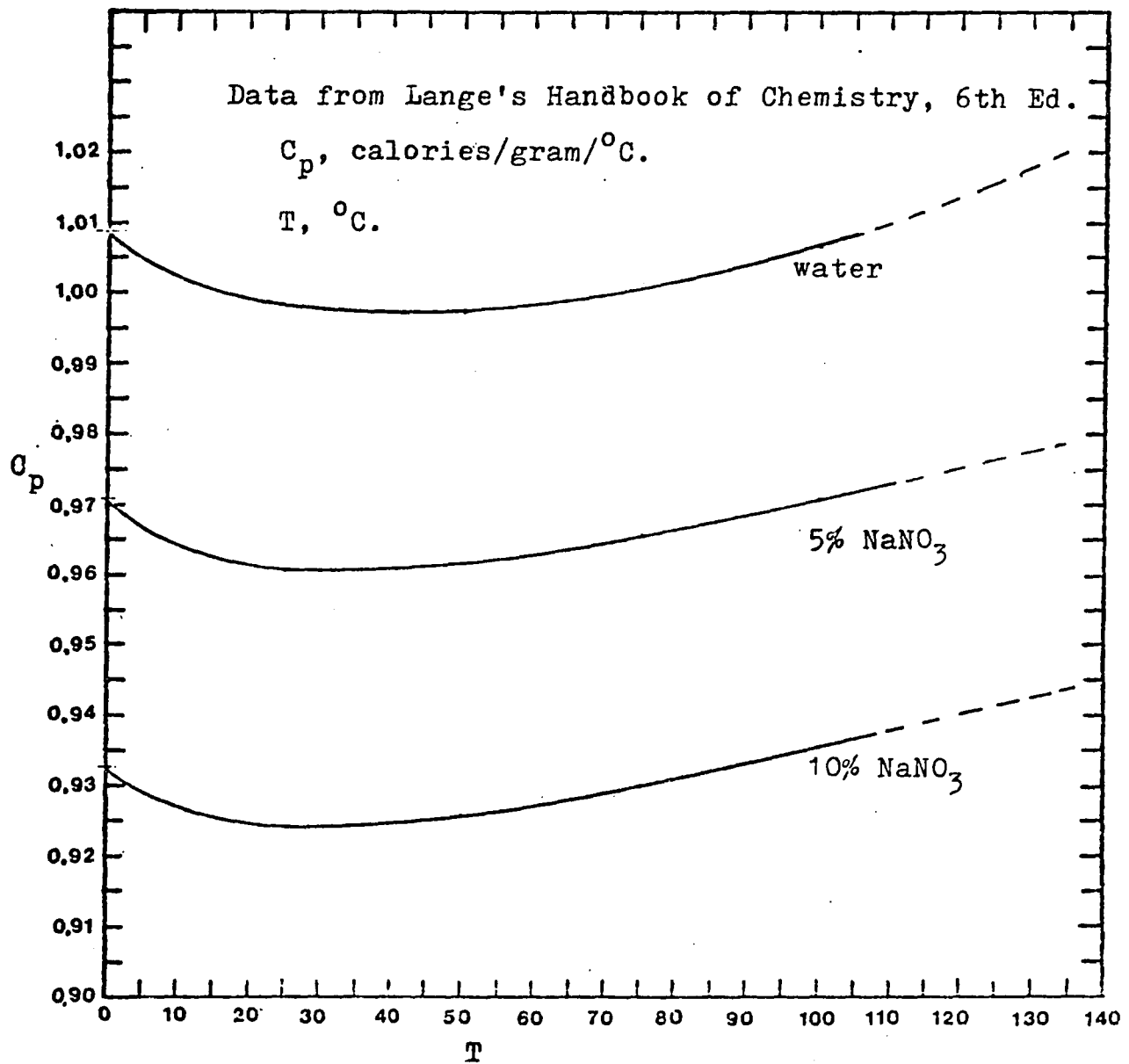Data from Lange's Handbook of Chemistry, 6th Ed.

C_p, calories/gram/^{o}C.

T, ^{o}C.

water

5% NaNO$_3$

10% NaNO$_3$

FIGURE (36)

Specific Heats of Aqueous N$_a$NO$_3$ Solutions

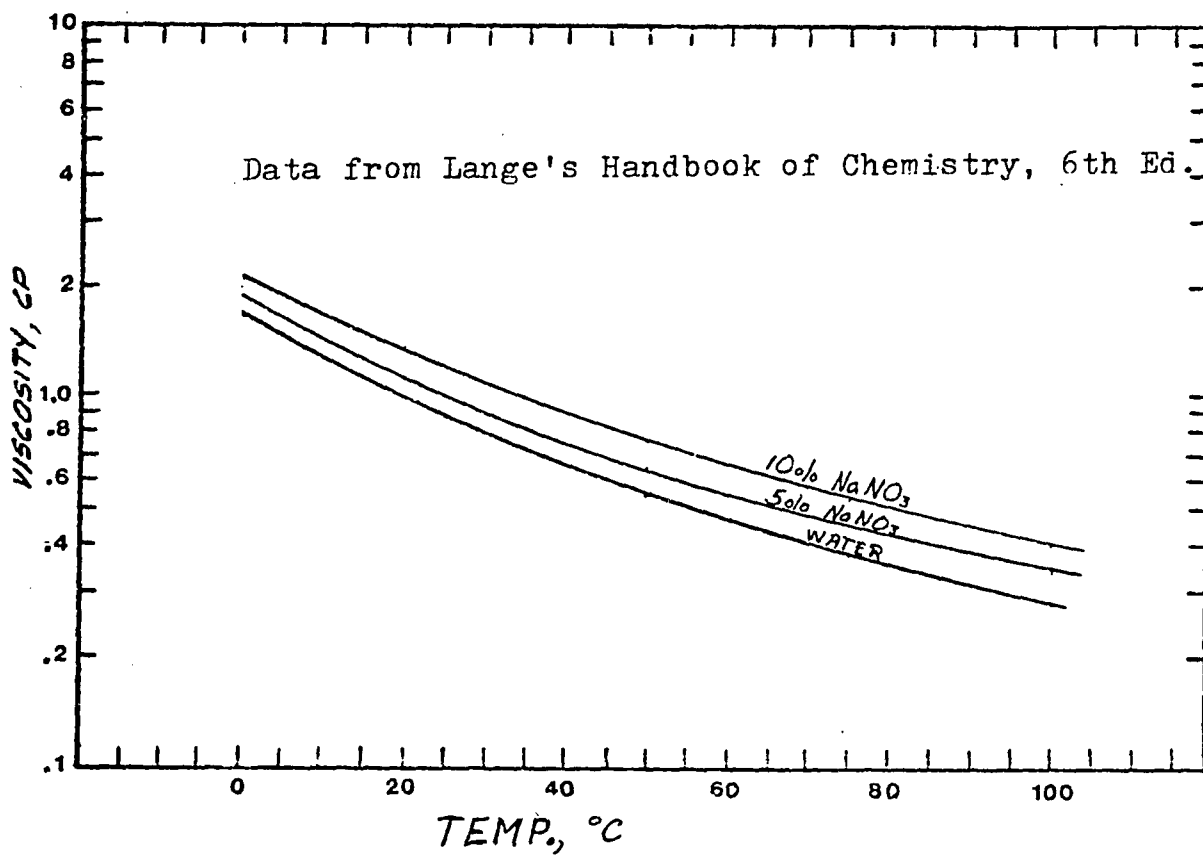Data from Lange's Handbook of Chemistry, 6th Ed.

FIGURE (37)

Viscosity of Aqueous NaNO$_3$ Solutions

APPENDIX V

DESIGN EXAMPLE: SALT-WATER-RESIN SYSTEM

The design is based on multiple tubes, each of which is similar in size to the packed columns used in the laboratory. With tubes of these dimensions, the heat transfer through each tube would be similar to that measured by Sweed and Gregory (1971) who reported that the temperature inside the column reached 90% of its ultimate value in 1.5 min. + 0.5 min. lag time in between half cycles. This is a reasonably low fraction of a typical half cycle time of 20-30 minutes. It is essential that the temperature changes be instantaneous if the equilibrium theory equations of Chen and Hill (1971) and Chen et al. (1972) are to be incorporated into the design equations. Also, even in those cases where the equilibrium theory does not apply, the concept of instantaneous temperature change is usually a basic one.

For a practical design example, it is necessary to make certain basic assumptions regarding the mechanical components of the system, the fluid(s) used for heating and cooling, the column packing, and the fluid system undergoing separation. It should be pointed out that the assumptions in the first two categories could apply to practically all systems. For the last two categories, an ion exchange resin and a dilute aqueous salt solution

have been selected because of the availability of data
and of the wide interest and applicability relating to
dilute aqueous salt systems. The assumptions relating
to the mechanical components are:

1. The parapump column assembly (heat exchanger)
is a 3 ft. diameter unit with the full complement of
2226 0.5 inch o.d. 18 BWG tubes on an 11/16 inch triangular
pitch with 6-inch baffle spacing. A tube length of 4 ft.
(122 cm.) would be adequate to approximate the laboratory
columns which are usually less then 100 cm. long. A
typical flow rate would be 1 cc/min./tube or 2.65×10^{-4}
GPM per tube.

2. The insulation is adequate to make the operation
essentially adiabatic and to restrict the heating and
cooling requirements to the process fluid, the adsorbent,
and the tube walls.

3. The process reservoir pump lines are short and of
sufficient diameter so that the line pressure drop between
the tubes and the reservoirs is negligible.

4. The flow in the feed and product lines is laminar
because of the low flow rate (less than 1 GPM).

5. All pumps operate at 50% efficiency for purposes
of estimating power consumption.

6. Operation is continuous and is limited to 8,000
hours per year or 333 operating days, assuming automatic
and trouble-free operation.

7. The equivalent length of the feed and product lines is arbitrarilly set at 100 ft. and the pipe diameter at 1 inch.

The assumptions relating to the column packing are:

1. The packing material may be assumed to be an ion retardation resin (Bio Rad AG 11 A8) with the properties (Appendix IV) listed as follows:

    a. Void fraction ε = 0.38

    b. Moisture = 36.8-40.3%

    c. Particle size D_p = 149 microns = 4.89×10^{-4} ft.

    d. Heat capacity c_s = 0.65 cal/gm/$^{\circ}$C.

2. The weight x specific heat of the packed column is easily calculated from the data in Appendix IV and includes a stainless steel tube, the packing, and the dilute aqueous solution saturating the packing. The value of $w_t c_t + w_s c_s + w_f c_f$ is determined as follows:

Tube is 0.5 in. o.d. 18 BWG, 0.402 in. i.d.

Internal volume per foot = .785 $(.402)^2 (12)$
(16.39) = 24.95 cm^3

Resin content = 0.475(24.95) = 11.85 gm. dry resin

Wet resin volume = 11.85/0.766 = 15.50 cm^3

Liquid volume = (24.95 - 15.50)+(0.39/0.61)
(11.85) = 17.026 cm^3

Volume of tubing = (3.14/4)(0.5^2 - 0.402^2)12
(16.39) = 13.62 cm^3

Weight of tubing = 13.62 (8.02) = 109.23 gm.

Weight x specific heat:

Resin: 11.85 x 0.65 = 7.70 cal/$^{\circ}$C

Water: 17.02 x 1.0 = 17.02 cal/$^{\circ}$C

Tubing: 109.23 x 0.12 = 13.11 cal/$^{\circ}$C

Total = 37.83 cal/$^{\circ}$C = 0.150 BTU/$^{\circ}$K/ft.

The assumptions relating to the heating and cooling fluid are:

1. The fluid used is water which will be indirectly heated by steam and indirectly cooled by a brine refrigeration system.

2. The temperature range used will be assumed at 55°C for the hot reservoir and 5°C for the cold reservoir. It is assumed that the water must be kept just slightly above freezing.

3. The jacket water densities and specific heats may be assumed equal to 1 at the specified temperatures (Appendix IV). However, in Eq. (III-27), the viscosity is raised to the 0.2 power which effectively narrows the range to within engineering accuracy.

4. The minimum water rate may be taken as one shell-side volume displacement of 104.7 gallons over a 2-minute period or 52.35 GPM, assuming perfect displacement. As shown in the calculations, the rate corresponds to a jacket

water temperature rise of $76.4^{\circ}F$ ($42.4^{\circ}C$). This is a
large temperature rise, but the controls could be arranged
so as to dump the hot water into the hot reservoir and vice
versa so as to minimize the effect on the reservoirs. Also,
the reservoirs could be made large enough to minimize the
overall temperature rise.

The assumptions relating to the process fluid are:

1. The fluid undergoing separation is a dilute
sodium nitrate solution, the properties of which are
shown in Appendix IV. The properties are measured over
the range $T_1 = 55^{\circ}C$ and $T_2 = 5^{\circ}C$ and are shown below:

     a. $\rho_1 = \rho_2 = 62$ lb/ft^3

     b. $c_i = c_2 = 0.54$ BTU/lb/$^{\circ}K$

     c. $\mu_1 = \mu_{TP} = \mu_F = 0.5$ cp $= 1.21$ lb$_m$/ft/hr

     d. $\mu_2 = \mu_{BP} = 1.5$ cp $= 3.629$ lb$_m$/ft/hr

2. The reservoir flow rate was assumed to be 2.65×10^{-4}
GPM/tube x 2,226 tubes = 0.59 GPM or 4.73 ft^3/hr. One impor-
tant constant relating to this rate and dependent on the
particular system is the dimensionless (experimentally
determined) separation parameter b. Most systems studied
thus far have had values of b varying from 0.05 to 0.15.

     a.   Assume a value of b of 0.1

     b.   The ratio of the bottom product rate to the
reservoir flow rate, $\emptyset_B$, must be less than b for good
separation. Assume a value of $\emptyset_B$ of 0.05.

     c.   A dimensionless feed rate, $\emptyset_B + \emptyset_T$, may be

assumed as typical, which means that the dimensionless top product rate is $\emptyset_T = 0.25$.

3. A typical half cycle time, π/ω, of 0.5 hr may be assumed, which means that the number, n, of cycles in 8,000 hours operating time is 8,000.

The process design for the parapump column assembly is:

<u>Flow</u> <u>rate</u> <u>in</u> <u>the</u> <u>columns</u> = 2.65×10^{-4} GPM/tube x 2226 tubes = 0.59 GPM = 4.73 ft^3/hr.

<u>Crossflow</u> <u>area</u> = $(.402 \text{ in})^2$ x .785/144 x 2226 tubes = 1.96 ft^2

<u>Column</u> <u>(tube)</u> <u>velocity</u> = 4.73/1.96 = 2.41 ft/hr

$$\text{Column pressure drop} = \frac{150(1-\epsilon)^2}{D_p^2 \epsilon^3 g_c} (u)(h)(v) \qquad (III-20)$$

$$= \frac{150 \ (.62)^2}{(4.89 \times 10^{-4})^2 (.38)^3 (4.17 \times 10^8)} (2.42)(4)(2.41)$$

$$= (10.54)(2.42)(4)(2.41) = 245.8 \text{ lb/ft}^2 = 1.71 \text{ psi}$$

for a batch pump at 20°C. For a continuous pump operating at 55°C during hot upflow and 5°C during cold downflow and at a $\emptyset_B$ of 0.05, corrections must be made for viscosity and flow rate. From Appendix IV, the viscosities at the hot and cold temperatures are 0.5 and 1.5 cp, respectively.

For the hot upflow half cycle, the pressure drop is

245.8 x (0.5/1)(0.95/1)- 116.8 lb/ft^2 = 0.81 psi.

For the cold downflow half cycle, the pressure drop is

245.8 x (1.5/1)(1.05/1) = 387.1 lb/ft^2 = 2.7 psi.

Shellside Pressure Drop

$$\frac{1.525 \times 10^{-4}(w)^2(2h-1)}{(0.005732N^{0.9474}-0.00173N)^2}$$

$$+ \frac{2.756 \times 10^{-4}(w)^{1.8}(0.07117N^{.4737}-0.0417)(2h)}{(0.003293N^{0.4737}-0.01563)^{1.8}}$$

$$(III-33)$$

Now since N = 2,226 tubes and h = 4 ft, the pressure

drop is now equal to $4.95 \times 10^{-5}w^2 + 3.967 \times 10^{-3}w^{1.8}$.

The minimum water rate was assumed to be 52.35 GPM or

7.281 lb/sec, and the corresponding pressure drop is

equal to 0.144 psi.

The corresponding temperature rise of the water can

be estimated from the data previously calculated. The

mass x specific heat of the tubing and contents was esti-

mated to be 0.150 BTU/$^\circ$K/ft of tubing. The duty is there-

fore 0.150 (4 ft) (2226) (50°) = 66,780 BTU over the two-

minute temperature changeover period. The temperature rise

of the water is therefore equal to (66,780/2)(1/52.35)(1/8.35)

(1/c_w) = 76.4°F = 42.4°C. This temperature rise is high by

a factor of at least five. Therefore, assume the temperature

rise is only 15.2°F. The resulting water rate would be
261.8 GPM and the new shellside pressure drop would be
2.63 psi. All the flow rates discussed are shown to be
in the turbulent range according to the Reynolds number

$$\text{Re} = DG_c/u = (.5/12)(7.28/.46)(1/.000672) = 981$$

which is well above the transition range of 42-225 given
by Donohue (1955).

Heat transfer during hot upflow = q_i =

$$\left[(w_t c_t + w_s c_s + w_f c_f)(N)(h) + Q(1-\emptyset_B)(\rho_1)(c_1)(\pi/\omega) \right] (T_1 - T_2)(n)$$

$$= \left[(0.150)(2226)(4) + 4.73(0.95)(62)(0.54)(0.5) \right] (50)(n)$$

$$- (1335.6 + 75.2)(50)(n) = 70591n = 70,591 \text{ BTU/cycle}$$

Note that the heat required to change the temperature of
the tubes (columns) required 94.7% of the total and that
this occurred during the first two minutes at a rate of
2,003,400 BTU/hr as compared with 8057 BTU/hr for the
remaining 28 minutes of the 0.5 hr half cycle.

Heat transfer during cold downflow = q_2 =

$$(w_t c_t + w_s c_s + w_f c_f)(N)(h)(T_1 - T_2)n$$

$$+ Q(1+\emptyset_B)(\rho_2 c_2)(\pi/\omega)(T_{2H} - T_2)n$$

(III-18)

If it is assumed that the incoming feed is at temperature T_1, then $T_1 = T_{2H}$ and $\rho_1 = \rho_2$; $c_1 = c_2$.

$$q_2 = \left[(.150)(2226)(4)+(4.73)(1.05)(62)(.54)(.5)\right] (50)n$$

$$= (1335.6+83.1)(50)n = 70,935n = 70,935 \text{ BTU/cycle.}$$

REFERENCES

Alexis,R.W.,Chemical Engineering Progress,63,69 (1967).

Andrews,M.A.,PhD Thesis, Princeton University, N.J. (1967).

Acrivos,A.,Industrial and Engineering Chemistry,48,703 (1956).

Apostolopoulos,G.P.,Industrial and Engineering Chemistry, 14, (1975).

Aris,R.,Industrial and Engineering Chemistry Fundamentals, 8,603,(1969).

Bird,R.B.,Stewart,W.E., and Lightfoot,E.N., Transport Phenomena, Wiley (New York, 1960).

Bringhurst,F.R., B.S.E. Thesis, Princeton University, Princeton, N.J.(1970).

Butts,T.J., Gupta,R., and Sweed,N.J., Chemical Engineering Science, 27, 855 (1972).

Butts, T.J., Sweed, N.H., and Camero, A.A., Industrial and Engineering Chemistry Fundamentals, 12, 467 (1973).

Carslaw, H.S., and Jaeger, J.C., Conduction of Heat in Solids, Oxford University Press, 2nd Ed. (1959).

Chen, H.T., and Hill, F.B., Separation Science, 6, 411 (1971).

Chen, H.T., Jaferi, J., and Stokes, J.D., Paper 9e, 73rd National AIChE Meeting, Minneapolis (1972a).

Chen,H.T., Rak,J.L., Stokes,J.D., and F.B. Hill, AIChE Journal, 18, 356 (1972).

Chen, H.T., Reiss, E.H., Stokes, J.D., and F.B. Hill, AIChE Journal, 19, 589 (1973).

Chen, H.T.,Lin, W.W., Stokes, J.D., and W.R. Fabisiac, AIChE Journal, 20, 306 (1974).

Chen, H.T., and J.A. Manganaro, AIChE Journal, 20, 1020 (1974).

Chen, H.T., and V.J.D'Emido, AIChE Journal, 21 813 (1975).

Donohue, D.A., "Heat Exchanger Design" Series, Petroleum Refiner, (Aug., Oct., Nov., 1955).

Goldstein, R.J., B.S.E. Thesis, Princeton University, Princeton, N.J. (1969).

Gregory,R.A., and N.H. Sweed, Chemical Engineering Journal, $\underline{1}$, 207 (1970).

Gregory, R.A., and N.H. Sweed, Chemical Engineering Journal, $\underline{4}$, 139 (1972).

Gregory, R.A., AIChE Journal, $\underline{20}$, 294 (1974).

Jenczewski, T.J., and A.L. Myers, AIChE Journal, $\underline{14}$, 509 (1968).

Jenczewski, T.J., and A.L. Myers, Ind. Eng. Chem. Fundamentals $\underline{9}$, 216 (1970).

Kim, D.K., and H.M. Hulburt, Northwestern University, Paper presented at the AIChE Meeting in San Francisco, California (Dec. 1971).

Kim, C.Y., M.S. Thesis, N.J.I.T., Newark, N.J. (1976).

Kowler, D.E., and R.H. Kadlec, AIChE Journal, $\underline{18}$, 1207 (1972).

Kunin, R. "Ion Exchange Resins", 2nd Ed., John Wiley & Sons, New York (1958).

Lee, H. and D.E. Stahl, Paper 92e. Presented at 65th Annual AIChE Meeting, New York (Nov., 1972).

Lin, W., M.S. Thesis, Newark College of Engineering, Newark, N.J., (1974).

Patrick, R.R., Schrodt, J.T., and R.I. Kermode, Separation Science, $\underline{7}$, 331 (1972).

Perry, Chilton, Kirkpatrick, "Perry's Chemical Engineers' Handbook", 5th Ed. (1970).

Pigford, R.L., Baker, B., and D.E. Blum, Industrial and Engineering Chemistry Fundamentals, $\underline{8}$, 144 (1969).

Rolke, R.W., and R.H. Wilhelm, Industrial and Engineering Chemistry Fundamentals, $\underline{8}$, 235 (1969).

Sabadell, J.E., and N.H. Sweed, Separation Science, $\underline{5}$, 171 (1970).

Schroeder, H.G. and C.E. Hamrin Jr., AIChE Journal, 21, 807 (1975).

Shendalman, L.H. and J.E. Mitchell, Chemical Engineering Science, 27, 1449 (1972).

Skarstrom, C.W., Annals New York Academy of Sciences, 72, 751 (1959).

Sweed, N.H., PhD Dissertation, Princeton University, Princeton, N.J. (1969).

Sweed, N.H. and R.H. Wilhelm, Industrial and Engineering Chemistry Fundamentals, 8, 221 (1969).

Sweed, N.H. and R.A. Gregory, AIChE Journal, 17, 171, (1971).

Sweed, N.H. and J.M. Rigaudeau, Paper 18c. Presented at the 66th Annual AIChE Meeting, Philadelphia (Nov. 1973).

Turnock, P.H. and R.H. Kadlec, AIChE Journal, 17, 335, (1971).

Wakao, N., Matsumoto, H., Suzuki, K., and A. Kawahara, Kagaku Kogaku, 32, 169 (1968).

Wankat, P.C., Industrial and Engineering Chemistry, 12, 372 (1973).

Wankat, P.C., Separation Science, 9, 85 (1974).

Wilhelm, R.H., Rice, A.W., and A.R. Bendelium, Industrial and Engineering Chemistry, 5, 141 (1966).

Wilhelm, R.H., Intracellular Transport, Academic Press, pp. 199-220, (New York, 1966).

Wilhelm, R.H., Rice, A.W., Rolke, R. W., and N.H. Sweed, Industrial and Engineering Chemistry Fundamentals, 7, 327 (1968).

Wilhelm, R.H., and N.H. Sweed, Science, 159, 522 (1968).

NOMENCLATURE

a	deviation of m from the mean of the values at T_1 and T_2
a_p	interfacial area of the sorbent particles per unit volume of packed bed
a_t	total cross section area of a packed tube
b	dimensionless equilibrium parameter defined by Equation (21)
b_1	largest value of b_1 in a multicomponent system
b_s	smallest value of b_i in a multicomponent system
b_k	value of b_i in a multicomponent system which is $\leq \emptyset_B$
b_k+1	value of b_i in a multicomponent system which is $\geq \emptyset_B$
B_s	shellside baffle spacing, ft.
c	heat capacity
c_f	heat capacity of process fluid
c_{HTF}	heat capacity of heat transfer fluid
c_s	heat capacity of solid adsorbent
c_t	heat capacity of tube wall
C_1	$V_T/(Q\pi/\omega)$, dimensionless
C_2	$V_B/(Q\pi/\omega)$, dimensionless
c_o	total utility costs, $/year
C_{BR}	brine refrigeration costs, $/ton-hr
C_{EL}	electricity costs, $/kw-hr
C_{ST}	steam costs, $/lb steam
d	i.d. of shell parapump assembly
d_1	i.d. of adsorbent packed column
$\mathcal{D}$	axial diffusivity
D_f	fluid diffusivity

D	o.d. of adsorbent packed column
D_i	i.d. of pipe or conduit
D_p	adsorbent particle diameter
E	pump efficiency, fraction
f	fanning friction factor
F_{N1}	shellside pressure drop factor related to resistance through baffle openings
F_{N2}	shellside pressure drop factor related to resistance to flow across tube banks
g_c	gravitational conversion factor, $(lb_m/hr^2/ft)(ft^2/lb_f)$ = $4.17x10^8$
h	packed column height
Hp	hydraulic horsepower
k	thermal diffusivity
K	constants (defined locally)
k_f	fluid phase mass transfer coefficient, bed volume/interfacial area/ time
l	length of pipe or conduit, ft.
L	wavefront propagation distances defined by Equations (17, 18)
M	x_i/y_i
m	dimensionless equilibrium parameter defined by Equation (6)
n	number of cycles of pump operation
N	number of packed columns or tubes in the parapump assembly
p	defined by Equation (30)
P_B	bottom product flow rate
q	defined by Equation (30)
q_i	total heat required during hot upflow half-cycle (including switchover period)

q_2	total cooling required during cold downflow half cycle (including switchover period
q_t	heat required to change temperature of packed tubes from T_1 to T_2 (switchover period)
Q	reservoir displacement rate, ft^3/hr.
r	packed column radius
t	time
T	temperature, $^\circ K$
ΔT_w	temperature change of heat transfer fluid
u	wavefront propagation velocity in packed column
v	velocity of process fluid in packed bed
v_o	interstitial velocity in the packed column at the mean of the upflow and downflow half-cycles
V_A	molar volume of a solute
V_S	volume of shellside fluid
V_T	top reservoir dead volume
V_B	bottom reservoir dead volume
w	mass flow rate of heat transfer fluid, lb/sec.
w_f	mass per unit length of process fluid
w_s	mass per unit length of solid adsorbent
w_t	mass per unit length of tube wall
x_i	concentration of solute in the solid phase, moles per unit weight of adsorbent
y_i	concentration of solute in the liquid phase, moles per unit volume of fluid
y_i^*	equilibrium concentration in fluid phase
z	axial distance along packed bed
$\hat{z}$	z/v

Greek

α	thermal diffusivity (local)
α_{ij}	constant separation factor of component i relative to component j
Ψ	association parameter used in Equation (66)
λ	mass transfer coefficient (cm^3/sec/gm. adsorbent)
δ	defined by Equation (50)
$\emptyset$	product volumetric flow rate/reservoir displacement rate, dimensionless
π/ω	duration of half cycle
ϵ	void fraction in packing, dimensionless
τ	switchover time
ρ	density
ρ_f	density of fluid
ρ_s	density of adsorbent
μ	viscosity

Subscripts

O	initial condition or condition at mean value of T_1 and T_2
1	upflow
2	downflow
B	stream from or to bottom of column
i	solute i
F	feed stream
HTF	heat transfer fluid
P	product stream
T	stream from or to top of the column
BP	bottom product
TP	top product

VITA

Candidate: John Daniel Stokes

Educational Background: B.S., Upsala College, East Orange, N.J., June, 1949; M.S., Newark College of Engineering, Newark, N.J., June, 1951; Dr. Engineering Science, New Jersey Institute of Technology, June, 1976.

Professional Background: Production Supervisor at Givaudan Corp., Clifton, N.J., 1951- 1955; Research Engineer at Hercules Powder Co., Parlin, N.J., 1955-1958; Process Design Engineer at Hoffmann La Roche, Inc., Nutley, N.J., 1958 to present. N.J. State Professional Engineer's License No. 10256, obtained in 1959.

Dissertation Research: Performed in the laboratories of New Jersey Institute of Technology, Newark, N.J. from Sept. 1972 to May, 1976.